FUNCTIONAL CHARACTERIZATION OF THE PARL MITOCHONDRIAL PROTEINS IN ZEBRAFISH (*DANIO RERIO*)

SANDRA NOBLE

Thesis submitted to the
Faculty of Graduate and Postdoctoral Studies
in partial fulfillment of the requirements
for the Doctorate in Philosophy degree in Biology

Department of Biology
Faculty of Science
University of Ottawa

PREFACE

This thesis was written following 'The thesis as a series of articles' format. Therefore, following a general introduction chapter, Chapter 2 includes the article entitled, "Zebrafish Parla- and Parlb-deficiency affects dopaminergic neuron patterning and embryonic survival" by Sandra Noble, Abid Ismail, Rafael Godoy, Yanwei Xi and Marc Ekker published in J. Neurochem. (2012) 122, 196–207. A copy of the permission granted from the publisher to use the published figures from this article in this thesis is included in Appendix C. Chapter 3 is entitled, "Transgenic zebrafish expressing mitochondrial targeted mCherry specifically in dopaminergic neurons" by Sandra Noble, Rafael Godoy and Marc Ekker and is currently in preparation for publication. Chapter 4 entitled, "Analysis of cleavage patterns of the zebrafish Parl proteins" comprises data that will be included in a research article to be written in the coming months once combined with data from another student. The thesis ends with a general discussion.

ACKNOWLEDGEMENTS

First and foremost, I would like to thank my supervisor, Dr. Marc Ekker, for his guidance and support throughout my Ph.D.

I would like to thank my Ph.D. Advisory Committee Members: Drs. Dennis Bulman, Shelley Hepworth and Mario Tiberi for their direction and guidance.

I am grateful for the help received from both past and present Ekker lab members, including, Vishal Saxena for teaching me about zebrafish husbandry and microinjection and his excellent care of the fish; as well as Gary Hatch for his technical advice, questions during lab meetings and discussions following lab meetings. Best wishes for success to the PD group; it was a pleasure working with them towards the same goal. I think their hard work will bring fruitful discoveries in the future.

I am thankful to my Mom and Dad for all of their support and always encouraging me to do my best.

STATEMENT OF CONTRIBUTIONS

The thesis, "Functional characterization of the Parl mitochondrial proteins in zebrafish (*Danio rerio*)" is composed of three related studies; all of which were collaborative efforts.

Chapter 2 entitled: "Zebrafish Parla- and Parlb-deficiency affects dopaminergic neuron patterning and embryonic survival" was a collaborative effort. Dr. Dennis Bulman communicated results before publication. I performed all the experiments including: synteny analysis, RT-PCR experiments, injection of all morpholinos and rescue mRNA sequences, *in situs* and scoring of morphant phenotypes. Abid Ismail, Rafael Godoy and I prepared zebrafish *pink1* and human *PARL* rescue constructs. Rafael Godoy and I performed the acridine orange and cell death assays, the scoring of morphant phenotypes in rescue experiments and the statistical analyses. Yanwei Xi and I performed the *in situs* for the rescue experiments. The experiments were conceived by Dr. Marc Ekker and me. I wrote the manuscript. Dr. Marc Ekker, Rafael Godoy and I helped in revising the manuscript.

Chapter 3 entitled: "Transgenic zebrafish expressing mitochondrial targeted mCherry specifically in dopaminergic neurons" was a collaborative effort. Rafael Godoy prepared electro-competent *E. coli* cells for homologous recombination. Gary Hatch and I prepared the targeting vector, subcloned it into the Tol2 vector and performed the electroporation of the targeting vector. Vishal Saxena (technician in Dr. Marc Ekker's laboratory) and I injected the transgenic construct into zebrafish. I screened zebrafish for a transgenic line and raised the fish. I isolated mitochondria and did western blotting. I performed confocal microscopy on live transgenic fish. Rafael Godoy and I performed fluorescent whole-mount *in situ* hybridization in combination with immunostaining to characterize the line. Rafael Godoy and I performed multiphoton confocal microscopy of fixed larvae. Rafael Godoy and I exposed fish to MPTP and I performed

live confocal microscopy. I quantified the relative fluorescence of the MPTP and control larvae. The experiments were conceived by Dr. Marc Ekker and me. I wrote the manuscript.

Chapter 4 entitled: "Analysis of cleavage patterns of the zebrafish Parl proteins" was a collaborative effort with Dr. Mario Tiberi's laboratory. I prepared the four *parla*-Flag and *parlb*-Flag constructs and synthesized the mRNA. I performed all zebrafish injections, protein extractions and western blotting experiments. Xiaodi Yang (technician in Dr. Mario Tiberi's laboratory) and I performed transfection, immunoprecipitation and western blotting experiments on the HEK cell line. I performed all transfection, immunoprecipitation and western blotting experiments on the HeLa and SH-SY5Y cell lines. Rafael Godoy helped with cell culture. I did the Coomassie blue gels. I also setup the same type of experiments for the MES23.5 dopaminergic cell line. Rafael Godoy and I prepared the MES23.5 cell culture media recipe. Melissa Lavictoire and I tested different elution methods and did the silver stained gel together. The experiments were conceived by Dr. Marc Ekker and me.

ABSTRACT

The aim of this thesis was the functional characterization of the zebrafish *parl* (Presenilin-Associated Rhomboid-Like) genes which code for mitochondrial proteins involved in cell survival. A mutation in PARL has been described in Parkinson's disease patients. I investigated the role of mitochondrial PD-related proteins using a zebrafish *parla* and *parlb* deficiency model. I found that the knockdown of both *parl* genes is lethal. Parla plays a larger role in patterning of the DA neurons in the ventral diencephalon than Parlb. The human PARL rescued the double morphant phenotype, suggesting function conservation between zebrafish and humans. I was able to rescue the mortality and DA neuron mispatterning observed in double morphants with synthetic *pink1* mRNA. This suggests that *parl* genes are epistatic to *pink1* in zebrafish.

To visualize mitochondria specifically in dopaminergic neurons of live zebrafish, I established a transgenic line Tg(*dat*:*tom20 MLS-mCherry*) where regulatory elements of the *dopamine transporter* (*dat*) were used to drive expression of a Tom20-mCherry fusion protein that is targeted to the mitochondria. I characterised the expression of Tom20-mCherry to the mitochondria of the majority of DA neuron groups. In addition, I observed a decrease in mCherry fluorescence following MPTP exposure of live fish.

The PD-related mutation in PARL is located in a cleavage site of the mammalian protein, which is necessary for the production of the beta peptide; however, this site is predicted to be absent in the zebrafish Parls. To establish the cleavage patterns of the zebrafish Parls and compare them to those of human PARL, I examined the cleavage of Parl-Flag constructs in cultured cells. I detected one band for Parla-Flag and two bands representing Parlb-Flag.

The *parla* and *parlb* deficiency model along with the characterization of the cleavage patterns of Parl and the Tg(*dat*:*tom20 MLS-mCherry*) transgenic line are tools which will help elucidate the role of mitochondrial proteins in PD research.

RÉSUMÉ

L'objectif principal de cette thèse était de caractériser la fonction du produit des gènes *parl* (Presenilin-Associated Rhomboid-Like) du poisson-zèbre (*Danio rerio*) qui codent pour des protéines mitochondriales impliquée dans la survie cellulaire. Une mutation du gène PARL humain a été décrite chez des patients souffrant de la maladie de Parkinson (MP). J'ai étudié le rôle de protéines mitochondriales associées à MP en produisant des poissons-zèbres morphants ayant perdu la fonction de *parla* et *parlb*. J'ai trouvé que l'inactivation des deux gènes *parl* avait un effet létal. Parla joue un rôle prépondérant dans la formation des neurones dopaminergiques (DA) dans le diencéphale ventral. Le gène PARL humain peut renverser ce phénotype morphant, ce qui suggère une conservation fonctionnelle. J'ai pu renverser la mortalité et la malformation des neurones DA des double-morphants avec un ARNm synthétique du gène *pink1*. Ceci suggère une relation d'épistasie dans laquelle *parl* est en amont de *pink1*.

Afin de visualiser spécifiquement les mitochondries des neurones dopaminergiques chez le poisson-zèbre, *in vivo*, j'ai produit une lignée transgénique, Tg(*dat*:*tom20 MLS-mCherry*), dans laquelle les éléments régulateurs du gène du transporteur de la dopamine (*dat*) dirigent l'expression d'une protéine de fusion Tom20-mCherry vers les mitochondries des neurones DA. J'ai montré l'expression du transgène dans la majorité des groupes de neurones DA. De plus, j'ai observé une diminution de la fluorescence de mCherry suite à une exposition des poissons au MPTP.

La mutation de la protéine PARL chez l'humain est située dans un site de clivage nécessaire à la production du peptide béta. Toutefois, ce site est absent dans la séquence prédite des Parls du poisson-zèbre. Afin de déterminer les profils de clivage des Parls du poisson-zèbre et de les

comparer à ceux de la protéine humaine, j'ai examiné le clivage de constructions Parl-Flag dans des cellules en culture. J'ai détecté une bande pour Parla-Flag et deux bandes pour Parlb-Flag.

Notre modèle de perte de fonction de *parla* et *parlb*, la caractérisation de leurs profils de clivage et la lignée transgénique Tg(*dat*:*tom20 MLS-mCherry*) sont des outils qui nous permettront de mieux comprendre le rôle des mitochondries dans la maladie de Parkinson.

TABLE OF CONTENTS

LIST OF FIGURES

LIST OF TABLES

LIST OF ABBREVIATIONS

BCA assay	bicinchoninic acid assay
bp	base pairs
Ccp1	cytochrome c peroxidase
Chr	chromosome
COS-7	mammalian cells from African green monkey kidney fibroblast-like cell line
DA	dopaminergic
dat	*dopamine transporter*
DC	diencephalic cluster
Dm	*Drosophila melanogaster*
dpf	days post-fertilization
Dr	*Danio rerio*
EGF	epidermal growth factor
EGFP	enhanced green fluorescent protein
EM	electron microscopy
HA	hemagglutinin tag
HEK	human embryonic kidney cells
hpf	hours post-fertilization
Hs	*Homo sapiens*
I-CliP	intramembrane-cleaving protease
IMM	inner mitochondrial membrane
IMS	intermembrane space
IP	immunoprecipitation
kb	kilobases
LC	locus coeruleus
LHON	Leber hereditary optic neuropathy
MFN1	mitofusin 1
MFN2	mitofusin 2
Mgm1	mitochondrial genome maintenance protein
MHB	midbrain hindbrain boundary
Mm	*Mus musculus*
MO	morpholino oligonucleotide

MPP+	1-methyl-4-phenylpyridinium
MPTP	1-methyl-4-phenyl-1,2,3,6-tetrahydropyridine
MLS	mitochondrial localising sequence
MTS	mitochondrial targeting sequence
mtYFP	mitochondrially targeted yellow fluorescent protein
NLS	nuclear localization signal
OB	olfactory bulb
Ol	*Oryzias latipes* (Medaka)
OMM	outer mitochondrial membrane
O/N	overnight
OPA1	optic atrophy 1
ORFs	open reading frames
PARL	Presenilin-Associated Rhomboid-like
PD	Parkinson's disease
Pr	pretectum
RAC	retinal amacrine cells
Rbd1p	yeast PARL orthologue
Rhomboid-7	fly PARL orthologue
RIP	regulated intramembrane proteolysis
ROM1	rhomboid-1 *C. elegan* PARL orthologue
S2	Drosophila melanogaster embryonic epithelial-like cell line
SDS-PAGE	sodium dodecyl sulfate-polyacrylamide gel electrophoresis
SNP	single nucleotide polymorphism
SP	subpallium
SREBP	sterol regulatory element-binding protein
Tg	transgenic
th	tyrosine hydroxylase
TILLING	Targeting Induced Local Lesions in Genomes
TMD	transmembrane domain
TMH	transmembrane helix
Tn	*Tetraodon nigroviridis* (Tetraodon)
TOM20	translocase of the outer mitochondrial membrane
Tr	*Takifugu rubripes* (Fugu)

UTR	untranslated region
VDAC1	voltage-dependent anion selective channel protein 1
vDC	ventral diencephalon
WT	wild type

CHAPTER 1.

INTRODUCTION: THE BIOCHEMISTRY OF PARL, THE MITOCHONDRIAL PRESENILIN-ASSOCIATED RHOMBOID-LIKE PROTEASE, IN DISEASE

1.1 MITOCHONDRIAL DYSFUNCTION IN PARKINSON'S DISEASE AND THE DOPAMINERGIC SYSTEM IN ZEBRAFISH

Parkinson's disease (PD) is the second most prevalent neurodegenerative disease in humans. The clinical hallmarks of PD which classify it as a movement disorder are tremor at rest, rigidity, bradykinesia, postural instability and responsiveness to dopaminergic medication (Lang and Lozano, 1998a, b). At the cellular level, PD is characterized by the loss of nigrostriatal dopaminergic (DA) neurons in humans (Dexter and Jenner, 2013). Many genes with mutations in inheritable PD have been found: *alpha-synuclein*, *Parkin*, *DJ-1*, *PINK1* and *LRRK2* (Cookson, 2005; Farrer, 2006; Klein and Schlossmacher, 2006; Whitworth et al., 2008). Recently, a mutation in the *PARL* gene was identified in two PD patients (Shi et al., 2011) (see Table 1.1).

Several biochemical abnormalities including mitochondrial dysfunction (complex I deficiency), free radical-mediated damage, inflammatory changes and proteasomal abnormalities have been observed in the substantia nigra of patients with sporadic PD (Schapira, 2007). Some of these biochemical changes are the result of known genetic defects which overlap in familial and sporadic PD. Studying the genetic basis of familial PD (5-20% of all PD cases), will help extend these findings to the 80-95% of sporadic PD cases (Dauer and Przedborski, 2003) since both may use common routes to dopaminergic cell death and dysfunction (Schapira, 2007).

1.2 PARKINSON'S DISEASE-RELATED GENES IN ZEBRAFISH AND EPISTATIC GENETIC PATHWAYS

Several models for dopaminergic neurotoxins and genes associated with familial Parkinson's disease have been identified: MPTP, rotenone, paraquat, 6-OHDA and *α-synuclein*, *Parkin*, *DJ-1*, *UCHL1*, *PINK1*, *LRRK2* and *PARL* (Bretaud et al., 2004; Cookson, 2005; Lam et al., 2005; McKinley et al., 2005; Farrer, 2006; Haque et al., 2008; Wen et al., 2008; Whitworth et al., 2008; Sallinen et al., 2009; Shi et al., 2011; Xi et al., 2011b). Each of these has been shown to perturb DA neurons to varying degrees.

We examined the role of the *parl* genes in zebrafish which we named, *parla* and *parlb* (Noble et al., 2012). *parla* codes for a 360 amino acid protein, while *parlb* codes for a 383 amino acid protein. Both *parla* and *parlb* transcripts are present during early development. In adult zebrafish, *parla* is expressed in the brain and muscle with lower expression levels in the liver and heart. Likewise, *parlb* is expressed in the brain and liver, but is not detected in the heart and muscle of adult fish.

Performing an *in vivo* loss-of function analysis using translation-blocking and splice-blocking morpholino oligonucleotides at the one-cell-stage, results in mild neurodegeneration, as evidenced by a lower density of dopaminergic neurons. Parla deficiency results in a 60% of larvae with severely mis-patterned DA neurons, while Parlb deficiency does not affect DA neurons. Double morphants exhibit patterning defects in DA neurons of the ventral diencephalon. This work was done using a *tyrosine hydroxylase* (*th1*) antisense cRNA probe for whole-mount *in situ* hybridization and was also confirmed by observing EGFP fluorescence in a zebrafish transgenic line, Tg(*dat:EGFP*), expressing EGFP under the control of the *cis*-

regulatory elements of the *dopamine transporter* (*dat*) (Xi et al., 2011b), following morpholino injection (Noble et al., 2012). Moreover, extensive cell death is observed throughout the entire body of double morphants, as well as an increase in larval mortality, which is confirmed through acridine orange staining. Single morphants, however, do not exhibit increased mortality. We believe that the functional redundancy of the zebrafish *parl* genes allows for a compensatory mechanism whereby the knockdown of a single *parl* subsequently triggers the up-regulation of its paralogs. Indeed, the knockdown of *parla* results in an increase in *parlb* expression by semi-quantitative RT-PCR, while the knockdown of parlb did not markedly affect *parla* or *parlb* transcription. Our results suggest that at least one functional Parl protein is required for early embryonic and larval survival in zebrafish.

The double morphant phenotypes of DA neuron mis-patterning and of mortality are rescued by wild-type human *PARL* mRNA co-injection with the *parla* and *parlb* morpholinos (Noble et al., 2012). However, mRNA encoding a catalytically inactive human PARL (S277G) co-injected with both *parl* morpholinos does not rescue the double morphant phenotype. Since human PARL can rescue the morphant phenotype, this suggests that Parl function is conserved between zebrafish and human.

The *Drosophila* PARL ortholog, *rhomboid-7*, acts in a common pathway with *Pink1* and *Parkin*, which are other known PD-related genes, where it is needed for mitochondrial fusion (Thisse and Thisse, 2008; Whitworth et al., 2008). In *Drosophila*, it has been shown that *rhomboid-7* is epistatic to *pink1* and that PINK1 is a substrate of *rhomboid-7* (Whitworth et al., 2008). Similarly, we found that the zebrafish *parl* genes are epistatic to the zebrafish *pink1* gene by knocking down the *parl* genes while simultaneously expressing zebrafish *pink1* (Noble et al., 2012). Since this epistatic relationship was previously unknown in vertebrates, our findings open

up the possibility that the same relationship could be true in higher vertebrates as well. Human *PINK1* mRNA also rescues the parl morphant phenotype, although to a lesser degree than seen with zebrafish *pink1*. Furthermore, a human kinase inactive K219M *PINK1* does not rescue larval mortality, while a human PD-linked G309D *PINK1* mutant results in a mild rescue. Our findings supports the idea that the zebrafish *parl* genes may function upstream of *pink1*, as part of a conserved pathway in vertebrates.

PINK1 cleavage in mammalian cell culture is reportedly inhibited by the lack of PARL (Jin et al., 2010). Seemingly, these observations are inconsistent with Rhomboid-7/PARL being epistatically upstream of PINK1. However, although PARL is shown to cleave PINK1 in mammalian cell lines, PINK1 is not exclusively proteolysed by PARL (Deas et al., 2011) and it has been shown that PINK1 turnover is facilitated by four known mitochondrial proteases: mitochondrial processing peptidase, ClpXP, m-AAA and PARL (Greene et al., 2012). Thus, cleavage of over-expressed zebrafish or human PINK1 in the absence of Parla and Parlb may be accomplished by compensatory mechanisms which would explain the seemingly non-intuitive ability of Pink1 to rescue the Parl phenotype in zebrafish, even though Pink1 is a substrate of Parl.

The loss-of-function of the *parl* genes may lead to larval death in zebrafish by altering Parl's role in mitochondria dynamics and cristae remodelling (Herlan et al., 2003; McQuibban et al., 2003; Cipolat et al., 2006). Parl normally cleaves OPA1, an anti-apoptotic inner mitochondrial membrane protein, within its transmembrane domain in the inner mitochondrial membrane to produce a soluble form of OPA1 which oligomerizes with membrane-tethered OPA1 to close the mitochondrial cristae junctions and prevent the release of cytochrome c which, in turn, guards against apoptosis (Gottlieb, 2006; Pellegrini and Scorrano, 2007).

1.3 REGULATED INTRAMEMBRANE PROTEOLYSIS (RIP) AND INTRAMEMBRANE-CLEAVING PROTEASES (I-CLIPS)

Regulated intramembrane proteolysis (RIP) is a signaling mechanism, conserved from bacteria to humans, by which biologically active soluble peptides are generated from membrane-bound precursor proteins (Brown et al., 2000; Sik et al., 2004). These peptides may function as transcription factors or soluble ligands in a paracrine manner (Brown et al., 2000; Freeman, 2004). RIP requires two sequential cleavages performed by different proteases. The first cleavage typically occurs near a transmembrane helix (TMH), while the second cut occurs within a TMH and is executed by an intramembrane-cleaving protease (I-CliP). This second RIP releases a bioactive peptide. Many examples of RIP exist. They include the sterol regulatory element-binding protein (SREBP) which is cleaved by the site-2-protease (a metalloprotease) I-CliP to generate a water soluble N-terminal domain that translocates to the nucleus where it acts as a transcription factor for sterol regulatory element DNA sequences; Presenilin-1 (an aspartyl protease) is an I-CliP which cleaves both Notch receptor and APP in the cell membrane; *Drosophila* Rhomboid-1 is an I-CliP which cleaves the TMH of Spitz and secretes a regulatory peptide, but without an initial cleavage outside the TMH.

1.4 THE RHOMBOID FAMILY

Three classes of intramembrane proteases exist: 1) metalloproteases; 2) aspartyl proteases; and 3) rhomboid serine proteases (Brown et al., 2000; Lemberg and Freeman, 2007). Rhomboids were first discovered in a genetic screen for mutants in *Drosophila*, where it was found that the mutant phenotype of embryonic flies was a pointed head skeleton (Mayer and Nüsslein-Volhard, 1988). Thus, they named each of the mutants after a pointed shape. One of these mutants was

designated *rhomboid*. Rhomboids are defined as genes that are predicted to encode functionally active proteases with all the necessary features of proteolytic activity (Lemberg and Freeman, 2007). However, rhomboid-like genes have been identified based on sequence conservation and do not share all the protease consensus features of classical rhomboids.

In bacteria and parasites, rhomboids are involved in intercellular signalling quorum sensing (Gallio et al., 2002) and host cell invasion (Brossier et al., 2005). The yeast PARL subfamily (Pcp1p/Rbd1p) is a mitochondrial I-CliP which cleaves Mgm1 and mediates mitochondrial fusion, respiration and growth rate (McQuibban et al., 2003). In *Drosophila*, rhomboids play a role in growth and development in the epidermal growth factor (EGF) signalling pathway (Koonin et al., 2003; Freeman, 2004). Similarly, rhomboid-1 (ROM1) in *C. elegans* also controls EGFR signalling (Dutt et al., 2004). A $PARL^{-/-}$ mouse model, links mammalian mitochondrial rhomboid function to the regulation of apoptosis (Cipolat et al., 2006).

The hallmark feature of the rhomboid subfamily is the presence of a six TMH core (Lemberg and Freeman, 2007). Within the conserved core, there is a predicted catalytic serine located in TMH4 (S277) and predicted catalytic histidine in TMH6 (H335) as well as a domain within the first loop and TMH2 which is of unknown function, and a highly conserved tryptophan-arginine ($_{136}WR_{137}$) motif in loop 1 which may be required for proteolytic activity (Lemberg et al., 2005; Lemberg and Freeman, 2007; Wang et al., 2007; Freeman, 2008). The close interaction of TMH4 and TMH6 which harbor the catalytic serine and histidine of PARL is essential to its folding and stability (Jeyaraju et al., 2011). Bacterial and archaeal rhomboids possess only six TMHs, while the majority of eukaryotic rhomboids have the six TMH core and an additional TMH located at either the N-terminus (1 + 6) in the case of the mitochondrial PARL subfamily or the C-terminus (6 + 1) in the rhomboid subfamily (Lemberg and Freeman, 2007) (figure 1.1).

Figure 1.1. PARL is a multi-pass transmembrane protease situated in the inner mitochondrial membrane (IMM). This mammalian mitochondrial rhomboid possesses a '1+6' transmembrane structure consisting of an additional transmembrane helix (TMH) at its N-terminus, followed by the 6 TMH core. A catalytic serine (S) and histidine (H) (red) are located approximately a third of the way into the membrane on the matrix side in TMH4 and TMH6, respectively. The interaction (represented by a red bar) between these two catalytic residues is essential for stability of the PARL protein. Three cleavage sites (black arrow heads) exist in PARL: the most distal α site releases PARL's mitochondrial targeting sequence (MTS, blue) upon import into the mitochondria; the β site releases the Pβ peptide (purple); the γ site within loop 1 may destabilize PARL when its degradation is required within specific tissues. Phosphorylation of three residues (S65, T69 and S70; yellow stars) within the Pβ domain regulate β-cleavage (inset). A Parkinson's disease mutation of a serine to an asparagine at amino acid position 77 is located in the β site and impairs PARL cleavage at this position. OMM, outer mitochondrial membrane.

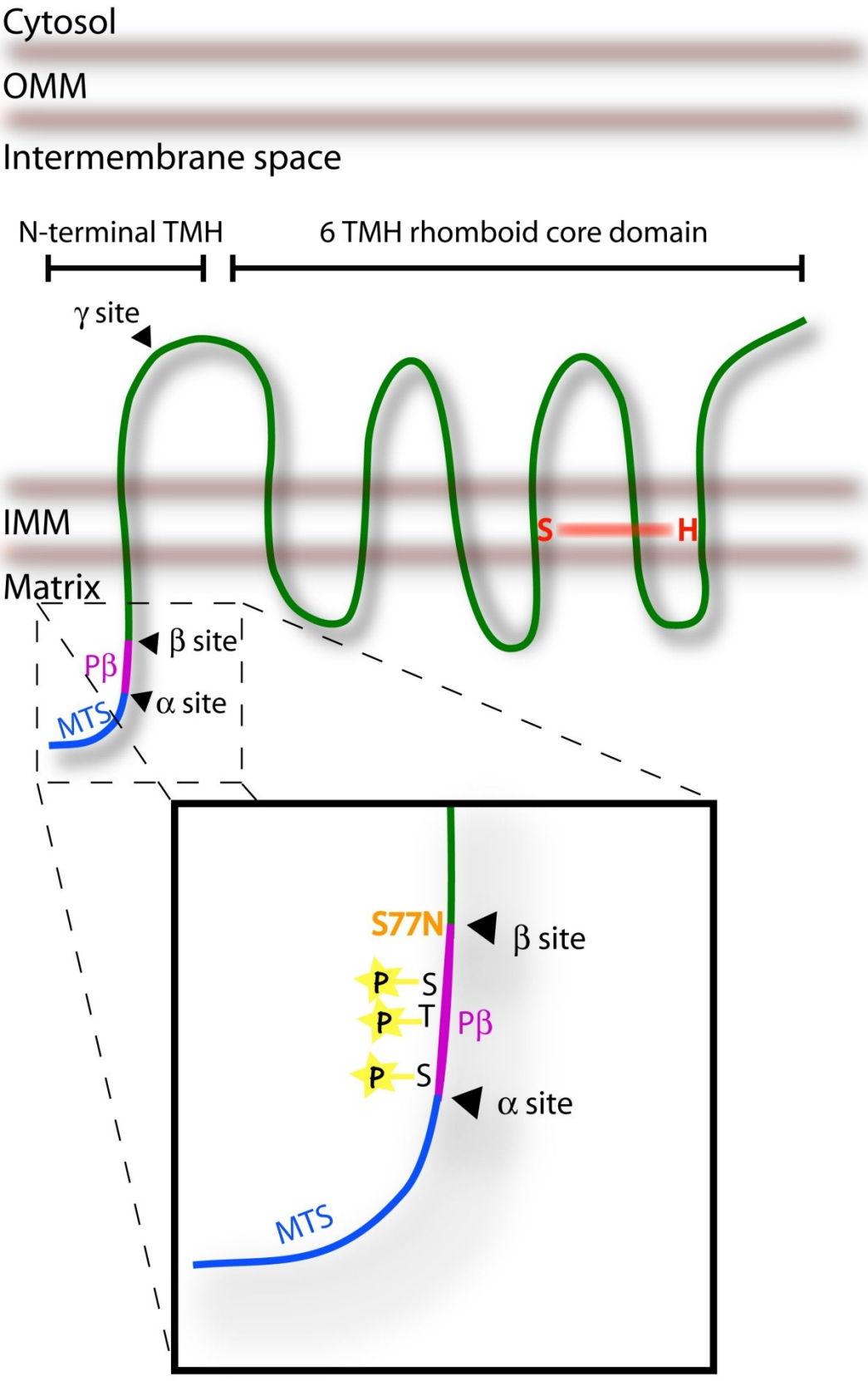
Cytosol
OMM
Intermembrane space
N-terminal TMH
6 TMH rhomboid core domain
γ site
IMM
S
H
Matrix
β site
Pβ
α site
MTS
S77N
β site
P
S
P
T
Pβ
P
S
α site
MTS

The rhomboid-like family of serine I-CliPs is divided into three subfamilies: 1) true active rhomboids, encompassing the PARL subfamily and the secretase subfamily; 2) novel inactive rhomboids called iRhoms; and 3) other inactive rhomboid-like proteins (Lemberg and Freeman, 2007) (figure 1.2). The mitochondrial PARL rhomboid-like proteases follow the 1 + 6 TMH arrangement and are missing the arginine (R) in loop 1 and a glutamate (E) between TMH2 and TMH3. In addition, the predicted catalytic serine and histidine which make up the serine protease catalytic dyad are shifted over by one TMH to TMH5 and TMH7, respectively. The active sites of PARL are believed to be located towards the matrix side of the mitochondrial membrane and the cleaved fragment of its substrate is released into the intermembrane space.

Figure 1.2. Summary of rhomboid protease classification. Three intramembrane protease classes exist. The rhomboid-like family of serine I-CliPs is divided into three subfamilies. The PARL subfamily is found within the rhomboids (green). Adapted from (Lemberg and Freeman, 2007; Freeman, 2008).

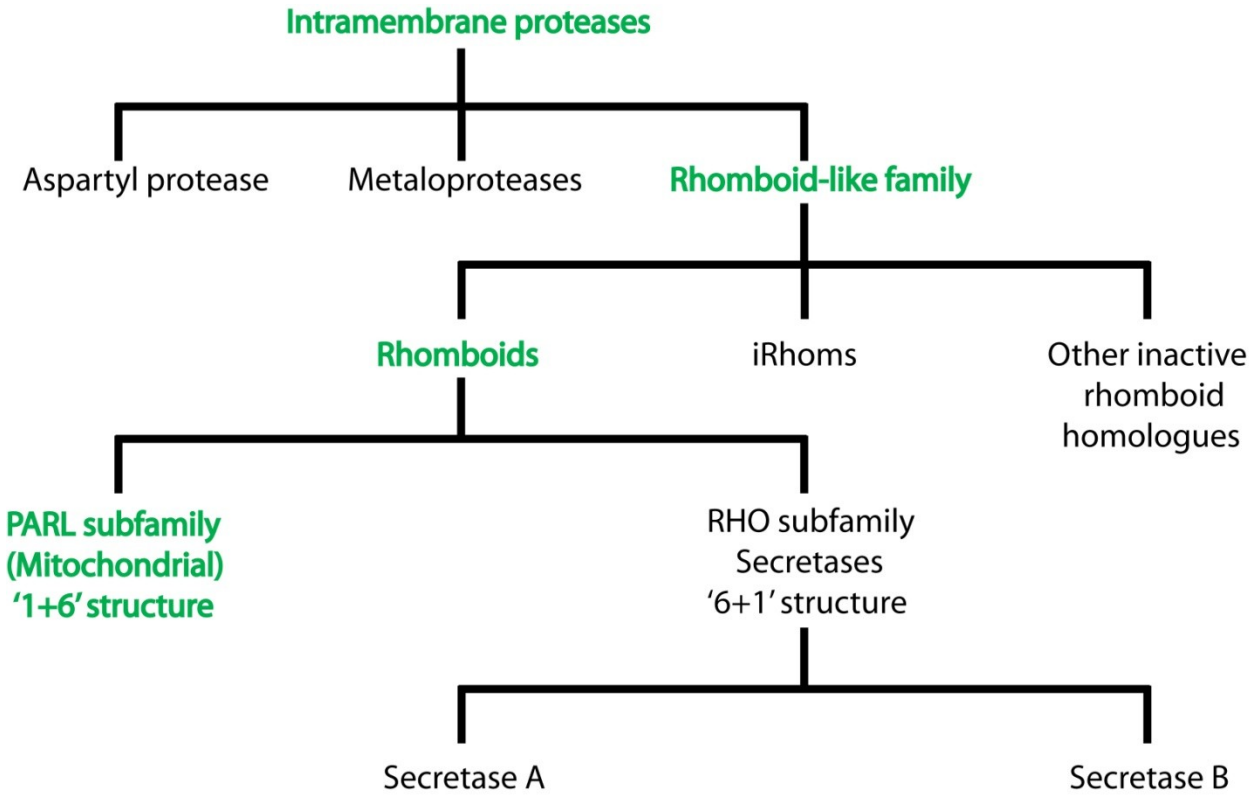
Intramembrane proteases
Aspartyl protease
Metaloproteases
Rhomboid-like family
Rhomboids
iRhoms
Other inactive rhomboid homologues
PARL subfamily (Mitochondrial) '1+6' structure
RHO subfamily Secretases '6+1' structure
Secretase A
Secretase B

The active site of rhomboids is located within the plane of the membrane at a depth of approximately 1/3rd of the way into the membrane on the matrix side (Freeman, 2004). A problem that all intramembrane proteases encounter is the hydrophobic environment of the lipid bilayer which is not readily conducive to hydrolysis reactions since they require water to break peptide bonds. One possible solution to this problem may be explained by the amphipathic properties of the TMHs. It is possible that small aqueous pockets are produced around the rhomboid active site when the TMHs are packed into the membrane, thus exposing a cavity that is accessible to the aqueous environment outside the lipid bilayer (Freeman, 2004, 2008). Another proposed solution is that of alternative topogenesis (Herlan et al., 2004). Mgm1 and Ccp1 are two substrates of yeast rhomboid-1 and they are single-pass transmembrane proteins. These substrates are not cleaved in their transmembrane domain (TMD), but instead at an alternative hydrophobic domain which is located outside of the membrane. During cleavage, the topology of the TMD is shifted such that the alternative hydrophobic domain is pulled into the plane of the hydrophilic region of the polar headgroups of the lipid bilayer while the primary TMD is pulled out of the membrane and into the mitochondrial matrix. Finally, water molecules do have some, albeit limited, access to lipid bilayers, thus these could be sufficient for proteolysis.

A second mystery is how the enzyme accesses the peptide backbone to be proteolysed. The alpha-helix of the substrate likely unfolds exposing the peptide backbone; however, the unfolding of TMHs in the membrane is unfavourable since the polar peptide bond would be exposed to the lipid bilayer (Hill and Pellegrini, 2010). If indeed water can gain access to TMHs, then the substrate preference for Gly/Val/Ile residues may facilitate the enzyme's access to the peptide backbone.

1.5 PARL, THE MAMMALIAN MITOCHONDRIAL RHOMBOID

PARL, short for Presenilin-Associated Rhomboid-Like, was originally identified in a yeast-two hybrid screen as an interacting partner of Presenilin-2 (Pellegrini et al., 2001). Many years after its discovery, it is now known that this interaction was an *in vitro* artifact and that PARL does not interact with presenilin *in vivo*. The PARL subfamily is composed strictly of mitochondrial localized members. The mammalian *PARL* gene codes for a 379 amino acid PARL protease, which has been shown to reside exclusively in the inner mitochondrial membrane, with its N-terminus facing the matrix and its C-terminus exposed to the IMS (Jeyaraju et al., 2006) . Not much is known about PARL substrate specificity and cleavage site determination, since very few substrates have been found and cleavage sites are not well identified (Hill and Pellegrini, 2010). One well-studied substrate is the yeast Mgm1, where replacing the GlyGlyMet motif in the TMH with ValValLeu which are larger amino acids blocks Pcp1/Rbd1 from cleaving Mgm1 (Herlan et al., 2003). This suggests that the GlyGly motif may also be central in PARL rhomboids, as it is in RHO rhomboids, for substrate recognition. However, the TMH of Ccp1, another substrate of Pcp1/Rbd1, does not share structural similarity to that of Mgm1. Thus, the mitochondrial rhomboids and RHO family members may not recognize the same motifs in the TMH of all their substrates.

1.6 GENETIC VARIANTS OF PARL IN DISEASE

A number of studies have been conducted which implicate mutations in PARL and PARL regulation and expression with diabetes, obesity, glaucoma, Leber hereditary optic neuropathy (LHON), metabolic syndromes and Parkinson's disease. The locations of these mutations along

with the cohort or animal model screened and the implications of the mutations are summarized in Table 1.1.

Table 1.1. Summary of PARL variants presented in chronological order of publication.

Mutation (SNP[1] identifier)	Location	Significance	Citation
Quantitative trait locus	Chr. 3	• Cohort screened: Caucasian families of predominantly Northern European ancestry residing in the US • Existence of a quantitative trait locus on chromosome 3 (3q27) which influences phenotypes fundamental to abdominal obesity-metabolic syndrome	(Kissebah et al., 2000)
Leu262Val	Exon 7	• Animal model screened: skeletal muscle[2] of diabetic, obese *Psammomys obesus* (Isreali sand rats) • PARL gene expression reduced in skeletal muscle • PARL associated with insulin resistance and type II diabetes	(Walder et al., 2005)
		• Cohort screened: US Mexican Americans of Northern European ancestry • Association found in diabetics with no family history, but not in people with a family history of diabetes • SNP associated with age-dependant insulin resistance resulting in high plasma insulin concentration • PARL expression in skeletal muscle is associated with mitochondrial oxidative capacity • Exercise training alleviates symptoms of type II diabetes by reducing glucose and insulin levels in plasma and increasing PARL expression in skeletal muscle in both rats and human	
Leu262Val	Exon 7	• Cohort screened: UK population • No association between SNP and insulin resistance, nor obesity, nor age	(Fawcett et al., 2006)
Leu262Val	Exon 7	• Cohort screened: Two Western Australian populations • No association between SNP and insulin resistance, nor glucose, nor obesity, nor metabolic syndrome	(Powell et al., 2008)
N/A[3]	N/A	• Animal model screened: rats with induced insulin resistance • PARL expression reduced in skeletal muscle • Reduced mitochondrial DNA content	(Tang et al., 2009)

		• Reduced expression of mitochondrial complex I and II expression and enzyme activity indicative of reduced mitochondrial viability	
Leu262Val	Exon 7	• Cohort screened: Irish Caucasian population with type II diabetes • No association between SNP and insulin resistance • SNP in people with type II diabetes may indicate earlier onset of disease and increased susceptibility to nephropathy and cardiovascular complications or may have more rapid onset of signs and symptoms, thus earlier diagnosis	(Hatunic et al., 2009)
C→T (rs1402000) G→A (rs3749446)	Intron 2 Intron 1	• Cohort screened: Thai and/or Chinese population with most common mitochondrial mutation (G11778A) in Leber hereditary optic neuropathy (LHON) • Strongly significant association between LHON and two intronic SNPs in PARL	(Phasukkijwatana et al., 2010)
G→A (rs12631031)	Intron 4	• Nominally significant association between LHON and this SNP	
C→A (rs11918588) G→T (rs6782942)	Intron 1 Intron 1	• Results in loss of predicted binding site for a neuronal-specific RNA binding protein, Nova-1, involved in alternative RNA splicing • RNA splicing abnormalities caused by Nova-1 are implicated in several neurological diseases	
G→A (rs3749446)	Intron 1	• No predicted functional effect	
C→T (rs1402000) A→G (rs12634358)	Intron 2 Intron 4	• Alter the TTT sequence known to act as a *cis*-acting element for neuronal-specific splicing of human APP (Shibata et al., 1996)	
G→C (rs3792588)	5' end in putative promoter region at position -197	• Association with LHON • Only 6 bp away from T-191C SNP (refer to (Curran et al., 2010) below)	
T→C (rs3792589)	5' end in putative promoter region at position -191	• Cohort screened: healthy, obese and/or diabetic Caucasians • T vs. C allele preferentially binds nuclear factors • -191C allele ablates the core sequence for Sp1 • Influences mitochondria content and integrity	(Curran et al., 2010)

Ser77Asp	β-cleavage site	• Cohort screened: Parkinson's disease (PD) patients • SNP at the β-cleavage site necessary for autocatalytic processing of PARL's N-terminus region • SNP found in two late-onset Parkinson's disease patients • Average age of onset is 57.7 years of age • One patient with and one without familial PD • Frequency of S77N variant in Parkinson's disease population is 1 in 1291	(Shi et al., 2011)
Ser77Asp	β-cleavage site	• Cohort screened: Early-onset Parkinson's disease patients • Sequenced exons 2, 8 and 9 of PARL where amino acids needed for PARL's function and activity are located • No disease-causing SNPs detected, thus the S77N variant is not a frequent cause of autosomal recessive early-onset Parkinson's disease	(Heinitz et al., 2011)

[1]Single nucleotide polymorphism.

[2]Skeletal muscle is the major site of peripheral insulin resistance.

[3]Not applicable.

1.7 PARL CLEAVAGE

PARL belongs to a subfamily of rhomboid proteins that functions as an intramembrane serine protease (McQuibban et al., 2003). Vertebrate specific phosphorylation and cleavage sites that are important for mitochondrial morphology have been located (Table 1.2) (Sik et al., 2004). In mammalian vertebrates, the phosphorylation state of this site dictates whether or not PARL will be cleaved and subsequently mediates mitochondrial fragmentation. Ultimately, induction of mitochondrial fragmentation triggers apoptosis.

Table 1.2. Summary of known PARL cleavage sites.

Cleavage site	Location	Significance
α site	G52-F53	• Constitutive • Removes MTS
β site	S77-A78	• Depends on I-CliP activity of PARL supplied *in trans*; • Depends on the phosphorylation state of S65, T69 and S70, where these sites must be dephosphorylated in order for this cleavage to occur; • Developmentally regulated; liberates Pβ nucleus-targeted peptide
γ site	Exact location unknown; located between amino acids 121-167 of mammalian PARL within the first loop connecting the first TMH to the 6 TMH rhomboid core	• Requires $_{155}$INKWW$_{159}$, W158 and W159 • Destabilizes PARL and may serve to negatively regulate PARL activity in mitochondria in a tissue-specific manner

The N-terminal domain of human PARL harbors two consecutive cleavage sites (figure 1.1 and figure 1.2). Overall, the N-terminal domain is conserved among vertebrates, particularly between mammals (Sik et al., 2004). Mammalian PARL is constitutively processed between position Gly52 and Phe53 which is the proximal α-cleavage site that removes PARL's mitochondrial targeting signal. Distal to the α-cleavage site is the β-cleavage site between residues Ser77 and

Ala78. It is this serine at the β-cleavage site where a missense mutation was found in Parkinson's disease (PD) patients (serine to an asparagine at codon 77 (Ser77Asn)) (Shi et al., 2011). β-cleavage of PARL occurs through a mechanism of proteolysis that requires an active form of PARL supplied *in trans* and is thus thought to be executed either by PARL itself, supplied *in trans*, or by an unidentified PARLase (Sik et al., 2004). However, typical rhomboid-mediated intramembrane proteolysis occurs within a hydrophobic environment. Thus, since the β-cleavage site of PARL is not embedded within a hydrophobic transmembrane domain, it is unlikely that PARL cleaves itself (Pellegrini and Scorrano, 2007).

In HEK 293 cells transfected with a PARL-Flag construct and subsequently immunoprecipitated with antibodies against the N-terminal of PARL or the C-terminal Flag, two bands are detected by western blotting: 42 kDa corresponding to full-length PARL and 37 kDa corresponding to α-cleaved PARL with the mitochondrial targeting sequence (MTS) cut off (Sik et al., 2004). The observation that full-length PARL is present in low amounts suggests that PARL is efficiently targeted to the mitochondria where it is subsequently α-cleaved. A third band of 33.5 kDa is detected by immunoprecipitation using the anti-Flag antibody and is generated by cleavage at the β site which is downstream of the MTS. Mutating the amino acids which are predicted to form the catalytic site of Rhomboid proteases, abolishes β-cleavage, but not α-cleavage. The N2a murine neuroblastoma cell line yields the same cleavage patterns seen in HEK cells; however, COS-1 and HeLa cell lines produced only α-cleaved PARL. This suggests that α-cleavage occurs constitutively, but β-cleavage requires PARL's I-CliP activity and could be cell-type dependent.

Sik and colleagues mapped the amino acid location of these two cleavage sites, by adding an hemagglutinin (HA) tag to the PARL-Flag construct at the N-terminal upstream of the first TMH (Sik et al., 2004). Since β-cleaved PARL is detected by both the HA and Flag antibodies, but not

the N-terminal antibody, the location of the β-cleavage site is narrowed down to a region between the N-terminal epitope and the HA tag. The cleavage sites were precisely mapped using N-terminal sequencing by Edman degradation. This places the α site between residues Gly52 and Phe53 which are conserved in all animal orthologs of PARL. However, the β site found between residues Ser77 and Ala78 is only conserved among mammals.

Mutating two residues on either side of the β-cleavage site, eliminates the 33.5 kDa band corresponding to β-cleaved PARL. Co-transfecting HEK 293 cells with a catalytically inactive PARL S277G mutant along with WT PARL results in PARL β-cleavage, but co-transfecting two catalytically inactive PARL mutants, S277G and H335G, does not. This suggests that PARL cleavage at the β site is dependent on PARL's activity supplied *in trans*. β-cleavage could thus be executed either by a protease (a PARLase) which is activated by PARL or by PARL itself supplied *in trans*.

β-cleavage of PARL releases a Pβ peptide of 25 amino acids in mammalian PARL that may mediate mitochondria-to-nucleus signaling which appears to be under developmental control and might be linked to neuronal development (Sik et al., 2004) (figure 1.3). The amino acid sequence of this Pβ peptide is vertebrate-specific and contains a nuclear localization signal (NLS). This nuclear localizing signal consists of three closely spaced pairs of positively charged amino acids located within amino acids 54-65. The first two pairs are conserved in vertebrates, while the third is specific to mammals. Tagging the region between the α and β sites (amino acids 53 – 77) with GFP and transfecting this construct in HEK 293 cells reveals a nuclear localisation of Pβ by fluorescent microscopy. In primary cultures of immature rat cortical neurons, the Pβ peptide is found primarily in the nucleus, where as in differentiated neurons it is predominantly located in mitochondria (figure 1.3). Thus, in the early stages of neuronal differentiation, PARL is α- and β-

cleaved generating a Pβ peptide which is shuttled to the nucleus. After differentiation, the generation of the Pβ is halted or considerably reduced, and is detected in the mitochondria but no longer in the nucleus. This suggests that β-cleavage of PARL may be under developmental control and the nuclear targeting of Pβ may play a function in neuronal development.

Figure 1.3. Proteolytic processing of mammalian PARL. Full-length PARL contains three cleavage sites described in Table 1.2: α, β and γ. Constitutive α-cleavage removes the mitochondrial targeting sequence (MTS; blue) and is followed by β-cleavage only if PARL undergoes dephosphorylation at three residues: S65, T69 and S70 (yellow stars) within the Pβ domain (purple). β-cleavage liberates the approximately 25 amino acid long Pβ peptide which may translocate to the nucleus and be involved in mitochondrial-to-nucleus signalling where it may activate nuclear responses linked to mitochondrial biogenesis. The translocation pathway and bottom panel: In embryonic kidney cells (HEK cells) Pβ is located in both the mitochondria and the nucleus. In primary cultures of immature rat cortical neurons (undifferentiated neuronal state), PARL is cleaved to liberate the Pβ peptide which is targeted to the nucleus (grey) by a nuclear localizing signal (NLS) located near the N-terminal of the Pβ peptide. Once differentiation is complete, as in differentiated neuronal cells, β-cleavage decreases or stops thus Pβ is detected in mitochondria. The destabilization pathway: γ-cleavage destabilizes PARL and may function to negatively regulate PARL activity in mitochondria. Images not drawn to scale.

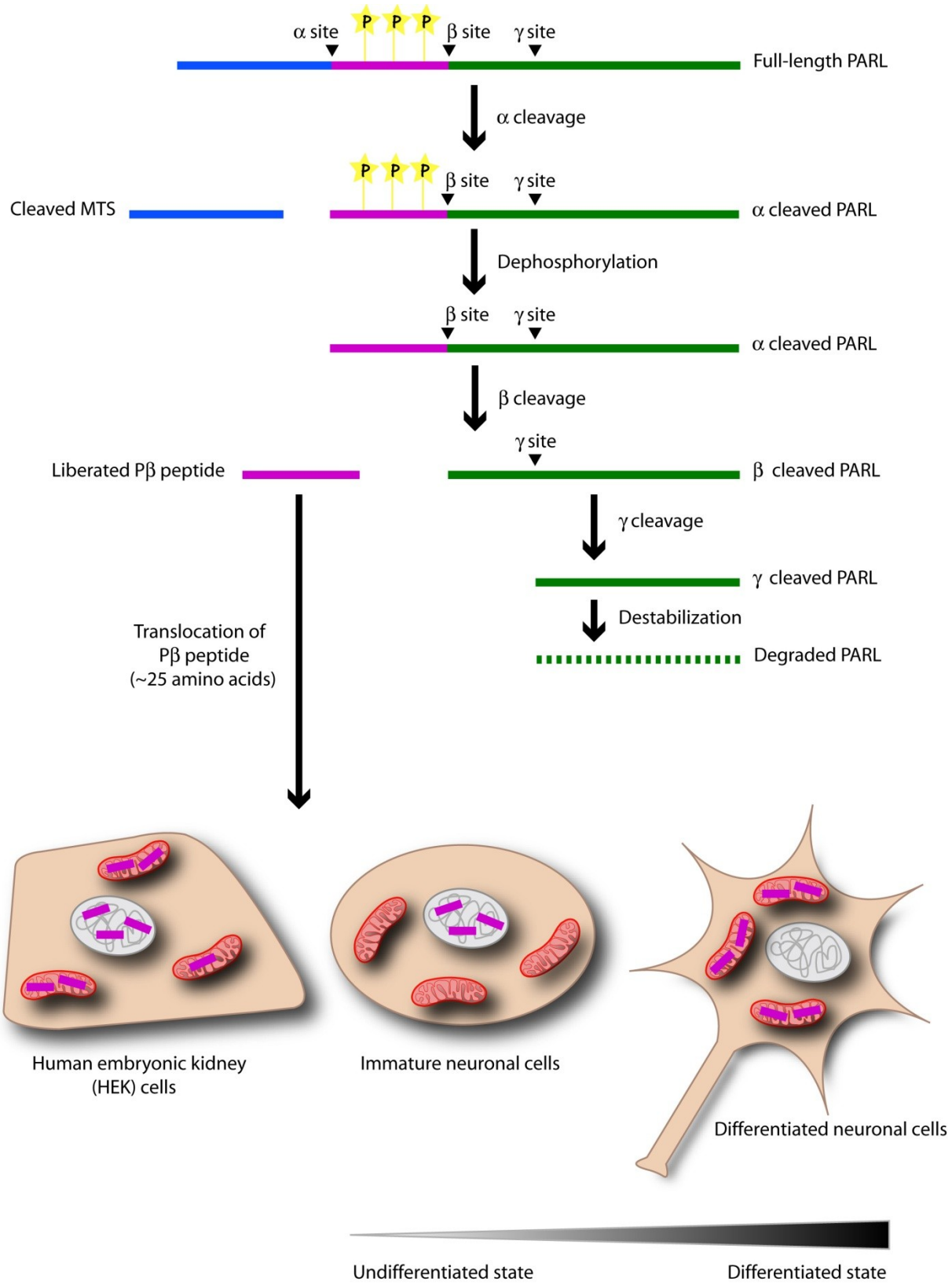
α site
P P P
β site
γ site
Full-length PARL
α cleavage
Cleaved MTS
α cleaved PARL
Dephosphorylation
β cleavage
Liberated Pβ peptide
β cleaved PARL
γ cleavage
γ cleaved PARL
Destabilization
Degraded PARL
Translocation of
Pβ peptide
(~25 amino acids)
Human embryonic kidney
(HEK) cells
Immature neuronal cells
Differentiated neuronal cells
Undifferentiated state
Differentiated state

PARL α- and β-cleavage is also observed *in vivo* in mitochondria lysates from human placenta, indicating that is it not an *in vitro* artifact (Jeyaraju et al., 2006). Similar to PARL transfected in HEK 293 cells, PARL originating from human placental tissue is phosphorylated at three sites Ser65, Thr69 and Ser70, located between the α- and β-cleavage sites and within the Pβ domain (figure 1.2 and figure 1.3). Substituting an Ala at each of these residues abolishes phosphorylation indicating that this post-translational event is specific to these three residues. In addition, most of the α-cleaved form of PARL exists in a triple-phosphorylated state.

Moreover, Pellegrini and colleagues who previously believed that the N-terminus of PARL faced the cytosol (from immunogold-labeling of electron microscopy (EM) sections), placing PARL in the outer mitochondrial membrane (Sik et al., 2004), now correct their previous observations and show by means of a permeability assay that PARL's C-terminus faces the intermembrane space, while the N-terminus, including the phosphorylated Pβ domain, is located in the mitochondrial matrix, placing PARL in the inner mitochondrial membrane (Jeyaraju et al., 2006). Phosphorylation at Ser65, Thr69 and Ser70 impairs β-cleavage, while deletion of the $_{84}$EETV$_{87}$ segment just after the Pβ domain promotes β-cleavage. In addition, a non-phosphorylated, β-cleaved form of PARL transiently expressed in HeLa cells results in mitochondrial fragmentation. It appears that PARL must be β-cleaved in order to initiate mitochondrial fragmentation. It is currently unknown what role the Pβ peptide plays. One hypothesis is that free Pβ could initiate mitochondrial fragmentation. However, mutating the Pβ domain by deleting amino acids 56-59 or 58-61, does not impair β-cleavage nor does it impair mitochondrial fragmentation. Overall, phosphorylation of residues Ser65, Thr69, and Ser70 within the Pβ domain inhibits PARL β-cleavage, and ultimately blocks mitochondria fragmentation, but the function of the Pβ peptide appears to be dispensable for initiation of PARL-induced

mitochondrial fragmentation (Jeyaraju et al., 2006). The identification of the PARL kinase, phosphatase, and protease may help elucidate the mechanism by which PARL-induced fragmentation occurs.

Recently, the Pellegrini group mapped a third cleavage site, termed γ-cleavage (Jeyaraju et al., 2011). This site is likely located within the first loop (amino acids 121-167 of mammalian PARL) which connects the first TMH to the 6 TMHs constituting the catalytic rhomboid domain of PARL. γ-cleavage is dependent on $_{155}$INKWW$_{159}$, since deleting this sequence blocks the γ-cleavage production. In addition, the W158G and W159G mutations reduce the amount γ-cleavage product by half, without affecting the production of α-cleaved PARL. Since γ-cleavage disrupts PARL's '1+6' structure, it is suggested that in mammalian systems, γ-cleavage destabilizes PARL and may serve to negatively regulate PARL activity in mitochondria (Jeyaraju et al., 2006; Jeyaraju et al., 2011). The cleavage pattern of PARL appears to be tissue-specific; for example, in rat muscle most of PARL is present in the α-cleaved form, in rat kidney most of PARL is found in the β-cleaved form, and in both the spleen and kidney where most of PARL is α-cleaved, it is also γ-cleaved (Jeyaraju et al., 2011). γ-cleavage is also observed in HeLa and HEK cells transfected with PARL.

γ-cleavage is believed to be specific to the tissues of the spleen and kidney in rats (Jeyaraju et al., 2011) and perhaps this tissue specific negative regulation of PARL through γ-cleavage may explain how PARL plays a cell specific role in dopamine (DA) neurons with respect to Parkinson's disease. Eliminating β-cleaved PARL in HeLa cells by either mutating (Leu79Glu) or deleting (Δ75-79) the β-cleavage site results in minimal generation of γ-cleaved PARL (Jeyaraju et al., 2011). Furthermore, blocking β-cleavage through the use of serine protease inhibitors, simultaneously blocks γ-cleavage. Thus, in order for γ-cleavage to occur efficiently,

β-cleavage must take place. Moreover, expression of γ-cleavage-impaired PARL in HeLa cells induces mitochondrial fragmentation (as does wild-type, but not a β-cleavage mutant PARL) suggesting that γ-cleavage is not required for β-cleavage-induced mitochondrial fragmentation.

1.8 PARL MODELS

A few models investigating PARL function exist. Here, we will present the salient features of each model and summarize the significant contributions of each while also comparing the phenotypes observed.

1.8.1 YEAST (*SACCHAROMYCES CEREVISIAE*)

The yeast orthologue of the *PARL* gene is referred to as *RBD1* and codes for the Rbd1p rhomboid protein which is localized to inner mitochondrial membrane (IMM) (McQuibban et al., 2003). Two substrates of the Rbd1p are known: cytochrome c peroxidase (Ccp1) and mitochondrial genome maintenance protein (Mgm1), the orthologue of *OPA1*, which is a dynamin-like GTPase which plays a role in mitochondrial membrane fusion (Esser et al., 2002; Herlan et al., 2003). *RBD1* deletion results in a reduced rate of cell growth, cellular respiration defects and mitochondrial disruption. Compared to the tubular structure of mitochondria around the cell cortex in wild-type yeast, the mitochondria of Rbd1 mutants are seen as small fragments which aggregate throughout the cell. These mitochondrial defects in Rbd1p mutant yeast are believed to be a consequence of lack of Mgm1p proteolytic cleavage by Rbd1p, since Mgm1p requires Rbd1p for its activation and for its function in regulating mitochondrial membrane fusion. Not surprisingly, Mgm1p mutants share the same phenotypes as Rbd1p mutants since mitochondrial membrane remodelling is regulated by cleavage of Mgm1p. The fact that human PARL rescues the abnormalities seen in yeast Rbd1p mutants, suggests that PARL function is

likely evolutionarily conserved in mammals. One disadvantage of the yeast model is the inability to study PARL function as it pertains to different organ systems and behaviour outputs at the whole animal level.

1.8.2 FLY (*DROSOPHILA MELANOGASTER*)

The fly orthologue of the PARL gene is known as *rhomboid-7* and codes for the Rhomboid-7 protein (McQuibban et al., 2006). Transfected Rhomboid-7 localizes to mitochondria in both COS-7 mammalian cells (African green monkey kidney fibroblast-like cell line) and fly S2 cells (*Drosophila melanogaster* embryonic epithelial-like cell line). Using RNA_i, to inhibit *rhomboid-7* gene expression in S2 cells, causes mitochondrial fragmentation. Over expression of mouse PARL or mouse OPA1 in COS-7 cells induces mitochondrial aggregation due to excess fusion. However, overexpression of catalytically mutant mouse PARL did not have this effect. Rhomboid-7 overexpression in S2 cells, also results in aggregation of the mitochondrial network. As in yeast (McQuibban et al., 2003), disruption of *opa1-like*, the fly orthologue of OPA1 also leads to fragmentation of the mitochondrial network of COS-7 cells (McQuibban et al., 2006). This places Rhomboid-7 and Opa1-like in the same pathway required for maintaining mitochondrial membrane dynamics in both the yeast and fly.

Drosophila *rhomboid-7* null mutants with the 5' end of the gene deleted lack the transcriptional start site and the first 18 codons disrupting the mitochondrial targeting sequence. Ninety percent of these flies die before building their pupa case at embryonic and larval stages. Surviving flies develop into adults; however, 10% of survivors die during eclosion because they get stuck while crawling out of their pupal case. Despite appearing morphologically normal, all survivors die within three days. All males are sterile. Homozygous females are fertile, but their progeny have

the same ailments as their parents. This indicates that the fly does not require Rhomboid-7 for its development, but that its absence reduces lifespan.

The testes of male mutants do not contain mature sperm and the seminal vesicles are small and empty. A critical mitochondrial fusion process occurs during sperm maturation in *Drosophila*. This involves the aggregation of all mitochondria adjacent to the nucleus which subsequently undergo immense membrane fusion to form a structure called the nebenkern. This mitochondrial derivative is made of two large entangled mitochondria which unfold and elongate to fill the flagellum of the sperm and provide energy for motility. The nebenkerns of Rhomboid-7 mutant flies are irregularly shaped since mitochondria do aggregate but fail to fuse. Opa1-like mutant flies exhibit the same early larval death and defective nebenkerns. Thus, Rhomboid-7 and Opa1-like play an essential role in mitochondrial membrane fusion, particularly during the formation of the nebenkern during spermatogenesis.

Adult Rhomboid-7 mutants have an obvious defect in the position of their wings which droop down to the side of their abdomen as opposed to being tucked and positioned on top of the abdomen. This wing defect results in flight muscle abnormalities. Numerous small mitochondria with reduced IMM cristae are located in the space between myofibrils. Throughout the first few days of life, fusion of several small mitochondria into larger ones is crucial for the development of normal muscle in flies. Thus, there is a requirement for Rhomboid-7 in tissues, such as flight muscle and spermatid development, which rely on unusually high levels of mitochondrial fusion.

Compared to the 60-day lifespan of wild-type flies, *rhomboid*-7 mutant flies live only three days and exhibit motor defects which render flight impossible and walking extremely difficult due to erratic twitching in the legs and head. Neurological dysfunction is also observed. Disruption of

Rhomboid-7 prevents normal synaptic transmission of photoreceptors, likely due to loss of mitochondrial function at the synapse.

Overall, since *rhomboid-7* mutants are not fully lethal as in the mitofusin MFN1 and MFN2 mouse model (Chen et al., 2003), it seems that Rhomboid-7 is not needed for all forms of mitochondrial dynamics. Rhomboid-7 is likely needed in regions with high energy demands. As in yeast, the loss of either fly Opa1-like or Rhomboid-7 leads to a similar phenotype, suggesting that they function in the same pathway. However, again as seen in yeast, *opa1-like* mutants exhibit a more severe phenotype than *rhomboid-7* mutants, suggesting that Opa1-like may play other roles which are independent from Rhomboid-7. An advantage of the fly model over that of yeast is the ability to disrupt mitochondrial function and observe more complex phenotypes than those seen is yeast. It is presumed that the loss of full mitochondrial function at the synapse is responsible for the defects in synaptic transmission. In turn, the dramatic effect on lifespan may be related to abnormal neuronal function in regions which rely heavily on the energy supplied by mitochondria.

1.8.3 MOUSE (*MUS MUSCULUS*)

Parl knockout (*Parl*$^{-/-}$) mice were generated by homologous recombination (Cipolat et al., 2006). Mice with floxed exon two of *Parl* were crossed with mice expressing Cre under the control of the ubiquitous PGK promoter. This results in a reading frame shift which introduces a premature stop codon and produces a non-functional protein in all cells.

Parl$^{-/-}$ mice develop normally up to the fourth postnatal week, after which, they experience severe growth retardation. These mice have lost muscle mass in the erector spinae, abdominal muscles and diaphragm. Since these muscles support proper posture and breathing, not

surprisingly, they have postural defects with hunched backs. All *Parl*$^{-/-}$ mice have a reduced lifespan and die between eight and twelve weeks after birth, likely due to problems with moving, breathing and general cachexia (loss of body mass that cannot be reversed nutritionally). Individual muscle fibers have a reduced diameter, but spinal motor neurons are normal and the peripheral nerve supply seems normal, suggesting that the premature death is muscle associated and not due to problems with muscle innervation. By eight weeks, the thymus and spleen undergo substantial atrophy and weigh only 10% of their expected mass, severely reducing the number of lymphocytes they produce. Females have underdeveloped uteri with normal ovaries, while males have cryptorchidism and their testis, epidydimis and accessory glands are reduced in size. Mild neurodegeneration is observed in the thalamus and striatum of *Parl*$^{-/-}$ mice. Delayed startle response to an auditory stimulus is present and could be due to defects in neural conduction, striatal dysfunction and or an increase in reaction time. Overall, the severe atrophy in several tissues is an indicator of increased apoptosis in *Parl* knockout mice.

Mitochondrial respiration does not require *Parl*, since no change in ATP levels, respiratory rates, nor mitochondrial membrane potential, was observed in cells and tissues from *Parl*$^{-/-}$ mice. Thus, the muscular atrophy and multisystemic failure may not be due to mitochondrial dysfunction. However, muscle fibers undergoing apoptosis are rapidly cleared away and become difficult to detect but in the thymus and spleen apoptosis determines cell fate and content. A large number of apoptotic T and B lymphocytes are present. Therefore, the large loss in cell population of these organs can be easily determined by the size of the organs themselves. These findings in combination with data from caspase-3 positive brain sections of the thalamus and striatum indicate that the increase in vulnerability to apoptosis may be responsible for the multisystemic failure seen in *Parl* knockout mice.

Cells derived from *Parl*$^{-/-}$ mice are sensitive to intrinsic apoptotic stimuli (e.g. BID), but not to extrinsic apoptotic stimuli (e.g. TNF-α). Wild-type PARL, but not catalytically inactive Parl (His335Gly), rescues the observed cell death. In the absence of PARL, H_2O_2 exposure and active BID cause rapid mobilization of cytochrome c from the inner mitochondrial membrane to the intermembrane space (IMS). Therefore, PARL plays an important role in remodeling the mitochondrial cristae and regulating the release of cytochrome c during apoptosis.

In mammals, OPA1 needs MFN1 in order to promote mitochondrial fusion, but does mammalian PARL control OPA1? Visually tagging mitochondria in *Parl*$^{-/-}$cells with mitochondrially targeted yellow fluorescent protein (mtYFP), demonstrates that the mitochondria appear morphologically identical to those in wild type cells. In addition, fusion rates were comparable between wild type and *Parl*$^{-/-}$ cells, as were the levels of OPA1. Surprisingly, contrary to findings in yeast, where Rbd1p maintains mitochondrial shape and is involved in apoptosis through a common pathway with MgM1p (McQuibban et al., 2003), mitochondrial fusion and shape are not affected by the absence of PARL in the mouse even in muscle tissue which is severely affected in *Parl*$^{-/-}$ mice. Thus, it appears that PARL does not function in regulating mitochondrial dynamics with OPA1 in *Parl*$^{-/-}$ mice (Cipolat et al., 2006).

Despite the fact that PARL does not work with OPA1 to regulate mitochondrial fusion, PARL and OPA1 do act in a common anti-apoptotic pathway. This is possible because OPA1 plays two potentially independent functions: 1) regulating mitochondrial fusion; and 2) functioning as an anti-apoptotic protein. Cell death induced by etoposide, staurosporine or H_2O_2, can be rescued by OPA1 in wild-type but not in *Parl*$^{-/-}$ cells, likely because PARL is needed for processing OPA1 into its soluble form which plugs the cristae junction and prevents the release of cytochrome c to inhibit apoptosis (Frezza et al., 2006; Gottlieb, 2006). Upon application of an intrinsic stimulus,

cytochrome c is released and mitochondrial membrane depolarization occurs, none of which can be rescued by OPA1 in *Parl*$^{-/-}$ cells, because without PARL, OPA1 cannot block apoptosis on its own (Cipolat et al., 2006). This observation places PARL and OPA1 in the same genetic pathway. Blocking OPA1 using shRNA$_i$ in wild type or *Parl*$^{-/-}$ cells, renders both more susceptible to apoptosis and cannot be rescued by PARL. In addition, overexpression of PARL in OPA1 silenced *Parl*$^{-/-}$ cells does not protect against apoptosis.

It has also been shown that both PARL and OPA1 are located in the IMM where they interact at the protein level. Co-immunoprecipitation and yeast two-hybrid experiments show that PARL and OPA1 interact. A small soluble form of OPA1 is present in the IMS in wild type cells, but was reduced in mitochondria from *Parl*$^{-/-}$ cells. This does not rule out the possibilities that PARL could be indirectly cleaving OPA1 or that another protease also cleaves OPA1, since some lower molecular weight OPA1 was found in the IMS in the absence of PARL. In addition, the cleavage of OPA1 could be regulated by its compartmentalization within mitochondria. Overall, PARL's function depends on its relationship with OPA1 which plays two independent roles: 1) its soluble form carries anti-apoptotic activity which prevents cytochrome c release and protects against cell death; and 2) its pro-fusion ability which depends on MFN1 promotes mitochondrial membrane fusion.

In summary, PARL functions as an anti-apoptotic protein. The mechanism which accounts for increased apoptosis in *Parl*$^{-/-}$ mice is based on the observation that cytochrome c is released faster from the mitochondrial cristae. This release hinges on a critical interaction with OPA1 and the generation of a soluble form of OPA1 located in the IMS. Under normal conditions, OPA1 oligomers composed of membrane-bound and soluble IMS OPA1 are subsequently formed to increase the tightness of the cristae junctions and prevent the escape of cytochrome c.

Following PARL deficiency, all three models discussed above suffer from growth arrest or premature death reinforcing that PARL's role in apoptosis is conserved throughout evolution (McQuibban et al., 2003). In addition PARL and OPA1 have been shown to act in the same pathway in all three models. A role was found for PARL in mitochondrial fusion/fission and mitochondrial respiration in both the yeast and fly models, however no correlation was found in the mouse model. The mouse model did help identify OPA1 as a substrate of PARL, suggesting that its proteolytic activity, but not its function in mitochondrial morphology if maintained in evolution.

1.9 ZEBRAFISH AS A MODEL FOR DISEASE

Danio rerio, commonly referred to as zebrafish, has emerged as an excellent model organism for the study of vertebrate development and disease in humans (Driever et al., 1994; Driever et al., 1996; Haffter et al., 1996; Hukriede et al., 1999; Dooley and Zon, 2000; Penberthy et al., 2002; Xi et al., 2011a). The zebrafish has several advantages compared to other vertebrate models. It has a small size (approximately 1.5 inches fully grown), rapid external embryonic development, optically clear embryos, is highly reproductive all year-round (a single female may produce up to 300 eggs per week), a short generation time (approximately 3 months), is easily accessible and maintained, and gene knockdown is easily achievable by antisense morpholino oligonucleotides (Gilbert, 2000). Moreover, its very rapid and synchronous embryonic development into a characteristic tadpole-like form enables phenotypic analysis at 24 hours post-fertilization (hpf) (Gilbert, 2000) and behavioral characterization starting at around 3-4 days post-fertilization (dpf) (*Zebrafish*, 2002). Research using zebrafish is supported by the completion of the zebrafish genome sequencing project (Link et al., 2006) and the widespread zebrafish genomic resources support research using zebrafish as a model organism in the study of human disease. Zebrafish

have been successfully used to study the pathology of human neurodegenerative diseases including Parkinson's disease, Huntington's disease, and Alzheimer disease and the orthologs of the primary disease-related genes have been identified in zebrafish (Xi et al., 2011a). The characteristics of the zebrafish as well as the genetic techniques to which it is amenable demonstrate the value of this model organism to the study of neurodegenerative diseases.

Through large-scale mutagenesis screens, more than 2000 mutations have been identified to have morphological, physiological and behavioral defects during development (Driever et al., 1996; Haffter et al., 1996; Amsterdam et al., 1999; Dal-Pra et al., 2011). Some zebrafish mutants and deficiency models are reminiscent of human diseases, including blood disorders, aging, muscular dystrophy, autism, heart disorders, solid tumor models, hematological disorders, kidney disorders, stroke, central nervous system disorders and ocular disorders (Tropepe and Sive, 2003; Keller and Murtha, 2004; Paffett-Lugassy and Zon, 2005; Guyon et al., 2007; Santoriello and Zon, 2012; Eisa-Beygi et al., 2013). A large number of mutants resulted from these screens and it is estimated that more than 30,000 genes exist in the zebrafish genome. This implies that more mutations remain to be discovered which can be obtained by smaller-scale and more targeted screens. Zebrafish as a whole-animal vertebrate model provides an advantage in terms of discovering new drugs through the development of automated high-throughput chemical screens (Lieschke and Currie, 2007). These types of screens are aided by the use of transgenic reporter lines which express a fluorescent protein that can be monitored after the application of a drug or treatment.

Zebrafish can be manipulated genetically using either forward or reverse genetic techniques (Lieschke and Currie, 2007). Microinjection of anti-sense morpholino oligonucleotides into one-cell zebrafish embryos can effectively suppress the translation or splicing of a particular mRNA

during early development (Nasevicius and Ekker, 2000). Exposure of dopamine (DA) neurons to 1-methyl-4-phenyl-1,2,3,6-tetrahydropyridine (MPTP), a dopaminergic neurotoxin that causes Parkinsonian symptoms in humans by targeting complex I of the electron transport chain, produces similar effects on DA neuron patterning and behaviour in zebrafish (Bretaud et al., 2004; Lam et al., 2005; McKinley et al., 2005).

Despite notable differences, the overall organization and divisions of the zebrafish nervous system show similarities to that of the human brain. The development of the zebrafish catecholaminergic system has been examined by morphological and genetic approaches (Holzschuh et al., 2001; Ma, 2003; Tay et al., 2011). In zebrafish, DA neurons are first detected at about 18 hpf in a cluster of cells in the ventral diencephalon (vDC). After 3 days post-fertilization (dpf), the central nervous system development is well advanced (Kimmel et al., 1995). It has been previously suggested by (Rink and Wullimann, 2002) that groups of DA neurons in the posterior tuberculum in the zebrafish vDC ascend to the basal telencephalon of the subpallium and that these were initially proposed as the equivalent to the dopaminergic system found in the substantia nigra of the human midbrain with projections to the striatum. Even though the neuroanatomical organization of DA neurons in zebrafish and mammals is similar, Tay and colleagues have suggested a homology between the diencephalic clusters of dopaminergic neurons in zebrafish and the A11 mammalian DA group and suggest that striatal dopaminergic innervation might involve local (telencephalic) circuits (Tay et al., 2011). These observations are based on projectome analysis of the catecholaminergic system in zebrafish and similar transcription factor expression.

These characteristics of the zebrafish as well as the genetic techniques to which it is amenable demonstrate the value of this powerful model organism to the study of the pathogenesis of human Parkinson's disease.

CHAPTER 2.

ZEBRAFISH PARLA- AND PARLB-DEFICIENCY AFFECTS DOPAMINERGIC NEURON PATTERNING AND EMBRYONIC SURVIVAL[1]

2.1 ABSTRACT

Many genes associated with familial Parkinson's disease contribute to mitochondrial morphology and function. Some of these genes, for example, *Pink1* and *Parkin*, are part of a common pathway. The presenilin-associated rhomboid-like (*PARL*) gene was recently linked to familial Parkinson's disease. The *PARL* gene product is found in the inner mitochondrial membrane and cleaves the optic atrophy 1 protein, involved in mitochondrial morphology and apoptosis. In *Drosophila*, the *PARL*-related *rhomboid-7* gene acts upstream of *pink1* and *parkin*. However, such a genetic relationship is still unknown in vertebrates. Here, we show that the zebrafish genome comprises two *parl* paralogs: *parla* and *parlb*. Morpholino-mediated loss of *parla* and/or *parlb* function resulted in mild neurodegeneration, as evidenced by a lower density of dopaminergic neurons. Patterning of dopaminergic neurons was also perturbed in the ventral diencephalon. Morphants exhibited extensive cell death throughout the entire body as well as increased larval mortality. The morphant phenotype could be rescued by injection of human *PARL* mRNA, but not catalytically inactive *PARL*, suggesting functional conservation between the human and zebrafish proteins. More importantly, the zebrafish *pink1* mRNA as well as the human *PINK1* mRNA, but not kinase-dead nor Parkinson's disease-linked mutant *PINK1*

[1] This chapter was published in J. Neurochem. (2012) 122, 196–207. A copy of the permission granted from the publisher to use the published figures from this article in this thesis is included in Appendix C.

mRNA, also rescued the morphant phenotype, providing evidence that *Parl* genes may function upstream of *Pink1*, as part of a conserved pathway in vertebrates.

2.2 INTRODUCTION

Parkinson's disease (PD) is a neurodegenerative disorder characterized by the loss of dopaminergic (DA) neurons in the substantia nigra pars compacta of the midbrain. Despite notable differences, the overall organization of the zebrafish brain shows similarities to that of the human brain. The development of the zebrafish catecholaminergic system has been examined by morphological and genetic approaches (Holzschuh et al., 2001; Ma, 2003; Tay et al., 2011). In zebrafish, DA neurons are first detected at 18 h post-fertilization (hpf) in a cluster of cells in the ventral diencephalon (vDC). After 3 days post-fertilization (dpf), the central nervous system development is well advanced (Kimmel et al., 1995). It has been previously suggested by Rink and Wullimann that groups of DA neurons in the posterior tuberculum in the zebrafish vDC ascend to the basal telencephalon of the subpallium and that these were initially proposed as the equivalent to the dopaminergic system found in the substantia nigra of the human midbrain with projections to the striatum (Rink and Wullimann, 2002). Even though the neuroanatomical organization of DA neurons in zebrafish and mammals is similar, Tay et al. have suggested a homology between the diencephalic clusters of dopaminergic neurons in zebrafish and the A11 mammalian DA group and suggest that striatal dopaminergic innervation might involve local (telencephalic) circuits (Tay et al., 2011).

Many genes with mutations in inheritable PD have been found: *a-synuclein*, *Parkin*, *DJ-1*, *UCHL1*, *PINK1* and *LRRK2* (Cookson, 2005; Farrer, 2006; Whitworth et al., 2008). Recently, a mutation in the PARL gene was identified in two PD patients (Shi et al., 2011). The human *PARL* gene codes for an evolutionarily conserved integral membrane protease of the inner

mitochondrial membrane, where it plays a role in regulated intramembrane proteolysis (Koonin et al., 2003). One of PARL's substrates is optic atrophy 1 (OPA1), an anti-apoptotic inner mitochondrial membrane protein, which in yeast, influences mitochondrial morphology (Herlan et al., 2003; McQuibban et al., 2003; Cipolat et al., 2006). *PARL* knockout mice die prematurely of progressive multisystemic atrophy (Cipolat et al., 2006). Loss of *PARL* in mouse embryonic fibroblasts disrupts OPA1 and remodels the mitochondrial cristae junction, triggering apoptosis through the release of cytochrome *c* (Cipolat et al., 2006; Frezza et al., 2006). The *Drosophila* PARL ortholog, *rhomboid- 7*, acts in a common pathway with other known PD-related genes, namely Pink1 and Parkin, where it is required for mitochondrial fusion (Thisse and Thisse, 2008; Whitworth et al., 2008). *Drosophila rhomboid-7* mutants display severe neurological defects and have a reduced lifespan (McQuibban et al., 2006).

We have identified two *Parl*-related genes in the zebrafish genome, *parla* and *parlb*, and performed an *in vivo* loss-of function using translation-blocking and splice-blocking morpholino oligonucleotides. Rescue experiments with *pink1* mRNA were also carried out to test the hypothesis that the zebrafish *parl* genes belong to a genetic pathway similar to that identified in *Drosophila*.

2.3 MATERIALS AND METHODS

2.3.1 ANIMAL MAINTENANCE

All experiments were performed according to the guidelines of the Canadian Council on Animal Care and were approved by the University of Ottawa animal care committee. Zebrafish and embryos were maintained at 28.5^{o}C according to methods described in Westerfield (Westerfield, 2000). Wild-type adult zebrafish were kept and bred in circulating fish water at 28.5^{o}C with a controlled 14-h light cycle. Embryos were collected at the one-cell-stage. A Narishige IM300

microinjector was used for microinjection. Wild-type (non-injected) and injected embryos were raised at similar densities in a 28.5^{o}C incubator. Embryos were killed with an overdose of tricainemesylate (ethyl 3-aminobenzoate methanesulfonate; Sigma-Aldrich, Oakville, ON, Canada).

2.3.2 MOLECULAR CLONING OF THE ZEBRAFISH *PARLA* GENE

The Ensembl zebrafish database contains two gene sequences related to other vertebrate Parl genes. We named them *parla* and *parlb*. Zebrafish *parla* is located on chromosome 15 and *parlb* on chromosome 2. The translational start site of the zebrafish *parla* gene was not annotated in a recent version of Ensembl. Starting from sequences likely corresponding to exon 2, we searched in the 5' direction upstream of this exon for putative open reading frames (ORFs), one of which would contain the start codon of *parla*. We searched about 6 kb upstream of the first annotated exon and translated, *in silico*, the three reading frames from the genomic DNA sequence provided by Ensembl. We identified 12 putative ORFs that could be exon 1 of *parla*. PCR was done with a forward primer anchored in the putative exon 1 of each putative ORF and a reverse primer was anchored in exon 2. A PCR product of the expected size was obtained for one of these putative ORFs and confirmed by sequencing. The following primers were successful in determining the location of the start codon of *parla*: forward primer 5'-AGGTGGGCTTCAGAGGACTT-3' and reverse primer 5'- TTGACCAGTCTGCCAAATGA-3'. The other ORFs did not yield any PCR products (data not shown).

2.3.3 SEMI-QUANTITATIVE RT-PCR

Total RNA was extracted from wild-type zebrafish at various time points in development, as well as from adult zebrafish tissues using RNeasy Mini Kit (Qiagen, Mississauga, ON, Canada), and reverse transcribed into cDNA using the SuperScript II RT kit (Invitrogen, Burlington, ON,

Canada), according to the manufacturer's instructions. The following primers were used for PCR reactions: *parla* forward primer, 5'-AGGGTCGCAGTTATGATGGC-3'; *parla* reverse primer, 5'-TCATGCACTGCTCTAAATGG-3'; *parlb'* forward primer, 5'-GAACCTGCTGCTTTGGAGTC-3'; *parlb'* reverse primer, 5'-TGAGCATCTGCACTTCCATC-3'; *parlb''* forward primer, 5'-CAGTGGTCCTGTGTTGTTGG-3'; *parlb''* reverse primer, 5'-CGCTTCCTCCAGATCAGTTC-3'; *β-actin* forward primer, 5'-TGGATGAGGAAATCGCTGCC-3'; *β-actin* reverse primer, 5'-CTTCTCTCTGTTGGCTTTGGG-3'. The following primers were used for the RT-PCR validation of the splice-blocking morpholino oligonucleotides (MO): *parla* e1i1 forward primer anchored in exon 1, 5'-CGGTGAGGGGTTTAGTGTTG-3'; *parla* e1i1 reverse primer anchored in exon 2, 5'-TTTGACCAGTCTGCCAAATG- 3'; *parlb* i3e4 forward primer anchored in exon 1, 5'-TTCACAGGCTGCTCTTTCG-3'; *parlb* i3e4 reverse primer anchored in exon 3, 5'-TCTCCAACAACACAGGACCA-3'; and the actin primers listed above. Band intensities were quantified using ImageJ software (National Institutes of Health, Bethesda, MD, USA).

2.3.4 *IN SITU* HYBRIDIZATION

In situ hybridization was performed according to Thisse and Thisse (Thisse and Thisse, 2008). Briefly, larvae were fixed at 3 dpf in 4% paraformaldehyde in phosphate-buffered saline, dehydrated in methanol, and stored in 100% methanol at -20^{o}C. A *tyrosine hydroxylase* (*th1*) digoxigenin labelled antisense riboprobe was synthesized according to (Xi et al., 2010). DA neuron patterning defects were scored according to criteria in Table 2.1 and in a blinded fashion.

Table 2.1. Classification of dopaminergic neuron defects.

Score	Phenotype
Normal	Normal neuron density; well-developed DA neuron groups; well-defined "U" shaped patterning; neuron patterning is comparable to that seen in WT fish
Low density	Reduced neuron density; fewer neuron clusters; spaces present within the "U" shaped patterning of neuron groups; but neurons still aligned
Mis-patterned	Normal or mildly reduced neuron density; large spaces between neuron clusters; neurons out of alignment
Severely mis-patterned	DA neuron patterning is severely altered; morphology of entire embryo often severely affected

Zebrafish larvae were fixed at 3 dpf followed by whole-mount *in situ* hybridization using a *th1* digoxigenin-labelled antisense riboprobe and DA neuron patterning defects were scored in a blinded fashion according to the phenotypes presented.

2.3.5 MORPHOLINO-MEDIATED KNOCKDOWN AND RESCUE EXPERIMENT CONSTRUCTS

The 5'-untranslated region of each *parl* gene was used to design translation blocking antisense MOs against each *parl* transcript. The following translation blocking MOs were obtained from Gene Tools (LLC, Philomath, OR, USA): *parla* MO 5'-AACCCCTCACCGC CATCATAACTGC-3'; *parlb* MO 5'-CATGAAGCAGCTCCTCCATGCCATG-3'. The following splice-blocking MOs were also designed and obtained from Gene Tools: *parla* e1i1 MO 5'- GTATGTGTGTTACCTGCTCCTCAGA-3' targeting intron 1 inclusion; *parlb* i3e4 MO 5'-GTGACCCTGCAGAAAATCAAGTGTA-3' targeting exon 4 excision. As controls, we used the following mis-matched MOs, each with 5 nucleotide substitutions equally distributed within the *parla* or *parlb* MO sequences that conserve base composition (shown in lower case): mis-match *parla* MO 5'-AACCCCTCAgCcCgATCATAAgTcC-3'; mis-match *parlb* MO 5'-CATcAAcCAcCTCCTCgATcCCATG-3'. We also injected a standard control MO: 5'-CCTCTTACCTCAGTTACAATTTATA-3'; and a *p53* MO: 5'-GCGCCATTGCTTTGCAAGA ATTG-3', all of which were obtained from Gene Tools. Each MO was reconstituted in nuclease-free water and diluted for injection to the desired concentration in a solution containing 0.1% Phenol Red and 1X Danieau Buffer.

A wild-type human *PARL* cDNA clone (Hs_*PARL*, accession no. BC014058) was purchased from The Centre for Applied Genomics (The Hospital for Sick Children, Toronto, ON, Canada). A catalytically inactive human *PARL S277G* mutant cDNA clone (Hs_*PARL* S277G, (Jeyaraju et al., 2006)) was obtained from Dr L. Pellegrini through Addgene (plasmid no. 13615; Addgene, Cambridge, MA, USA). A zebrafish *pink1* cDNA clone (Dr_*pink1*, GenBank: BC086729) was purchased from Open Biosystems (Huntsville, AL, USA). A wild-type human *PINK1*, kinase-

dead human *PINK1* K219M mutant and PD-linked human *PINK1* G309D mutant cDNA clones (Haque et al., 2008) were a gift from Dr D. Park, University of Ottawa. Wild-type Hs*_PARL* cDNA was PCR amplified using forward primer: 5'-GAGAATTCGATGGCGT GGCGAGGCTGG-3' and reverse primer: 5'-CGGAATTCTTACTTAGAGCCACCTCCTTT-3'. Hs*_PARL* S277G cDNA was amplified by PCR using forward primer: 5'-AGATCTATGGCGTGGCGAGGCT-3' and reverse primer: 5'-ACTAGTTCACTTGTCAT CGTCGTC-3'. Dr*_pink1* cDNA was PCR amplified using forward primer: 5'-CCGAATTCGATGTCAGTAAAGCATGTTCTCAG-3' and reverse primer: 5'-CCGAATTCCTATGGCTGAGTGTTTGACATC-3'. Each PCR amplicon was flanked by *Xenopus* β-globin 5' and 3' UTRs and cloned into the pT7TS vector. Hs*_PINK1* K219M and G309D cDNA were digested with *Bgl*II and *Xba*I and subcloned into the *Bam*HI and *Xba*I sites of a pCS2+ expression vector with a poly A tail. *In vitro* mRNA synthesis was carried out using the mMESSAGEmMACHINE kit (Ambion, Streetsville, ON, Canada). 50 pg of synthetic mRNA were microinjected together with 2.5 ng of *parla* MO and 2.5 ng of *parlb* MO in zebrafish embryos at the one-cell-stage.

2.3.6 ACRIDINE ORANGE STAINING

Live embryos were stained with 10 μg/mL of acridine orange (3,6- Bis(dimethylamino)acridine hydrochloride zinc chloride double salt; Sigma-Aldrich, St Louis, MO, USA) in embryo media for 30 min in the dark at 22^{o}C. Embryos were washed three times with fresh embryo media, anesthetised in tricainemesylate (ethyl 3-aminobenzoate methanesulfonate; Sigma-Aldrich, Oakville, ON, Canada) and visualized under a Leica fluorescent dissection microscope. At least 10 embryos were examined from each group.

2.3.7 STATISTICAL ANALYSIS

Differences in mean survival were analyzed by two-tailed unpaired Student's *t*-tests with at least three independent experiments, each comprising a minimum of 50 embryos. For the percentage of larvae affected by *parl* knockdown, tests for independence between treatments were done using chi-square tests (χ^2). Predetermined *p*-values ≤ 0.05 were considered statistically significant ($p < 0.05$, $p < 0.01$, $p < 0.001$). The number of biological replicates is indicated in corresponding sections of text or figure legends. All analyses were performed using Excel (Microsoft).

2.4 RESULTS

2.4.1 THE ZEBRAFISH PARL PROTEINS ARE CONSERVED AMONG VERTEBRATES

The zebrafish *parl* genes were identified by performing an Ensembl BLASTP search of the zebrafish genome using the human PARL protein coding sequence. The BLASTP search result identified two sequences similar to the human PARL sequence within the zebrafish genome. One of the orthologs is located on chromosome 15 (gene: LOC792889, protein: ENSDARP00000055977), while the other is located on chromosome 2 (gene: zgc:112986, protein: ENSDARP 00000057438). We arbitrarily designated these two PARL sequences *parla* and *parlb*, respectively. The PARL genes showed conservation at the amino acid level with other vertebrate PARL proteins (figure. 2.1). The predicted Parla protein shows a higher (67%) overall amino acid identity to human PARL when compared with Parlb (55%). In mammalian cells, Parl is targeted to the mitochondria, where it undergoes post-translational processing which involves removal of the mitochondrial targeting sequence and the generation of a Pβ peptide which is

targeted to the nucleus (Sik et al., 2004; Jeyaraju et al., 2006). This processing and localization has not been examined in zebrafish. Based on amino acid sequence analysis, the Pβ domain does not appear to be conserved in zebrafish suggesting that the zebrafish Parl proteins may not be processed in the same way as in mammals and may not produce a Pβ peptide which is shuttled to the nucleus.

Figure. 2.1. Amino acid alignment of PARL homologues. PARL is a conserved mitochondrial inner membrane protease with a mitochondrial targeting sequence (MTS) shaded in blue, a nuclear localization signal (NLS) shaded in purple, and seven transmembrane domains shaded in green. Red circles highlight amino acid residues that form the predicted catalytic sites of rhomboid-like proteases. Each of the teleost fish, zebrafish (Dr), medaka (Ol), fugu (Tr), tetraodon (Tn), have two *parl* genes (*parla* and *parlb*), while humans (Hs), mice (Mm) and *Drosophila* (Dm) have one *PARL* gene.

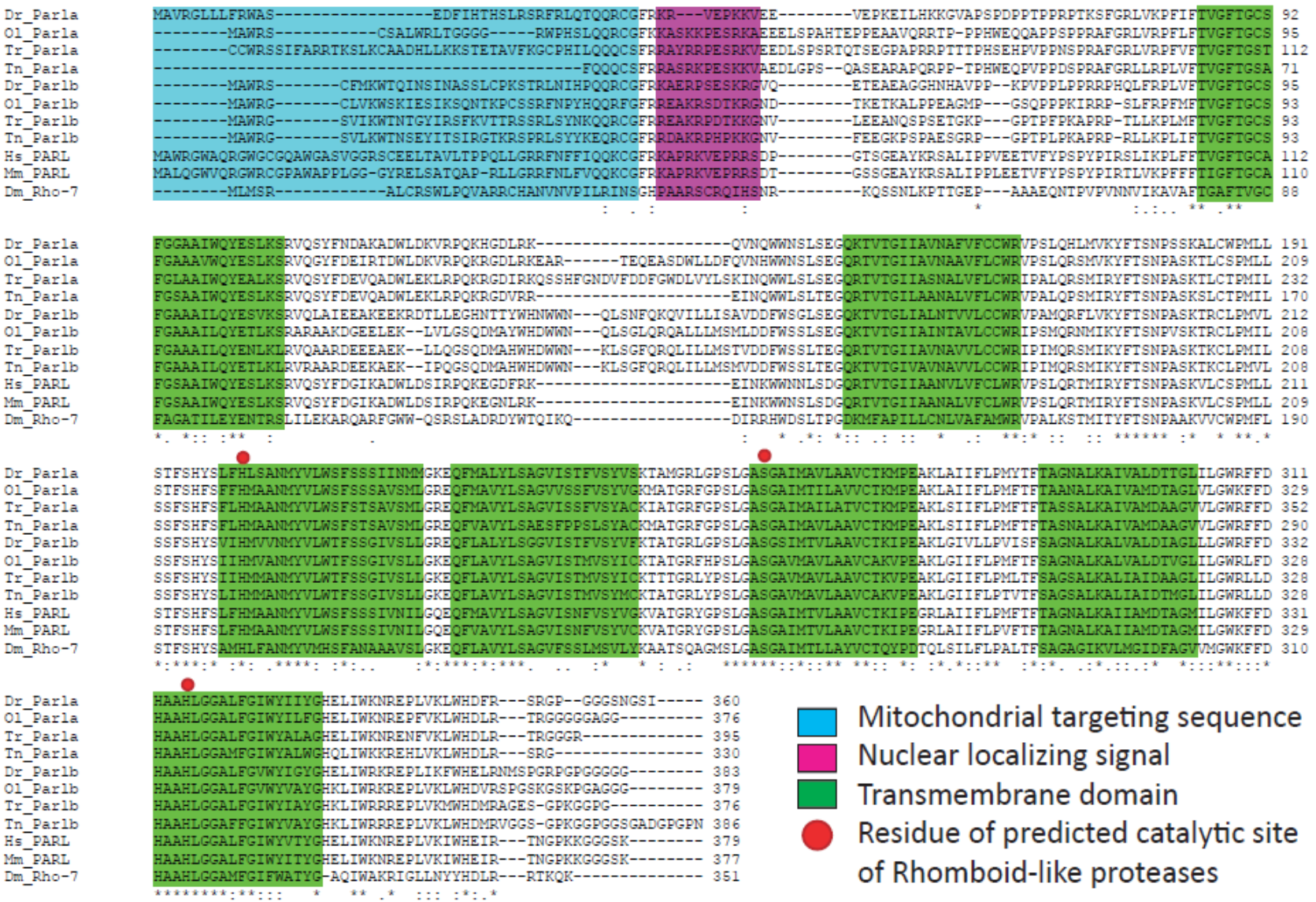
Dr_Parla
Ol_Parla
Tr_Parla
Tn_Parla
Dr_Parlb
Ol_Parlb
Tr_Parlb
Tn_Parlb
Hs_PARL
Mm_PARL
Dm_Rho-7
Mitochondrial targeting sequence
Nuclear localizing signal
Transmembrane domain
Residue of predicted catalytic site of Rhomboid-like proteases

2.4.2 SYNTENY ANALYSIS REVEALS TWO PARALOGOUS ZEBRAFISH *PARL* GENES

Synteny analysis of genes near *PARL* in the human and zebrafish showed that *PARL* and several genes located upstream and downstream of *PARL*, on human chromosome 3 mapped to chromosome 2 in zebrafish (figure. 2.2). The zebrafish ortholog of human *CHRD* (chromosome 3), *chrd*, was found along with *parla* on chromosome 15 of the zebrafish. These results indicate that the two *parl* sequences in the zebrafish are paralogs that evolved after a duplication event; most likely the whole genome duplication that occurred before the diversification of teleosts (Postlethwait et al., 2004). The synteny between human *PARL* and the genes around it on the same chromosome is more conserved on chromosome 2 of the zebrafish, where *parlb* is found.

Figure. 2.2. Synteny analysis of genes near *PARL* in human and zebrafish. Zebrafish *parla* and *parlb* map to chromosomes 15 and 2, respectively, while human *PARL* is found on chromosome 3. The synteny between human *PARL* and the neighbouring genes is conserved on chromosome 2 of the zebrafish, where *parlb* is located. The ortholog of the *CHRD* gene found near zebrafish *parla* is also found near the human *PARL* gene. A small chromosomal region is shown.

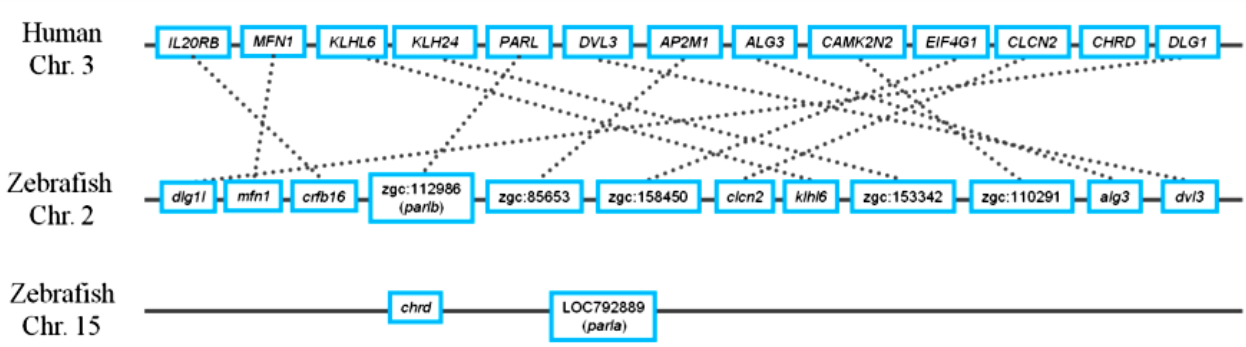
Human
Chr. 3
IL20RB
MFN1
KLHL6
KLH24
PARL
DVL3
AP2M1
ALG3
CAMK2N2
EIF4G1
CLCN2
CHRD
DLG1
Zebrafish
Chr. 2
dlg1l
mfn1
crfb16
zgc:112986
(parlb)
zgc:85653
zgc:158450
clcn2
klhl6
zgc:153342
zgc:110291
alg3
dvl3
Zebrafish
Chr. 15
chrd
LOC792889
(parla)

2.4.3 BOTH *PARL* MRNA TRANSCRIPTS ARE EXPRESSED DURING EMBRYONIC DEVELOPMENT AND IN ADULT TISSUES

The temporal and spatial mRNA expression of *parla* and *parlb* were analyzed by RT-PCR. The *parla* mRNA was not detected maternally [at 2 h post-fertilization (hpf)], but was present throughout embryonic development from 4 hpf to at least 7 days post-fertilization (dpf) (figure 2.3a and 2.3b). In adult zebrafish, *parla* was highly expressed in the brain and muscle tissues with lower expression in the liver and heart (figure 2.3a). The *parlb* gene was expressed at a very low level maternally, but transcripts were more abundant from 4 hpf to at least 7 dpf, as well as in the brain of adult zebrafish, followed by the liver (figure 2.3a and 2.3b). No *parlb* expression was detected in heart and muscle tissues (figure 2.3a). The combined expression patterns of *parla* and *parlb* in zebrafish is reminiscent of the ubiquitous expression of *PARL* in human adult and fetal tissues (Pellegrini et al., 2001). Ubiquitous expression of *parla* and *parlb* mRNA was also confirmed at 3 dpf by whole-mount *in situ* hybridization (data not shown).

Figure. 2.3. Semi-quantitative RT-PCR analysis of *parla* and *parlb* expression. (a) Expression of *parla* and *parlb* in zebrafish embryos, larvae and adult tissues. (b) *parla* and *parlb* expression between 2 hpf and 24 hpf. *parla* expression was first detected at 4 hpf. (c) Expression of *parla* and *parlb* following knockdown with 2.5 ng or 5 ng of splice-blocking MO. Primers anchored in exons 1 and 2 of *parla* generated a band of 236 bp in WT embryos at 24 hpf. The intensity of this band was reduced by more than 90% in morphants. Conversely, primers anchored in exons 1 and 3 of *parlb* generated a band of 285 bp in WT embryos. The intensity of this band was reduced by more than 85% in morphants. *β-actin* was used as a loading control. In all cases, a negative control containing no cDNA template was used for the PCR reactions and resulted in no amplification product.

(a)

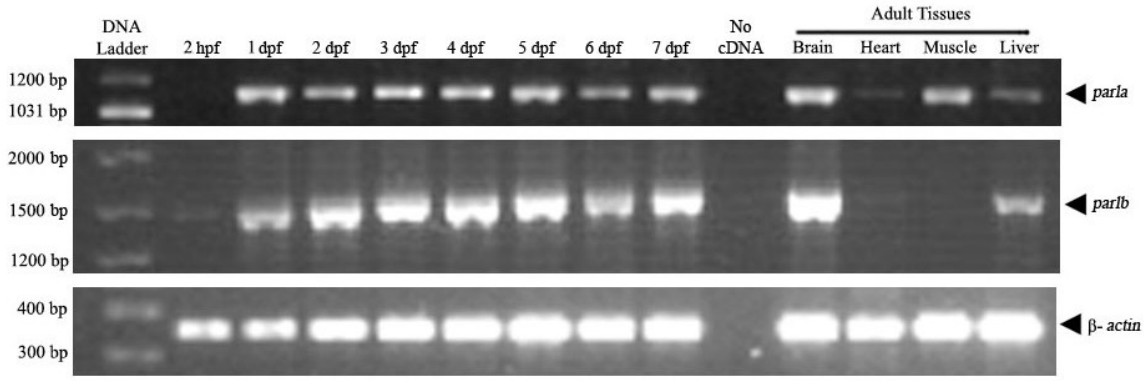
DNA Ladder
2 hpf
1 dpf
2 dpf
3 dpf
4 dpf
5 dpf
6 dpf
7 dpf
No cDNA
Adult Tissues
Brain
Heart
Muscle
Liver
1200 bp
1031 bp
parla
2000 bp
1500 bp
1200 bp
parlb
400 bp
300 bp
β- actin

(b)

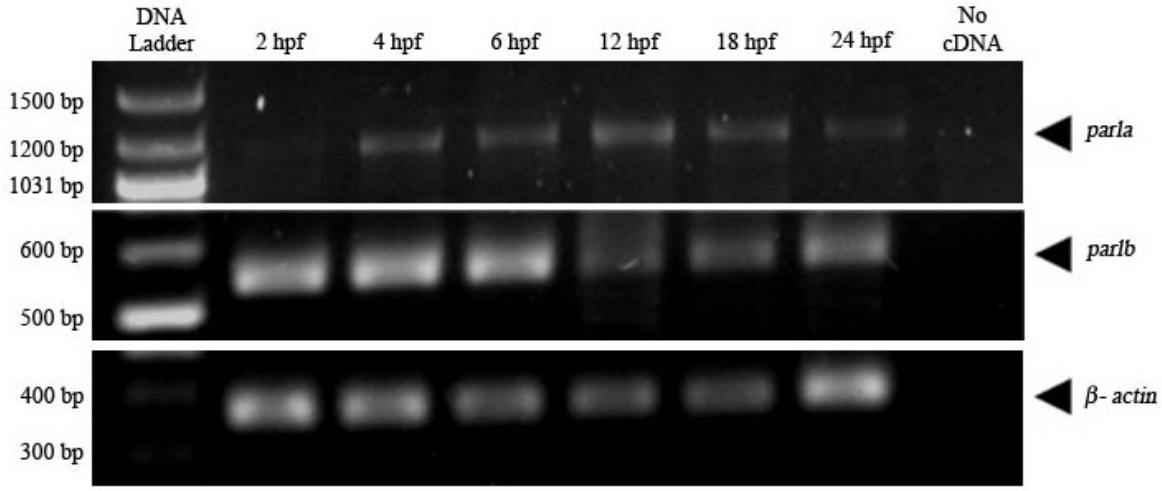
DNA Ladder
2 hpf
4 hpf
6 hpf
12 hpf
18 hpf
24 hpf
No cDNA
1500 bp
1200 bp
1031 bp
parla
600 bp
500 bp
parlb
400 bp
300 bp
β- actin

(c)

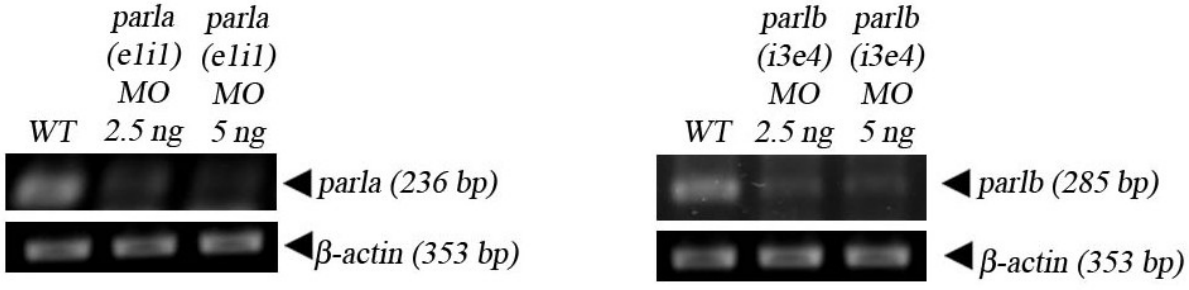
parla (e1i1) MO
parla (e1i1) MO
WT
2.5 ng
5 ng
parla (236 bp)
β-actin (353 bp)
parlb (i3e4) MO
parlb (i3e4) MO
WT
2.5 ng
5 ng
parlb (285 bp)
β-actin (353 bp)

2.4.4 EMBRYONIC SURVIVAL IS SEVERELY REDUCED BY MORPHOLINO-MEDIATED KNOCKDOWN OF BOTH ZEBRAFISH *PARL* GENES

We designed translation blocking MOs (the *parla* MO and the *parlb* MO) as well as splice-blocking MOs (the *parla* e1i1 MO and the *parlb* i3e4 MO) against each of the two zebrafish *parl* transcripts. These MOs were injected alone or in various combinations into one-cell embryos. The resulting phenotypes were compared with those of embryos injected with mis-matched MOs, with a standard control MO or with un-injected fish. We first tested various amounts of translation-blocking MOs. When compared with the survival of embryos injected with control MOs (63.7%), administration of 5 ng of either *parla* MO or *parlb* MO separately, had no statistically significant effect on survival at 3 dpf (data not shown). However, when both MOs were co-injected at 2.5 ng each (total MO concentration equalling 5 ng), the average survival at 3 dpf was 48.2% and significantly different from controls ($p < 0.01$; six experimental replicates; each with at least 300 fish. Mortality ranged between 33% and 64%). Mortality was already observed at 1 dpf but increased at 2 and 3 dpf (data not shown). In contrast, when one of the *parl* MOs was replaced by its mis-matched control and co-injected with its paralog's translation blocking MO (e.g. mismatched *parla* MO + *parlb* MO), no increase in mortality was observed (data not shown). These results suggest that the zebrafish needs at least one functional Parl protein for early embryonic and larval survival.

We next tested splice-blocking MOs targeted against *parla* or *parlb*. The *parla* e1i1 MO (2.5 or 5 ng) caused a greater than 90% decrease in the intensity of the 236 bp band corresponding to the wild-type (WT) *parla* transcript (figure 2.3c). Similarly, the *parlb* i3e4 MO (2.5 or 5 ng) caused a greater than 85% reduction in the intensity of the 285 bp band corresponding to the WT *parlb* transcript (figure 2.3c). We did not detect any band corresponding to intron 1 inclusion in the

case of the *parla* e1i1 MO or exon 4 excision in the case of the *parlb* i3e4 MO (data not shown), presumably because the incorrect splicing events led to premature stop codons and targeting of the *parl* mRNAs for non-sense-mediated mRNA decay. Based on these decreases in normal mature transcripts, we predict that morphants had almost total losses of normal Parl protein function. Injection of 2.5 ng each of the *parla* e1i1 MO and the *parlb* i3e4 MO gave results similar to those obtained after injecting both translation blocking MOs at the same concentrations. Over half of the larvae died (five experimental replicates, each with a minimum of 50 larvae). We also injected the *parla* MO and *parlb* MO along with a MO directed against the *p53* mRNA (Robu et al., 2007). Co-injection of the *p53* MO did not significantly reduce mortality (data not shown) indicating that the phenotypes observed (see above paragraphs and sections below) were unlikely attributable to off-target effects of the MOs and that the mortality observed is unlikely to proceed through p53-mediated DNA damage leading to apoptosis.

2.4.5 CELL DEATH IS DETECTED IN *PARL* MORPHANTS

We stained live embryos at 1, 2 and 3 dpf with acridine orange (figure 2.4) to see if the embryonic mortality observed in *parl* double morphants could be explained by the loss of Parl function in preventing apoptosis. Apart from a non-specific signal detected in the nasal pits and autofluorescence in the yolk, we observed almost no staining in wild-type embryos throughout 3 dpf (Fig. 2.4a–2.4c). In contrast, in *parla* morphants staining was present throughout the entire body of the embryos at 1, 2 and 3 dpf (Fig. 2.4d–2.4f). Acridine orange staining in *parlb* morphants was present throughout the entire embryo at 1 dpf but decreased in surviving embryos afterwards (Fig. 2.4g–2.4i). Consistent with the increased mortality, uniform staining was seen at 1 dpf in *parl* double morphants and persisted through 2 and 3 dpf (Fig. 2.4j–2.4l).

Figure. 2.4. Acridine orange staining of *parl* morphants. The staining of live embryos over the first 3 days of development revealed no staining in WT embryos, except for the nasal cavity (a–c). Wide-spread cell death is observed throughout *parla* single morphants (5 ng) (d–f). *parlb* single morphants (5 ng) had more abundant staining at 1 dpf (g), but reduced staining at 2 dpf and 3 dpf (h, i). Wide-spread cell death is observed throughout *parla* (2.5 ng) and *parlb* (2.5 ng) double morphants (j–l). Representative lateral views of the head region are shown with anterior facing left.

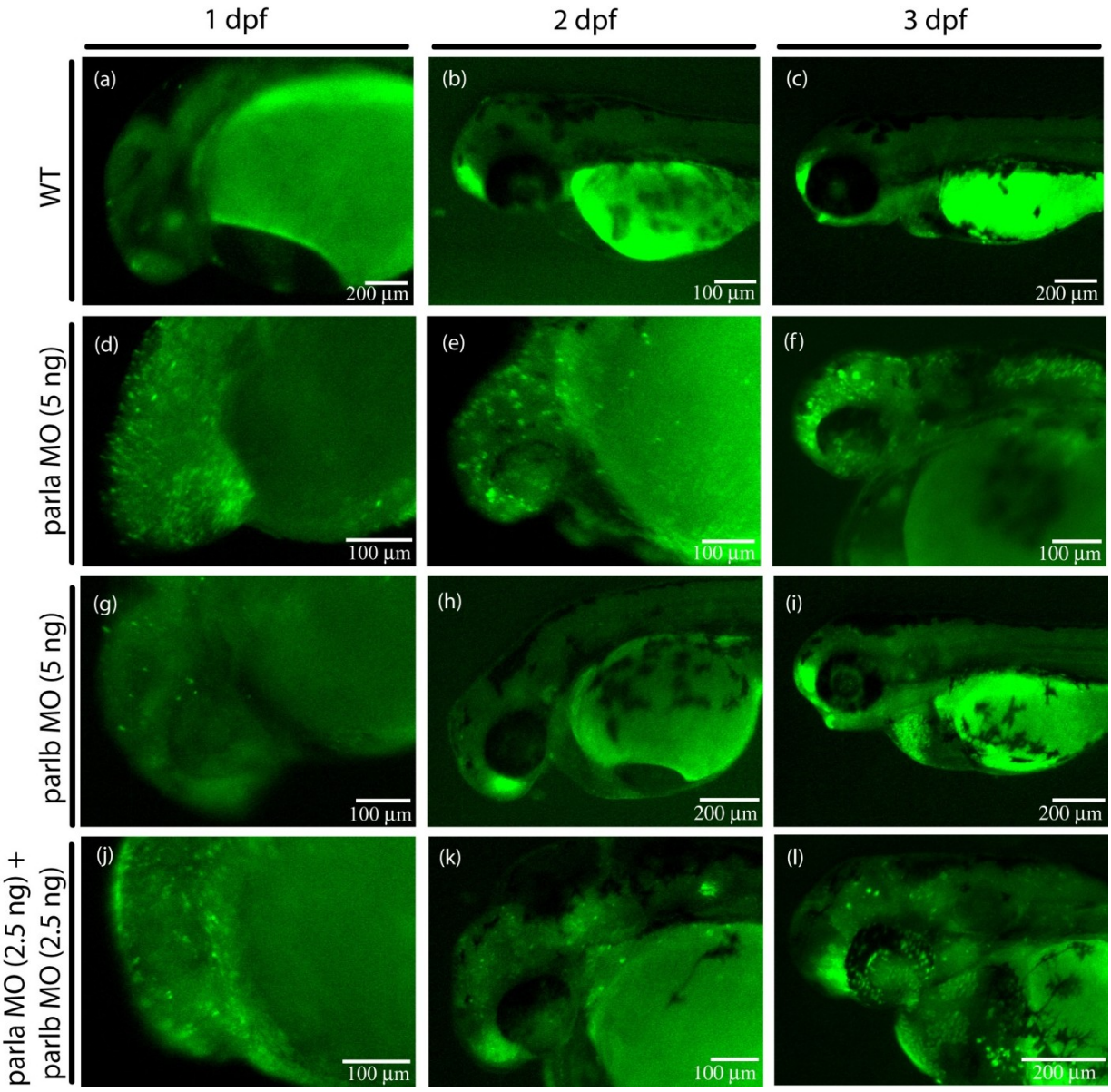
1 dpf
2 dpf
3 dpf
WT
parla MO (5 ng)
parlb MO (5 ng)
parla MO (2.5 ng) + parlb MO (2.5 ng)
(a)
(b)
(c)
(d)
(e)
(f)
(g)
(h)
(i)
(j)
(k)
(l)
200 µm
100 µm
100 µm
200 µm
100 µm
100 µm
100 µm
200 µm
200 µm
100 µm
100 µm
200 µm

2.4.6 DOPAMINERGIC NEURONS ARE PERTURBED BY KNOCKDOWN OF BOTH ZEBRAFISH *PARL* GENES

The central nervous system of the zebrafish is well advanced at 3 dpf (Kimmel et al., 1995) and we chose this time-point to examine the patterning of the DA neurons. We did this first using whole mount *in situ* hybridization with a *tyrosine hydroxylase* (*th*) antisense cRNA probe. In the current study we used *th1* which, together with *th2*, *aadc*, *dat* and/or *vmat2* have been used to label various DA neuron populations (Yamamoto et al., 2011); although it should be noted that Lin's group has recently reported that *th2* may actually label serotonergic clusters in the vDC and the caudal hypothalamus (Hc), namely DC3, DC5 and DC7 (Ren et al., 2013). We also injected the *parla* and *parlb* MOs in a line of transgenic zebrafish, Tg(*dat:EGFP*), in which the green fluorescent protein (GFP) is expressed under the control of *cis*-regulatory elements of the *dopamine transporter* (*dat*) gene (Xi et al., 2011b). We focused on groups of DA neurons in the zebrafish posterior tuberculum of the vDC. Surviving embryos were fixed at 3 dpf for observation of DA neuron patterning (Fig. 2.5a) and scored into four categories based on the definitions in Table 2.1.

The percentage of morphants that fall into each of these categories is presented alongside larval mortality in Fig. 2.5c. Knockdown of *pink1*, another PD-related gene we have studied previously in zebrafish, was used for comparisons because its knockdown causes obvious DA neuron mispatterning compared with control MO injected embryos (chi-square test, $p < 0.001$) (Xi et al., 2010). Significant differences in phenotype distribution were seen between treatment groups. 60% of *parla* single morphants had severely mis-patterned DA neurons compared with only 23% which received the control MO (chi-square test, $p < 0.001$). In comparison, *parlb* single morphants exhibited 9% more larvae in the low density category compared with the larvae which

received the control MO (chi-square test, $p < 0.001$). Double morphants co-injected with 2.5 ng of *parla* MO and 2.5 ng of *parlb* MO exhibited a larger total percentage of affected larvae (77%) when examining perturbed DA neuron patterning and mortality together compared with control MO injected larvae (61%) (chi-square test, $p < 0.001$). The *parla* morphants had a higher total percentage of affected larvae (96%) than *parlb* morphants (61%). These results suggest that in zebrafish, proper DA neuron development depends particularly on Parla function.

The specific loss of *th1* observed in the vDC was corroborated with a reduced number and perturbed patterning of GFP-positive cells at 3 dpf in Tg(*dat:EGFP*) larvae injected with both *parla* and *parlb* MOs (Fig. 2.5b).

Figure. 2.5. Altered DA neurons in parl morphants. (a) Categories of DA neuron patterning seen in larvae deficient in Parla and/or Parlb. *Tyrosine hydroxylase* (*th1*) mRNA (a) as well as EGFP under the control of *cis*-regulatory elements of the *dopamine transporter* (*dat*) (b) in the Tg(*dat:EGFP*) transgenic line served as markers of DA neurons. DA neurons in the vDC (white arrowhead) are perturbed in *parl* double morphants compared with WT at 3 dpf. At least 10 transgenic larvae were examined in each group. Dorsal views shown with anterior facing left. Scale bar, 50 μm. (c) Morphant phenotype at 3 dpf. DA neuron perturbations are divided into categories. Percentages are indicated in each bar. A minimum of 190 fish were examined in each group. The amount (ng) of injected MO is indicated.

(a)

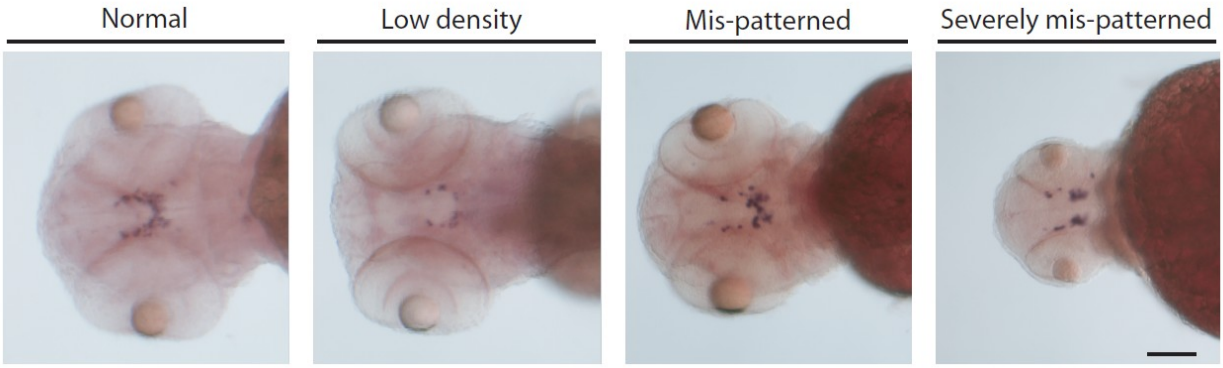
Normal
Low density
Mis-patterned
Severely mis-patterned

(b)

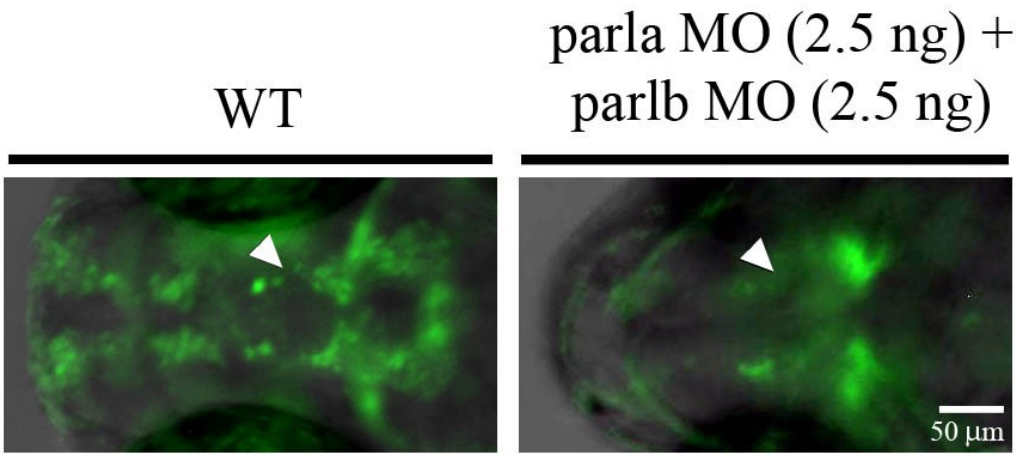
WT
parla MO (2.5 ng) +
parlb MO (2.5 ng)
50 µm

(c)

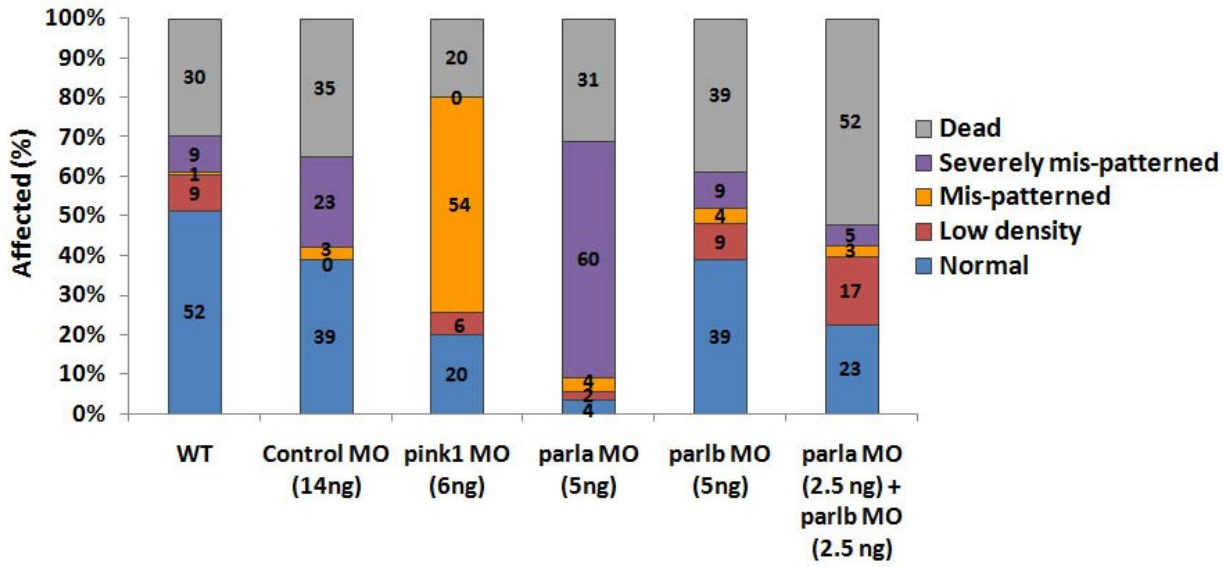
Affected (%)
100%
90%
80%
70%
60%
50%
40%
30%
20%
10%
0%
30
9
1
9
52
35
23
3
0
39
20
0
54
6
20
31
60
4
2
4
39
9
4
9
39
52
5
3
17
23
WT
Control MO (14ng)
pink1 MO (6ng)
parla MO (5ng)
parlb MO (5ng)
parla MO (2.5 ng) + parlb MO (2.5 ng)
Dead
Severely mis-patterned
Mis-patterned
Low density
Normal

2.4.7 OVER-EXPRESSION OF HUMAN *PARL* MRNA RESCUES LARVAL MORTALITY AND DA NEURON PERTURBATIONS IN *PARL* DOUBLE MORPHANTS

To further ascertain the specificity of the MO-induced phenotype, we tested the ability of human *PARL* (Hs_*PARL*) mRNA to rescue the morphant phenotypes. Over-expression of Hs_*PARL* along with the knockdown of the two *parl* genes significantly increased larval survival to 79.4% (chi-square test, $p < 0.001$) at 3 dpf, an increase of 22.8% compared with *parl* double morphants injected with 2.5 ng of each *parl* MO. In addition to rescuing mortality, human *PARL* mRNA also significantly rescued the DA neuron perturbations seen at 3 dpf in *parl* double morphants (Fig. 2.6; chi-square test, $p < 0.001$). The distribution of larvae injected with human *PARL* mRNA and scored by classification of DA neuron defects was not significantly different from WT (chi-square test, $p = 0.092$). We also injected mRNA coding for a catalytically inactive human *PARL* (S277G) along with both *parl* MOs. The mutant mRNA had much less ability to rescue larval mortality. Thus, while WT PARL could rescue the morphant phenotype by up to 75% (Fig. 2.6), embryos injected with inactive human *PARL* mRNA showed 74% higher mortality than in embryos injected with WT human *PARL* mRNA ($p < 0.01$) and only a mild rescue (18%; data not shown). The ability of human PARL to rescue the morphant phenotype also suggests that Parl function is conserved between zebrafish and human.

Figure. 2.6. Human *PARL* mRNA (Hs_*PARL*) or zebrafish *pink1* mRNA (Dr_*pink1*) rescues larval mortality and DA neuron alterations. Co-injections of *parla* and *parlb* MOs along with either human *PARL* mRNA or zebrafish *pink1* mRNA resulted in reduced larval mortality compared with *parl* double morphants alone. Morphants were grouped into categories based on DA neuron perturbations observed after knockdown of specified transcript(s) (see Table 2.1). Morpholino injections were performed on three independent clutches of embryos, each with at least 40 embryos. Percentages are indicated in each bar. Amounts of injected MOs and mRNA transcripts are indicated.

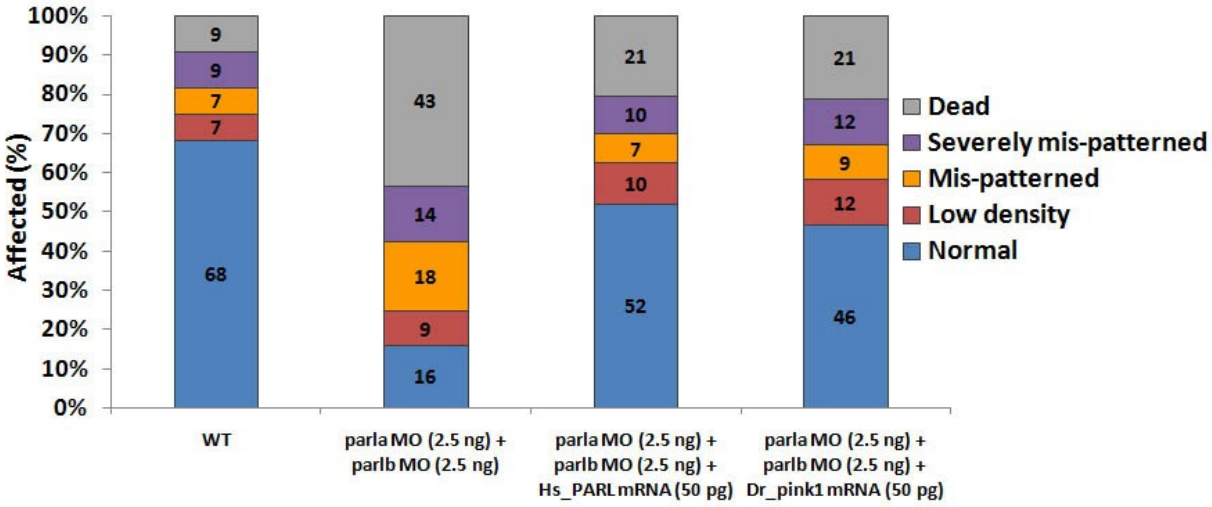
100%
90%
80%
70%
60%
50%
40%
30%
20%
10%
0%
Affected (%)
9
9
7
7
68
43
14
18
9
16
21
10
7
10
52
21
12
9
12
46
Dead
Severely mis-patterned
Mis-patterned
Low density
Normal
WT
parla MO (2.5 ng) + parlb MO (2.5 ng)
parla MO (2.5 ng) + parlb MO (2.5 ng) + Hs_PARL mRNA (50 pg)
parla MO (2.5 ng) + parlb MO (2.5 ng) + Dr_pink1 mRNA (50 pg)

2.4.8 THE PARKINSON'S DISEASE-RELATED GENE *PINK1*, IS GENETICALLY DOWNSTREAM OF THE *PARL* GENES IN ZEBRAFISH

To date, it has been shown that rhomboid-7 is epistatic to *pink1* only in an invertebrate model, the *Drosophila* (Whitworth et al., 2008). Currently, the epistatic relationship of these two PD-related genes is unknown in vertebrates. To see if the *parl* genes are epistatic to the *pink1* gene in vertebrates, we over-expressed the zebrafish *pink1* mRNA in embryos while simultaneously knocking down both *parl* genes. This reduced larval mortality by half compared with *parl* double morphants (chi-square test, $p < 0.001$). As well as rescuing larval mortality, DA neuron alterations were also significantly reduced by zebrafish *pink1* mRNA compared with *parl* double morphants at 3 dpf (figure 2.6; chi-square test, $p < 0.001$). Analogous to *Drosophila* (Whitworth et al., 2008), our results suggest that the *parl* genes are epistatic to *pink1* in zebrafish, which opens up the possibility that this genetic relationship possibly also exists in higher vertebrates too. The human *PINK1* mRNA was also able to rescue the *parl* morphant phenotype ($p < 0.01$; data not shown), albeit to a lesser degree than the zebrafish *pink1* (about 50% rescue of larval mortality with human *PINK1* compared with about 75% rescue with zebrafish *pink1*).

We also tested whether a human kinase-dead K219M *PINK1* or the human PD-linked G309D *PINK1* mutant could rescue the larval mortality observed in parl double morphants. We injected kinase-dead *PINK1* mRNA along with both parl MOs. This mutant mRNA did not rescue larval mortality at all with the same mortality rate as larvae that had been injected with the two MOs alone. The PD-mutant *PINK1* mRNA produced a mild rescue (18% rescue compared with 50% rescue obtained with WT human *PINK1*; $p < 0.05$; data not shown).

2.5 DISCUSSION

The combined loss-of-function of the *parla* and *parlb* genes in zebrafish resulted in a high rate of mortality in early larvae. In contrast, loss of function of a single *parl* gene had no major effect on survival. At the cellular level, the main phenotype observed in 3-day-old larvae deficient in *parla* was a larger proportion of fish with severely mis-patterned DA neurons as described in Table 2.1, compared with controls. In contrast, *parlb* morphants did not demonstrate a significant change in DA neuron patterning compared with controls.

In mice, loss of *Parl* function is lethal (Cipolat et al., 2006). In contrast, loss-of-function of one of the two zebrafish *parl* paralogs did not result in increased mortality. This implies that the functional redundancy of the zebrafish *parl* genes confers some advantage to the fish (Postlethwait et al., 2004). We hypothesized that single *parl* knockdowns may have resulted in the compensatory up-regulation of the paralog's mRNA expression. After knockdown of *parla*, we observed an increase in the expression of both *parla* and *parlb* transcripts by semi-quantitative RT-PCR (data not shown). The knockdown of *parlb* did not have marked effects on transcription of either *parla* or *parlb* (data not shown).

How the loss-of-function of the *parl* genes specifically leads to larval death in zebrafish remains unknown. This could be accomplished by altering Parl's role in mitochondria dynamics and cristae remodelling. Parl's protease function is normally responsible for cleaving OPA1 within its transmembrane domain in the inner mitochondrial membrane. This produces a soluble form of OPA1 which oligomerizes with membrane-tethered OPA1 to gate the mitochondrial cristae junctions and prevent the release of cytochrome *c* which, in turn, guards against apoptosis.

Flies with a *rhomboid*-7 mutation exhibit the same abnormal phenotypes as *pink1* or *parkin* mutant flies suggesting that the two gene products act in a common pathway (McQuibban et al.,

2006). Based on an overexpression eye phenotype assay, it has been suggested that *Drosophila rhomboid-7* is epistatically upstream of *pink1* and that PINK1 is a substrate of rhomboid-7 (Whitworth et al., 2008). Studies carried out in mammalian cell culture have shown that PINK1 cleavage is inhibited by the lack of PARL (Jin et al., 2010). These observations are seemingly inconsistent with Rhomboid-7/PARL being epistatically upstream of PINK1. Although PARL was shown to cleave PINK1 in mammalian cell lines, PINK1 was not exclusively proteolysed by PARL (Deas et al., 2011). Four mitochondrial proteases were found to facilitate PINK1 turnover: mitochondrial processing peptidase; ClpXP, m-AAA and PARL (Greene et al., 2012). We have shown that the lack of both Parl proteins can be rescued by the expression of either zebrafish or human PINK1. Thus, cleavage of over-expressed Pink1 by compensatory mechanisms may explain the seemingly surprising ability of Pink1 to rescue the parl phenotype in zebrafish, despite the fact that PINK1 is a substrate of Parl.

We observed higher levels of cell death in morphants with acridine orange staining at 1 dpf (figure 2.4) which parallels the high mortality observed before 2 dpf. At later time points, the rate of death and relative number of acridine orange stained cells decreased (figure. 2.4 and 2.5c). It should be noted that although acridine orange staining provides a rapid assessment of cell death *in vivo*, this dye method may not only stain apoptotic cells but may also stain necrotic cells as well as acidic intracellular compartments such as lysosomes. The activation of cell death upon Parl deficiency could be occurring through Parl's inability to prevent mitochondrial fission and/or Parl's inability to proteolytically produce soluble OPA1 which would normally prevent the widening of the cristae junction and inhibit the release of cytochrome *c* from the mitochondria.

Dose-dependent lethality in the *parl* double-morphants was accompanied by disarranged DA neurons of the posterior tuberculum in the vDC of surviving larvae. In this respect, loss of *parla* function seems to have a more profound impact than loss of *parlb* (figure 2.5). Defects in the patterning of DA neurons was assessed by examining *th1* expression and the results were corroborated in a line of transgenic fish where GFP is expressed under the control of regulatory sequences from the dopamine transporter, *dat*, gene (Xi et al., 2011b). Thus, changes in two different markers likely reflect changes in the number and positions of cells. In addition to the effects observed in the ventral diencephalon, other *th1*-expressing cells in *parl* morphants were affected. Thus, we also saw decreases or disappearance of the few *th1*-expressing cells in the locus coeruleus, medulla oblongata, arch-associated neurons and sympathetic neurons in *parl* double morphants (data not shown). This is not surprising, because noradrenergic locus coeruleus neurons, as well as serotonergic (raphe), cholinergic, cerebral cortex, olfactory bulb neurons, the autonomic nervous system, hippocampal structures and cholinergic cortical inputs have been reported to be affected in PD-patients indicating that the neurodegeneration is not exclusive to DA neurons (Dauer and Przedborski, 2003).

Our findings are in agreement with loss of PARL function in other organisms. It has been previously established that the global lack of *PARL* in a mouse knockout model results in loss of muscle mass, postural defects and mild neurodegeneration of the thalamus and striatum (Cipolat et al., 2006). Ultimately, these mice die prematurely because of dysfunctional muscle-associated movement and breathing problems between 8 and 12 weeks. Similarly, *Drosophila rhomboid-7* mutants show a disruption of myofilament spacing in their flight muscles causing them to have droopy wings and rendering them unable to fly (McQuibban et al., 2006; Whitworth et al., 2008). In addition, these flies have disrupted mitochondrial organization and are unable to undergo

mitochondrial fusion during spermatogenesis and muscle maturation which both rely heavily on mitochondrial energy production. Once again, severe motor defects are seen when *rhomboid-7* is disrupted, ultimately leading to death in 3-day-old flies. Similar to the PARL mouse model, our zebrafish *parla*- and *parlb*-deficiency model exhibits neuronal defects, namely in the neurons responsible for DA transmission. Our results suggest that the *parl* genes are essential for the proper patterning of at least some of the zebrafish DA neurons and that the survival of the embryos and larvae depends on the function of the *parl* genes and their downstream target, *pink1*.

Functional studies of several PD-related genes have now been reported in zebrafish (Xi et al., 2011a). These include *parkin*, *pink1*, *dj-1* and *lrrk2*. Parkin-deficient zebrafish showed an ~20% reduction in the number of *th* positive ventral diencephalic DA neurons at 3 dpf which is exacerbated to ~50% following exposure to MPTP (DA neurotoxin) (Flinn et al., 2009). Although mitochondrial morphology appears normal, respiratory chain complex I activity is reduced. In contrast, another study with a MO targeting exon 2 of *parkin* did not result in DA neuron loss, morphological, nor behavioural defects, but the fish were more vulnerable to stress-induced cell death (Baulac et al., 2009; Fett et al., 2010). We and others have shown that translation-blocking morpholino-mediated loss of Pink1 function results in DA neuron defects (Anichtchik et al., 2008; Sallinen et al., 2010; Xi et al., 2010). The *pink1* morphant phenotypes included moderate decreases in DA neurons, abnormal morphology with no apparent loss of neurons and impaired locomotor dysfunction that could be rescued with a dopamine D_1 receptor agonist. Moreover, fewer than 20% of pink1 morphants live past 10 dpf. Loss of Pink1 function sensitized larvae to a sub-effective dose of MPTP in one of the studies. Similarly, zebrafish deficient in Dj-1 did not exhibit a loss of DA neurons, but were more susceptible to hydrogen

peroxide, proteasome inhibition and apoptosis (Bretaud et al., 2007; Baulac et al., 2009). MOs have been used to target *lrrk2* in zebrafish (Sheng et al., 2010; Ren et al., 2011). A translation blocking MO caused severe embryonic lethality with decreased TH-labelling and expression in surviving larvae. A splice-blocking MO was used which deletes the WD40 domain of Lrrk2 and resulted in a weaker phenotype with loss of *Th* and *Dat* positive DA neurons, disorganized DA neuron axon tracts and locomotor defects (Sheng et al., 2010). A much milder phenotype was observed by Ren and collaborators (Ren et al., 2011) even though the same splice-blocking MO was used. Overall, the range of phenotypes arising from the loss of function of genes associated with familial PD resembles those observed in the current study on Parl. They were also suggestive of common pathways involving some of these genes, something for which we provide direct evidence in the case of *parla/b* and *pink1* (Fig. 2.6).

The amenability of zebrafish to genetic manipulations facilitates the elucidation of genetic interactions in a vertebrate model. The rescue of *parl* morphants by zebrafish *pink1* mRNA has implications for our understanding of Parl function in the study of Parkinson's disease. The ability of *pink1* to increase larval survival and to restore DA neuron patterning in *parl* morphants suggests that the same epistatic relationship between the *parl* genes and the PD-related *pink1* gene exists in a vertebrate model as in the invertebrate, *Drosophila*. Investigations of this conserved genetic pathway in zebrafish, a vertebrate model organism, may prove to be beneficial in the understanding of Parkinson's disease and, possibly, in the development of therapeutic strategies.

2.6 ACKNOWLEDGEMENTS

We thank Dr Dennis Bulman for communication of results prior to publication, Dr Luc Poitras, Gary Hatch and Dr Mélanie Debiais-Thibaud for advice and discussions, Vishal Saxena for

zebrafish husbandry and Dr M. Emdadul Haque for the human *PINK1* cDNA clones. This work was supported by the Canadian Institutes of Health Research (grant no. MOP-93803) and by the Ottawa chapter of the Parkinson Society of Canada. The authors declare no competing interests.

CHAPTER 3.

TRANSGENIC ZEBRAFISH EXPRESSING MITOCHONDRIAL TARGETED mCHERRY SPECIFICALLY IN DOPAMINERGIC NEURONS

3.1 ABSTRACT

In order to visualize mitochondria in dopaminergic neurons of live zebrafish, we used the regulatory elements of the *dopamine transporter* (*dat*) to drive the expression of an mCherry reporter in the dopamine neurons of a transgenic zebrafish line, Tg(*dat*:*tom20 MLS-mCherry*). In this transgenic line, mCherry was targeted to the mitochondria by fusing mCherry in frame with the mitochondrial localising signal (MLS) of Tom20. Western blotting analysis of both mitochondrial fractions and cytosolic fractions from transgenic zebrafish larvae show that mCherry is indeed targeted to the mitochondria. We have taken confocal images of live fish to characterize the transgenic line from 1 day-post-fertilization (dpf) to 9 dpf. In addition, using combined fluorescent whole-mount *in situ* hybridization and immunostaining on fixed larvae, we localized *dat* mRNA expression and the mCherry protein as well as *tyrosine hydroxylase* (*th1*) mRNA expression and the mCherry protein. Treating these transgenic larvae with the dopaminergic neurotoxin MPTP at 1mM, starting at either 2 dpf or 3 dpf, resulted in a visible and significant decrease in fluorescence of mCherry positive dopamine neurons compared to untreated larvae.

3.2 INTRODUCTION

Mitochondria are responsible for energy production, apoptosis, calcium storage, signalling events and metabolism. Dysfunctional mitochondria and oxidative metabolism are two theories

that may explain nigrostriatal dopaminergic (DA) neurodegeneration in Parkinson's disease (PD). Mitochondria may contribute to DA neuron cell death in PD due to changes in their membrane potential or in their structure and dynamics (Schapira, 2011; Dexter and Jenner, 2013). A defect in cellular energy production could predispose the DA neurons to death following exposure to other toxin or genetic defects, all together increasing the neuron's susceptibility to apoptosis. In a healthy neuron, the production and clearance of harmful oxidants which are produced from cellular metabolism are tightly regulated (Lang and Lozano, 1998a). It has been suggested that in PD patients there is an abundance of reactive oxygen species and increased oxidative stress.

To facilitate the study of mitochondrial function under specific physiological and/or genetic conditions, some tools which allow us to visualize mitochondria are available. Mitochondria in the somites and pharyngeal arch are visible by confocal microscopy in transgenic zebrafish embryos expressing EGFP targeted to the mitochondria under the control of a ubiquitous promoter which demonstrates that live imaging of mitochondrial fusion and fission events is possible *in vivo* (Kim et al., 2008). In addition, the transport and trafficking of mitochondria in Rohon-Beard sensory nerve cells is visible in distal axon branches at the thin rim of the fin fold where the cell membrane is labeled with YFP and the mitochondria are labeled with CFP (Plucińska et al., 2012). Another strategy which has been used to visualise mitochondria in live zebrafish embryos is the transient labeling of mitochondria by injection of a construct coding for a fusion protein between the mitochondrial localizing signal of the zebrafish cytochrome c oxidase subunit VIII and EGFP (Rahn et al., 2013). These transgenic and transient models label the whole fish or the entire nervous system, but none have looked in the brain nor specifically at DA neurons.

In this study, we have developed a transgenic mitochondrial zebrafish model which specifically labels the mitochondria of DA neurons in the zebrafish by creating a fusion protein between the mitochondrial localising signal (MLS) of Tom20 and the mCherry fluorescent protein all under the control of the *cis*-regulatory elements of the *dopamine transporter* (*dat*). This transgenic line allowed the observation of mitochondria in real-time specifically in DA neurons in order to better our understanding of the pathogenesis of PD following chemical neurotoxin exposure. By exposing the fish to a DA neurotoxin, MPTP, we demonstrated the ability to target mitochondria and induce mitochondrial damage in vivo.

3.3 MATERIALS AND METHODS

3.3.1 ANIMAL MAINTENANCE

All experiments were performed according to the guidelines of the Canadian Council on Animal Care and were approved by the University of Ottawa animal care committee. Zebrafish and embryos were maintained at 28.5^{o}C according to methods described in (Westerfield, 2000). Wild-type adult zebrafish were kept and bred in water at 28.5^{o}C with a controlled 14-h light cycle. Embryos were collected at the one-cell-stage. A Narishige IM300 microinjector was used for microinjection. Embryos were raised at similar densities at 28.5^{o}C. Embryos were killed with an overdose of tricainemesylate (ethyl 3-aminobenzoate methanesulfonate; Sigma-Aldrich, Oakville, ON, Canada).

3.3.2 TRANSGENIC CONSTRUCT AND ZEBRAFISH TRANSGENESIS

To prepare the targeting construct we used pBluescript II KS+ as a backbone and placed mCherry downstream and inframe with the translational start site of the zebrafish *tom20* MLS, which was a generous gift from Dr. Philippe Vernier's lab in France. Downstream of mCherry

we included a stop codon followed by a floxed Neomycin resistance (Neo^R) cassette. We used the same *cis*-regulatory elements used to create the Tg(*dat:EGFP*) transgenic line. Flanking this targeting construct, we included two arms (Arm A and Arm B, about 250 bp each) which are sequences homologous to the region of the *dat* locus flanking the EGFP sequence in the construct used to generate the Tg(*dat:*EGFP) transgenic line. Exon 1 of *dat* and the ATG within it was not included in Arm A, thus the translational start site of the construct is located at the ATG of the *tom20* MLS. The pBluescript II KS+ targeting construct was digested with the *Not*I enzyme to linearize the targeting fragment of about 3kb. To insert this targeting fragment into the *dat* plasmid by homologous recombination we electroporated the DY380 electrocompetent *E. coli* strain which contains a temperature inducible RecET homologous recombination system (Liu et al., 2003) and already contained the dat:EGFP construct. These cells already contained the Tg(*dat:EGFP*) BAC sequence with the cis-regulatory elements of the *dat* gene flanked by Tol2 arms from previous work we have published (Xi et al., 2011b). These Tol2 arms, when co-injected with transposase mRNA (35 ng/µL), facilitate efficient integration of the targeting vector (50 ng/µL) into the genome of the zebrafish when injected into embryos at the one-cell stage. We screened for positive recombined colonies using the neomycin antibiotic followed by PCR with a pair of primers anchored at the 3' end of the Neo^R and in exon 2 of *dat*. The recombinant plasmid was injected into WT zebrafish embryos at the one-cell stage, followed by fluorescent screening for mCherry positive DA neurons. Primary injected fish were raised to adulthood and screened for germline transmission by out-crossing with WT fish.

3.3.3 WESTERN BLOTTING AND MITOCHONDRIA ISOLATION

Mitochondrial and cytosolic fractions were prepared from 5 dpf fish using the Mitochondria Isolation Kit for Tissue (Thermo Scientific, Rockford, IL, US). Protein concentration was

determined by bicinchoninic acid (BCA) assay and 20 µg was loaded into each lane of a 12% SDS-PAGE gel. The following antibodies were used for western blotting: rabbit anti-dsRed (1:1000) (Clontech, Mountain View, CA, US), rabbit anti-actin (1:1000) (Sigma-Aldrich, Oakville, ON, Canada), rabbit anti-VDAC1/Porin (1:1000) (Abcam, Boston, MA, US), donkey anti-rabbit-IgG-HRP antibody (1:5000) (GE Healthcare, Little Chalfont, Buckingshire, UK).

3.3.4 LIVE TWO-PHOTON CONFOCAL IMAGING

Live embryos and larvae were embedded in 1% low melting point agarose and imaged using a Nikon A1 MP Multiphoton Confocal Microscope equipped with a 25X water dipping objective. Max intensity projection images are composed of z-stacks approximately 200 µm in thickness.

3.3.5 COMBINED FLUORESCENT WHOLE-MOUNT *IN SITU* HYBRIDIZATION AND IMMUNOSTAINING

For *in situ* and immunostaining experiments, 3 dpf larvae were fixed in 4% paraformaldehyde, washed in PBST and dehydrated in methanol and stored at -20°C. A *tyrosine hydroxylase* (*th*) cRNA probe and a *dopamine transporter* (*dat*) cRNA probe were synthesised as described previously (Xi et al., 2011b) and labeled with digoxigenin and developed using Tyr-Cy3 (Perkin-Elmer, Woodbridge, Ontario). The following antibodies were used to detect mCherry: rabbit anti-dsRed (Clontech, Mountain View, CA, US) and anti-rabbit AlexaFluor® 488 (Molecular Probes, Burlington, ON, Canada). For *in situ* and immunostaining experiments, larvae were mounted on slides and images were acquired with a Zeiss LSM 510 upright confocal microscope equipped with a 20X air objective.

3.3.6 MPTP TREATMENT

MPTP (1-Methyl-4-phenyl-1,2,3,6-tetrahydropyridine; Sigma-Aldrich, Oakville, ON, Canada) was dissolved at 10 mM in autoclaved MilliQ water and used at a working concentration of 1 mM in 1X embryo media. mCherry positive embryos and larvae were exposed to MPTP starting at either 48 hpf or 72 hpf with daily fresh MPTP-containing media changes. Control fish received 1X embryo media only. Live fish were imaged by confocal microscopy as described above.

3.3.7 STATISTICAL ANALYSIS OF FLUORESCENCE QUANTIFICATION

Differences in mean fluorescent intensity were analyzed by two-tailed unpaired Student's t-tests with three biological replicates. Z-stacks comprising individual DA neuron regions were compiled and fluorescence pixel intensity was measured using ImageJ. DA neuron regions from control fish were compared to those from fish treated with 1 mM MPTP. Predetermined p-values ≤ 0.05 were considered statistically significant ($p < 0.05$, $p < 0.01$, $p < 0.001$). All analyses were performed using Excel (Microsoft).

3.4 RESULTS

3.4.1 TRANSGENIC CONSTRUCT DESIGN FOR THE ESTABLISHMENT OF A TRANSGENIC ZEBRAFISH LINE

Based on a construct we previously used to generate a Tg(*dat:EGFP*) zebrafish transgenic line expressing EGFP under the control of the cis-regulatory elements of the *dat* gene (Xi et al., 2011b), we designed a new construct (figure 3.1A) to express a fluorescent fusion protein targeted to the outer mitochondrial membrane by fusing mCherry with the mitochondrial

localizing signal (MLS) of zebrafish *tom20*, coding for a receptor located in the outer mitochondrial membrane and that is part of the mitochondrial translocation system (Kanaji et al., 2000).

Figure 3.1. Transgenic construct to produce Tg(*dat:tom20 MLS-mCherry*) zebrafish line. **(A)** The targeting vector was designed to contain two homologous arms, A and B (yellow). These arms facilitated the replacement of the EGFP (green), previously used in the generation of the Tg(*dat:EGFP*) transgenic line, with the fusion protein between the mitochondrial localising signal (MLS) of Tom20 (light blue) and mCherry (red). Tol2 left and right arms (light green) flanking the sequence enhance transgenesis efficiency. Neomycin resistance cassette (Neo^R) was flanked by loxP sites (arrow heads). Polyadenylation signals (pA) are shown in grey. Exons of the *dat* gene are depicted by black boxes. The total size of the inserted DNA is 27 kb, containing the *dat* genomic sequence except for the last coding exon and 3'-flanking region. **(B)** Western blotting demonstrates that the mCherry protein is localized to the mitochondria of transgenic fish. Mitochondria were isolated from Tg(*dat:tom20 MLS-mCherry*) and WT larvae at 5 dpf. mCherry was abundantly detected in the mitochondrial fraction of transgenic larvae, but was not as prominent in the cytosolic fraction. The voltage-dependent anion selective channel protein 1 (VDAC1) was used as a mitochondrial marker and Actin was used as a cytosolic marker. Western blots are representative of at least two independent experiments.

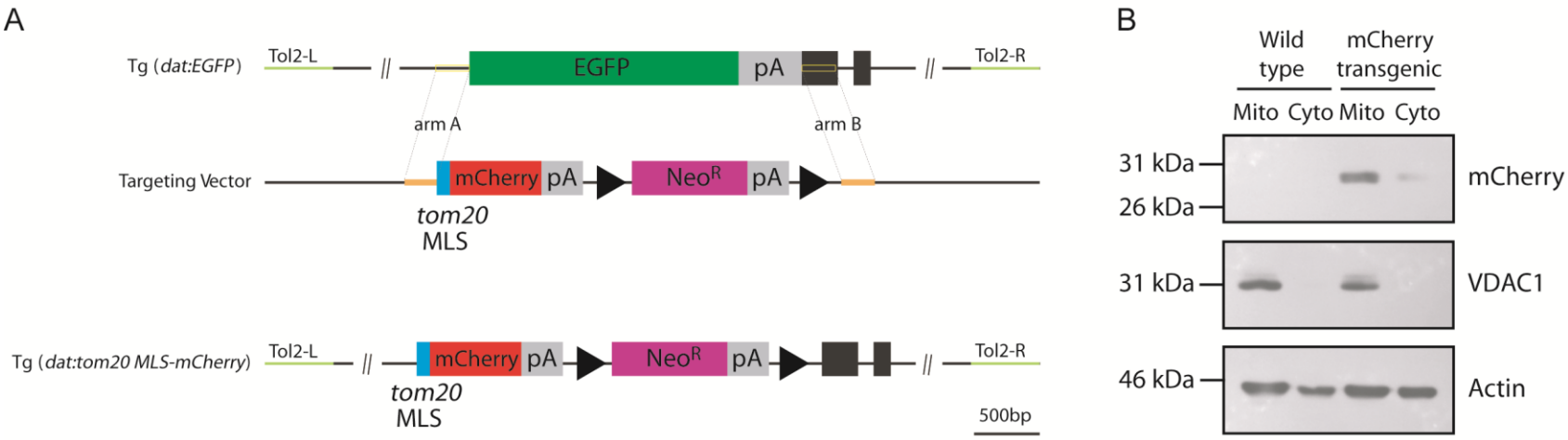
A
Tg (dat:EGFP)
Tol2-L
EGFP
pA
Tol2-R
arm A
arm B
Targeting Vector
mCherry
pA
NeoR
pA
tom20
MLS
Tg (dat:tom20 MLS-mCherry)
Tol2-L
mCherry
pA
NeoR
pA
Tol2-R
tom20
MLS
500bp
B
Wild type
mCherry transgenic
Mito Cyto Mito Cyto
31 kDa
26 kDa
mCherry
31 kDa
VDAC1
46 kDa
Actin

We injected the recombined plasmid into one-cell stage WT embryos and screened for mCherry positive fluorescent DA neurons. Primary injected fish were raised to adulthood (approximately 4 months) and screened for germ line transmission by out-crossing with WT fish. From these injections, we obtained seven transgenic lines. For further studies we chose line 1 which expressed strong mCherry fluorescence in several DA neuron clusters (figure 3.2A and 3.2B). Furthermore, the subpallial region which is believed to be the area responsible for movement in zebrafish was also labeled in this line. The expression pattern of mCherry in the chosen line was observed in a total of three lines. While this study was underway, we identified another line which had weaker expression of mCherry in the pretectum, but stronger expression in the ventral diencephalon (vDC), however since these DA neurons are deeper in the brain they were harder to image and thus this line was not selected for further analysis (figure 3.2A and 3.2B). The differences in mCherry expression in these lines could be due differences in the mCherry intensity and/or an insertional effect.

Figure 3.2. mCherry expression in the Tg(*dat:tom20 MLS-mCherry*) line. (A) Live dorsal and lateral composite fluorescent and bright field images of 3 day-old larvae taken with a dissecting microscope. The following clusters of cells express mCherry: olfactory bulb (OB); subpallium (SP); pretectum (Pr); diencephalic clusters 2 and 3 (2/3); caudal hypothalamus (Hc); midbrain hindbrain boundary (MHB); locus coeruleus (LC). Fluorescence ventral to the eye (in the jaw) is likely ectopic. **(B)** Two-photon confocal live images taken from 2 dpf to 9 dpf. Images are dorsal facing up and anterior facing left. All scale bars represent 50 μm.

A

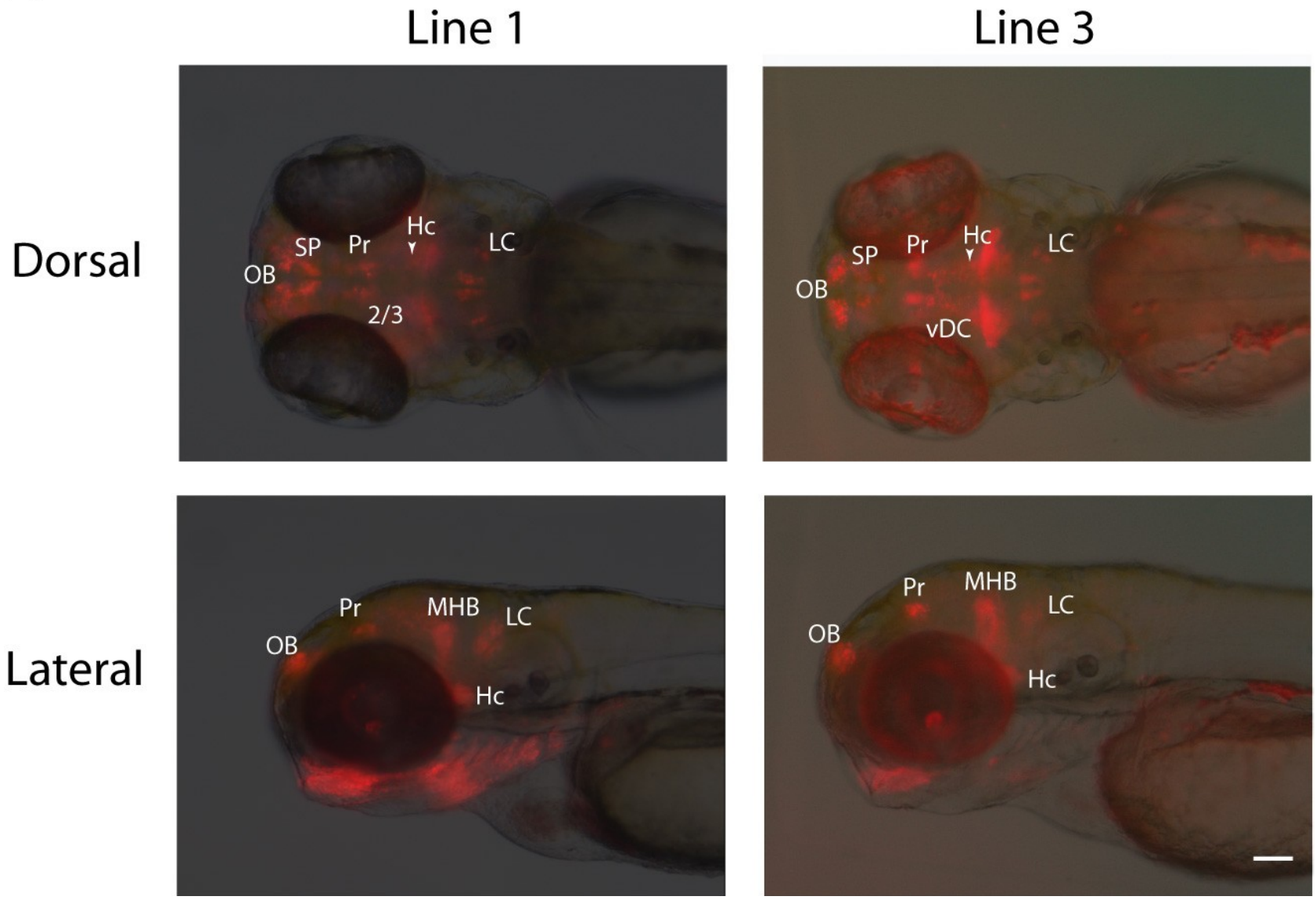

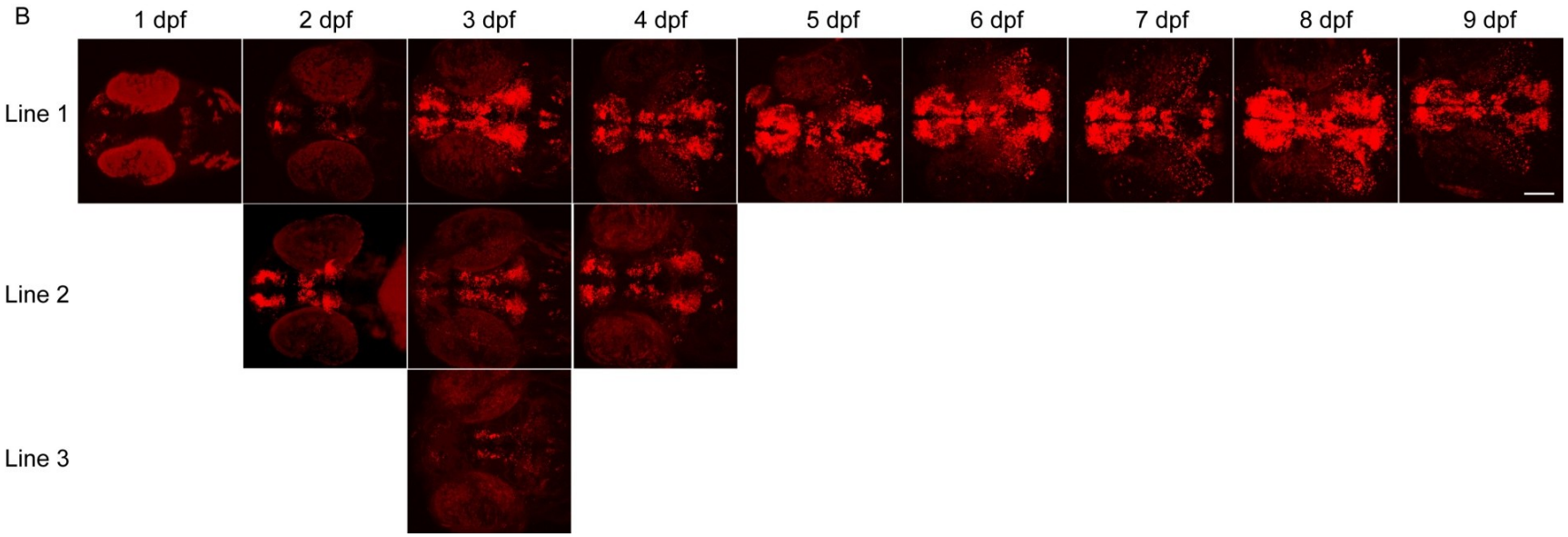
B
1 dpf
2 dpf
3 dpf
4 dpf
5 dpf
6 dpf
7 dpf
8 dpf
9 dpf
Line 1
Line 2
Line 3

3.4.2 mCherry is properly targeted to the mitochondria in transgenic zebrafish

We isolated mitochondria from transgenic larvae at 5 dpf and compared the amounts of the mCherry protein in the mitochondrial fraction to that in the cytosolic fraction by western blotting (figure 3.1B). A band representing mCherry is detected in the mitochondrial fraction from transgenic fish, while a low amount of mCherry is detected in the cytosolic fraction of transgenic fish likely due to the transient transport of the Tom20 MLS-mCherry fusion protein to the mitochondria. The voltage-dependent anion selective channel protein 1 (VDAC1/Porin) was used as a mitochondrial control, whereas Actin was used as a cytosolic control.

3.4.3 Co-localization of mCherry patterning with dopaminergic neuron markers in transgenic zebrafish larvae

We examined the expression of mCherry in the transgenic Tg(*dat:tom20 MLS-mCherry*) zebrafish line. mCherry fluorescence in this line is visible within the first 24 hpf which is in agreement with observations of DA neuron characterization from the Driever lab (Tay et al., 2011). We have three transgenic lines which express mCherry in the olfactory bulb (OB), subpallium (SP), pretectum (Pr), diencephalic clusters 2 and 3 (DC2 and DC3), caudal hypothalamus (Hc) (figure 3.2) and retinal amacrine cells (RAC) (figure 3.3). Using the same construct, we also obtained a separate line which strongly expresses mCherry in the vDC. Global dorsal and lateral views of live larvae were taken at 3 dpf to compare the overall mCherry expression in the two lines (figure 3.2A). In addition, two-photon confocal images were also taken from 2 dpf to 9 dpf (figure 3.2B). The pattern observed in the Tg(*dat:tom20 MLS-mCherry*) fish closely resembles the pattern of EGFP expression seen in the Tg(*dat:EGFP*) line, with the exception of some clusters in the ventral diencephalon.

Figure 3.3. mCherry co-localization with *th* and *dat* in transgenic zebrafish larvae. Fluorescent whole-mount *in situ* hybridization using a fluorescent cRNA probe for *tyrosine hydroxylase* (*th*) or the *dopamine transporter* (*dat*) both shown in blue in combination with immunostaining using an antibody against the mCherry reporter shown in red at 3 dpf. DA neuron groups are labeled: Olfactory bulb (OB); subpallium (SP); pretectum (Pr); diencephalic neuron groups 2 and 3 (DC2 and DC3); caudal hypothalamus (Hc); locus coeruleus (LC); retinal amacrine cells (RAC). Images were taken with an upright LSM 510 confocal microscope equipped with a 20X air objective. Each image is a rendered series of z-stacks of approximately 90 µm thick. Scale bar represents 50µm. All images are dorsal facing up and anterior facing left.

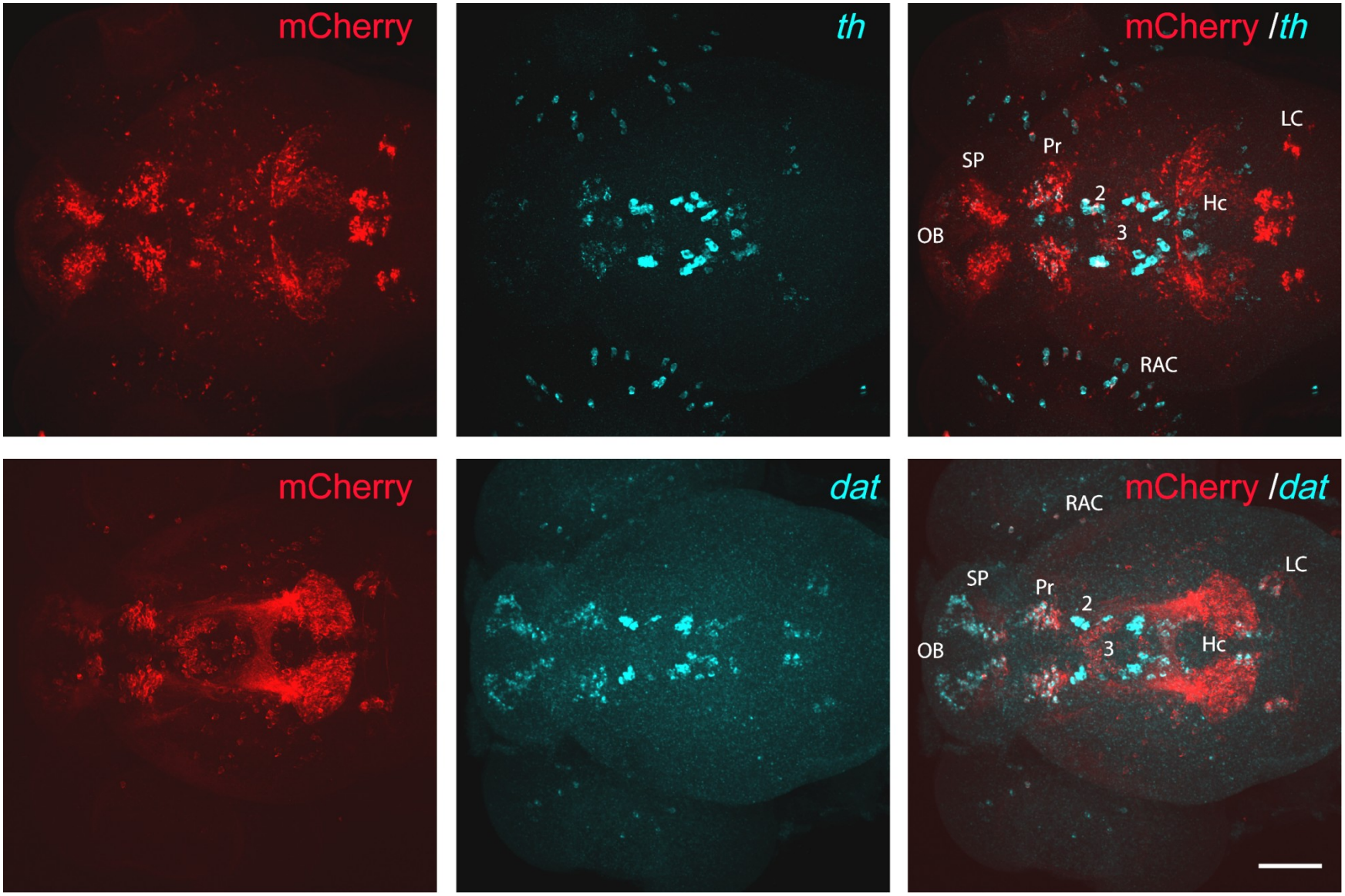
mCherry
th
mCherry /th
LC
Pr
SP
2
Hc
OB
3
RAC
mCherry
dat
mCherry /dat
RAC
LC
SP
Pr
2
OB
3
Hc

We co-localized the mCherry reporter by whole-mount immunostaining with either *tyrosine hydroxylase* (*th1*) or the *dopamine transporter* (*dat*) by whole-mount *in situ* hybridization (figure 3.3). The analysis of individual z-stacks revealed co-localisation between mCherry and *th1* in the pretectum (Pr), subpallium (SP), diencephalic clusters 2 and 3 (DC2 and DC3), olfactory bulb (OB), anterior preoptic area (POa), caudal hypothalamus (Hc), preoptic area (PO) and retinal amacrine cells (RAC) (figure 3.4A – D). Similar analysis revealed co-labeling between mCherry and *dat* positive cells in the pretectum (Pr), locus coeruleus (LC), diencephalic clusters 2 and 3 (DC2 and DC3), olfactory bulb (OB), subpallium (SP), anterior preoptic area (POa), retinal amacrine cells (RAC), caudal hypothalamus (Hc) and preoptic area (PO) (figure 3.5A – E). However, certain *th1* positive (figure 3.4C – C") and *dat* positive (figure 3.5B – C") diencephalic clusters, namely DC4, DC5 and DC6, did not appear to be labeled in our Tg(*dat:tom20 MLS-mCherry*).

3.4.4 MPTP NEUROTOXIN TREATMENT REDUCES MCHERRY EXPRESSION IN TG(*DAT:TOM20 MLS-MCHERRY*) LARVAE

In order to demonstrate that mitochondria could be targeted in the Tg(*dat:tom20 MLS-mCherry*) line, we exposed embryos to MPTP, which is a DA neurotoxin. At 2 dpf, dechorionated embryos were screened for mCherry fluorescence. Starting at 2 dpf, approximately 30 to 50 embryos were treated with 1 mM MPTP for 72 hours (figure 3.6A). A visible reduction of mCherry fluorescence in live MPTP treated fish was distinguishable from untreated fish at 120 hours post-fertilization (figure 3.6B) and 144 hours post-fertilization (figure 3.6C). We quantified the fluorescent pixel intensity representing the mCherry signal in five separate regions of DA neurons in control and MPTP treated fish using ImageJ software. Composite z-stacks of each DA

region were analysed individually. At 120 hpf, a significant decrease in fluorescence was observed in the pretectum (29%, $p < 0.05$), olfactory bulb (33%, $p < 0.05$), subpallium (34%, $p < 0.05$), DA neuron clusters 2 and 3 (40%, $p < 0.05$) and caudal hypothalamus (Hc) (44%, $p < 0.05$). Moreover, the observed decrease in mCherry signal was more pronounced at 144 hpf in the pretectum (32%, $p < 0.05$), olfactory bulb (41%, $p < 0.01$), subpallium (55%, $p < 0.01$), DA neuron clusters 2 and 3 (57%, $p < 0.05$) and caudal hypothalamus (Hc) (62%, $p < 0.01$). Similar effects were observed when MPTP treatment was started at 3 dpf and continued for 48 hours (data not shown). Overall, these results suggest that these DA neuron regions in the Tg(*dat:tom20 MLS-mCherry*) line are susceptible to the neurotoxin, MPTP, which targets mitochondria in DA neurons.

Figure 3.4. Confocal z-stacks of mCherry co-localization with *tyrosine hydroxylase* (*th1*) in transgenic zebrafish at 3 dpf. mCherry (red) and *th1* (blue) positive cells are labeled in individual 6.4-µm thick optical sections. DA neuron groups are labeled: pretectum (Pr); subpallium (SP); diencephalic clusters 2 and 3 (DC2 and DC3); olfactory bulb (OB); anterior preoptic area (POa); caudal hypothalamus (Hc); preoptic area (PO); and retinal amacrine cells (RAC). Regions which co-localize have white labels. Regions which do not appear to co-localize are labeled in blue (DC4, DC5 and DC6). Images were taken with an upright LSM 510 confocal microscope equipped with a 20X air objective. Scale bar represents 50µm. All images are dorsal facing up and anterior facing left.

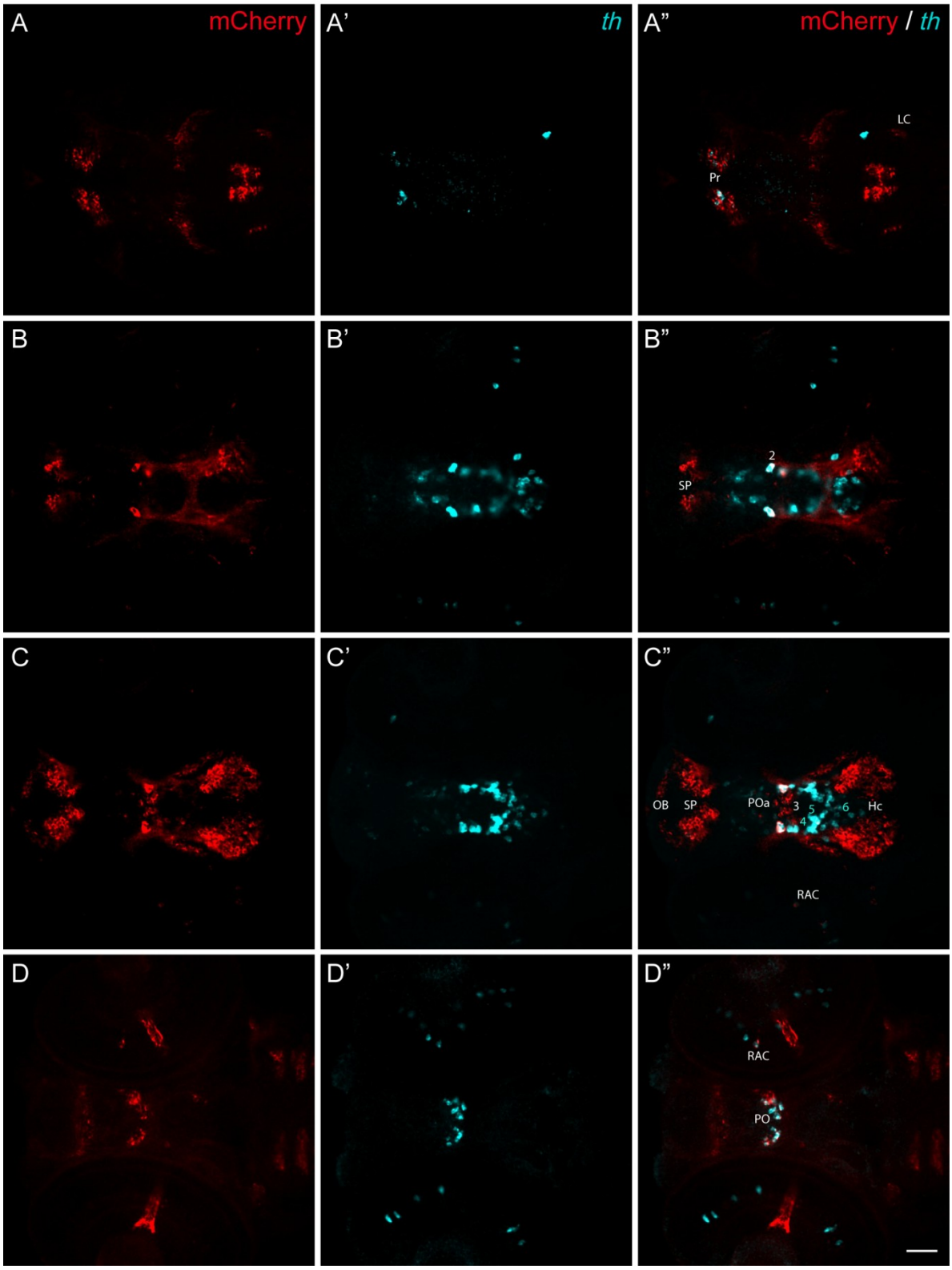
3 dpf
A
mCherry
A'
th
A"
mCherry / th
LC
Pr
B
B'
B"
2
SP
C
C'
C"
OB
SP
POa
3
5
4
6
Hc
RAC
D
D'
D"
RAC
PO

Figure 3.5. Confocal z-stacks of mCherry co-localization with *dopamine transporter* (*dat*) in transgenic zebrafish at 3 dpf. mCherry (red) and *dat* (blue) positive cells are labeled in individual 6.4-µm thick optical sections. DA neuron groups are labeled: pretectum (Pr); locus coeruleus (LC); diencephalic clusters 2 and 3 (DC2 and DC3); olfactory bulb (OB); subpallium (SP); anterior preoptic area (POa); retinal amacrine cells (RAC); caudal hypothalamus (Hc); and preoptic area (PO). Regions which co-localize have white labels. Regions which do not appear to co-localize are labeled in blue (DC4, DC5 and DC6). Images were taken with an upright LSM 510 confocal microscope equipped with a 20X air objective. Scale bar represents 50µm. All images are dorsal facing up and anterior facing left.

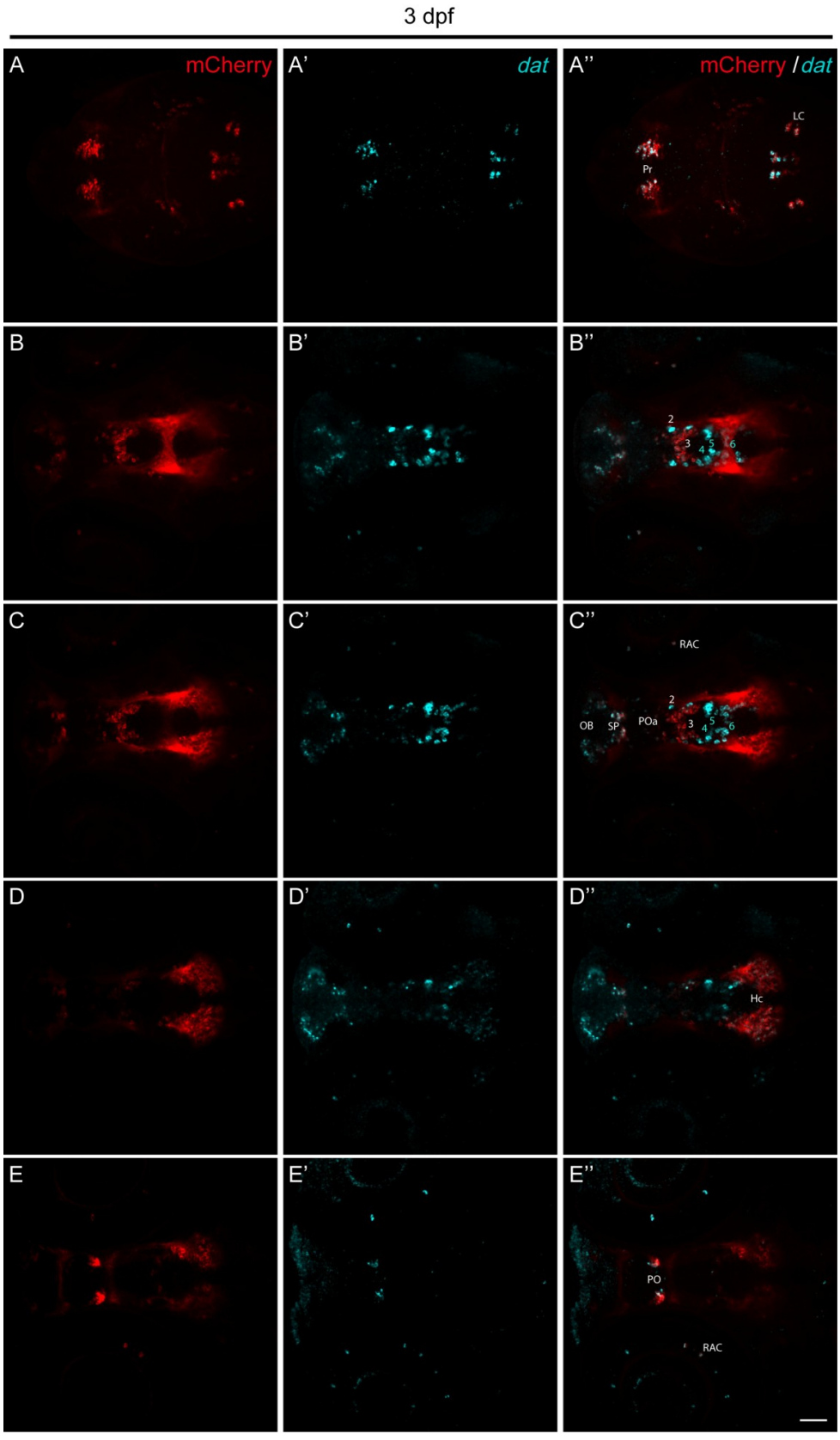
3 dpf
A
mCherry
A'
dat
A''
mCherry / dat
LC
Pr
B
B'
B''
2
3
4
5
6
C
C'
C''
RAC
OB
SP
POa
2
3
4
5
6
D
D'
D''
Hc
E
E'
E''
PO
RAC

Figure 3.6. MPTP neurotoxin exposure in transgenic larvae. (A) 1 mM MPTP treatment started at 48 hpf visibly diminished mCherry fluorescence at 120 hpf and 144 hpf compared to control untreated larvae. The treatment regime is shown above with images corresponding to each time point below. Quantification of fluorescent pixel intensity at 120 hpf **(B)** and 144 hpf **(C)** revealed a significant reduction in mCherry labeled DA neuron regions: pretectum (Pr); olfactory bulb (OB); subpallium (SP); diencephalic clusters 2 and 3 (DC2 and DC3); and caudal hypothalamus (Hc). Confocal images are representative of at least three independent experiments with 30 – 50 embryos per treatment and control group. Scale bar represents 50μm. All images are dorsal facing up and anterior facing left.

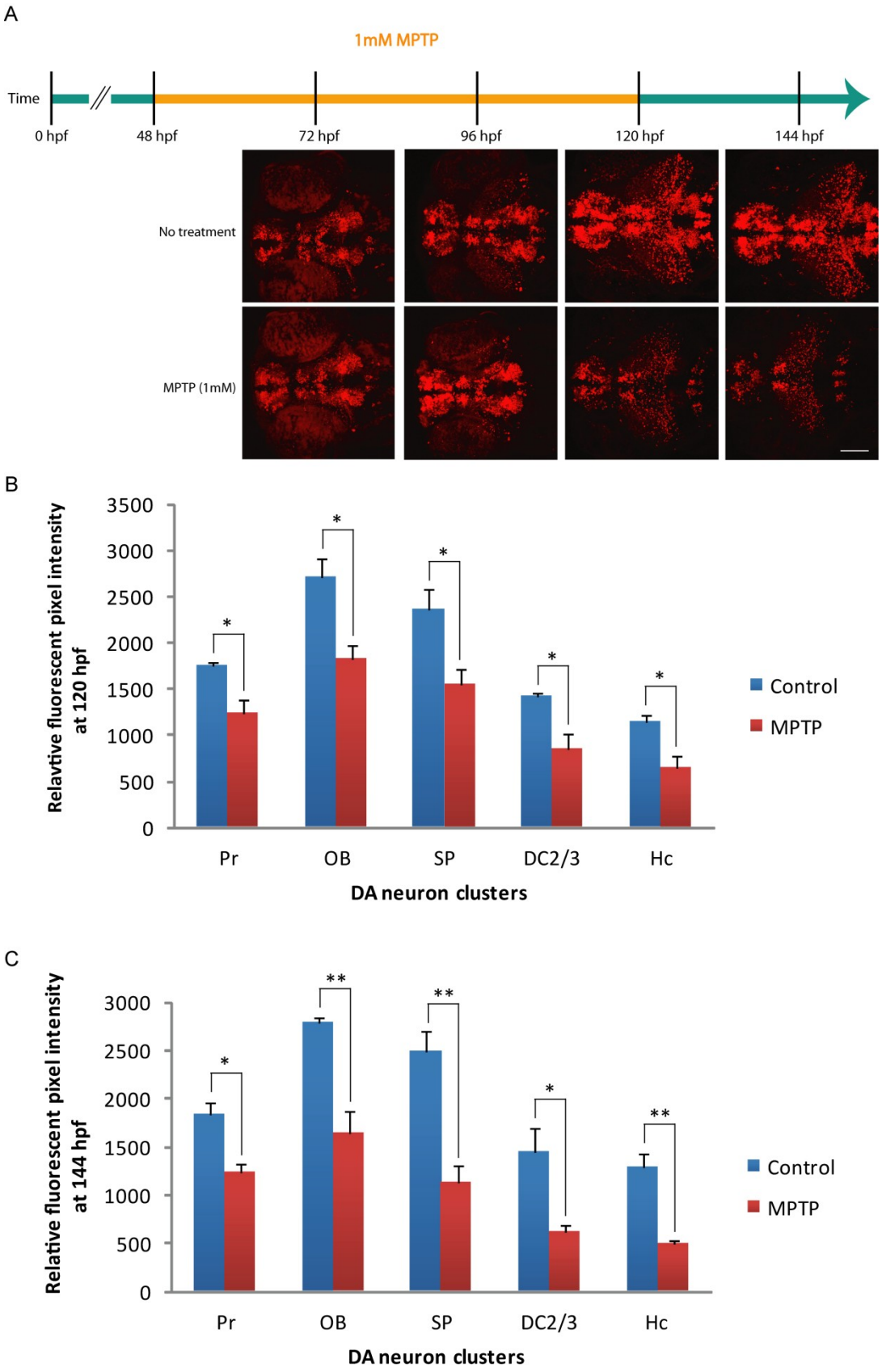
A
1mM MPTP
Time
0 hpf
48 hpf
72 hpf
96 hpf
120 hpf
144 hpf
No treatment
MPTP (1mM)
B
Relavtive fluorescent pixel intensity at 120 hpf
3500
3000
2500
2000
1500
1000
500
0
Pr
OB
SP
DC2/3
Hc
DA neuron clusters
Control
MPTP
C
Relative fluorescent pixel intensity at 144 hpf
3000
2500
2000
1500
1000
500
0
Pr
OB
SP
DC2/3
Hc
DA neuron clusters
Control
MPTP

3.5 DISCUSSION

We generated a transgenic zebrafish model for the study of mitochondria specifically in DA neurons. Using Tg(*dat:tom20 MLS-mCherry*) embryos and larvae, we observed a significant reduction in mCherry fluorescence in the olfactory bulb, pretectum, subpallium and diencephalic clusters 2 and 3 and caudal hypothalamus following MPTP exposure for 3 days compared to untreated fish. Our findings are in agreement with other MPTP studies in zebrafish which show selectively perturbed DA neurons and results in behavioural deficits which mimic PD (Anichtchik et al., 2004; Bretaud et al., 2004; Lam et al., 2005; McKinley et al., 2005; Wen et al., 2008; Sallinen et al., 2009; Xi et al., 2011b).

Once the active form of MPTP, MPP+, enters a DA neuron, MPP+ targets mitochondria and inhibits complex I of the electron transport chain (ETC) leading to cellular energy depletion and reduction in DA cell markers. As a consequence, MPTP is used in research to model dopamine deficiency, since it causes a 30 to 40 percent decrease in complex I activity in the substantia nigra pars compacta (Mann et al., 1992). McKinley and colleagues have previously shown that the mechanism of DA neuron toxicity induced by MPTP is conserved in zebrafish (McKinley et al., 2005). Using our transgenic model, strategies can be designed to prevent DA neuron loss, specifically at the level of mitochondrial dysfunction.

The case of MPTP toxicity points out that PD could be the result of one single event as opposed to a continual insult to the brain (Lang and Lozano, 1998a). Although, it may appear that only one insult is at the root of the disease, a predetermined genetic susceptibility may also be at play. In fact, most PD patients do not have a clear family history of autosomal dominant PD, suggesting that the gene(s) associated with the disease has(have) a low penetrance or that the

cause of the disease is multifactorial, meaning that a combination of genetic predisposition and environmental exposure may be required.

Interestingly, dopamine metabolism may produce toxic by-products which could increase the oxidative state of DA neurons in PD patients (Jenner, 1998; Dexter and Jenner, 2013). If this is true, then prescribing levodopa, a dopamine precursor may actually be harmful and hasten cell death in the substantia nigra pars compacta. At one point this generated apprehension among some patients which resulted in the decision to delay the use of levodopa treatment (Olanow, 1992); however, the possibility that levodopa has toxic effects is not widely accepted based on the clinical observations that humans without Parkinson's disease who are given levodopa do not show signs of its toxicity (Rajput et al., 1997; Parkkinen et al., 2011).

We described the patterning of DA neurons in the Tg(*dat:tom20 MLS-mCherry*) line and observed a Parkinson's disease-relevant phenotype following exposure of these fish to MPTP. The amenability of zebrafish to transgenesis and drug exposure facilitated our observation of mitochondria within specific DA cell populations and allowed us to examine changes following neurotoxin exposure. Since dysfunctional mitochondria may contribute to DA neuron death and mitochondria are known to possess a dynamic morphology that is regulated by mitochondrial shaping proteins (Cipolat et al., 2006), our transgenic line can be used in the context of neurodegeneration and mitochondrial dynamics (fusion and fission) specifically in DA neurons *in vivo*.

CHAPTER 4.

ANALYSIS OF CLEAVAGE PATTERNS OF THE ZEBRAFISH PARL PROTEINS

4.1 INTRODUCTION

PARL belongs to a subfamily of rhomboid proteins that functions as an intramembrane serine protease (McQuibban et al., 2003). Vertebrate specific phosphorylation and cleavage sites that are important for mitochondrial morphology have been located (Sik et al., 2004). In mammalian vertebrates, the phosphorylation state of this site dictates whether or not PARL will be cleaved and subsequently mediate mitochondrial fragmentation. Ultimately, induction of mitochondrial fragmentation triggers apoptosis. Identifying and characterizing these cleavage sites (if indeed they are conserved) in the two zebrafish Parl proteins could facilitate the functional study of the cleaved Parl peptides in the zebrafish model.

The N-terminal domain of human PARL harbors two consecutive cleavage sites (figure 4.1A). Overall, the N-terminal domain is poorly conserved between vertebrates, but is well conserved between mammals. Mammalian PARL is constitutively processed at the proximal α-cleavage site that is associated with PARL's import into mitochondria. Distal to the α-cleavage site is the β-cleavage site between residues Ser-77 and Ala-78. It is this serine at this β-cleavage site where a mutation was found in PD-patients (serine to an asparagine at codon 77 (Ser77Asn)) (Shi et al., 2011). PARL β-cleavage is thought to be executed either by PARL itself, supplied *in trans*, or by an unidentified PARLase. According to Sik and colleagues, β-cleavage occurs through a mechanism of proteolysis that requires an active form of PARL supplied *in trans* (Sik et al., 2004). However, typical rhomboid-mediated intramembrane proteolysis occurs within a

hydrophobic environment. Thus, since the β-cleavage site of PARL is not embedded within a hydrophobic transmembrane domain, it is unlikely that PARL cleaves itself (Pellegrini and Scorrano, 2007).

Figure 4.1. *parl*-Flag constructs. (A) Full-length mammalian PARL contains three cleavage sites: α, β and γ. Constitutive α-cleavage removes the MTS (blue) and is followed by β-cleavage only if PARL undergoes dephosphorylation at three residues: S65, T69 and S70 (yellow stars) within the Pβ domain (purple). **(B)** *parl*-Flag pGEM-4Z constructs were linearized with *Xba*I for mRNA synthesis using the T7 polymerase followed by mRNA microinjection into zebrafish embryos. **(C)** *parl*-Flag pcDNA3 constructs containing a CMV promoter were used for cell transfection. Each *parl*-Flag sequence was flanked by UTRs. **(D)** The quality of the synthesized mRNA was checked by running it on a 1% agarose gel.

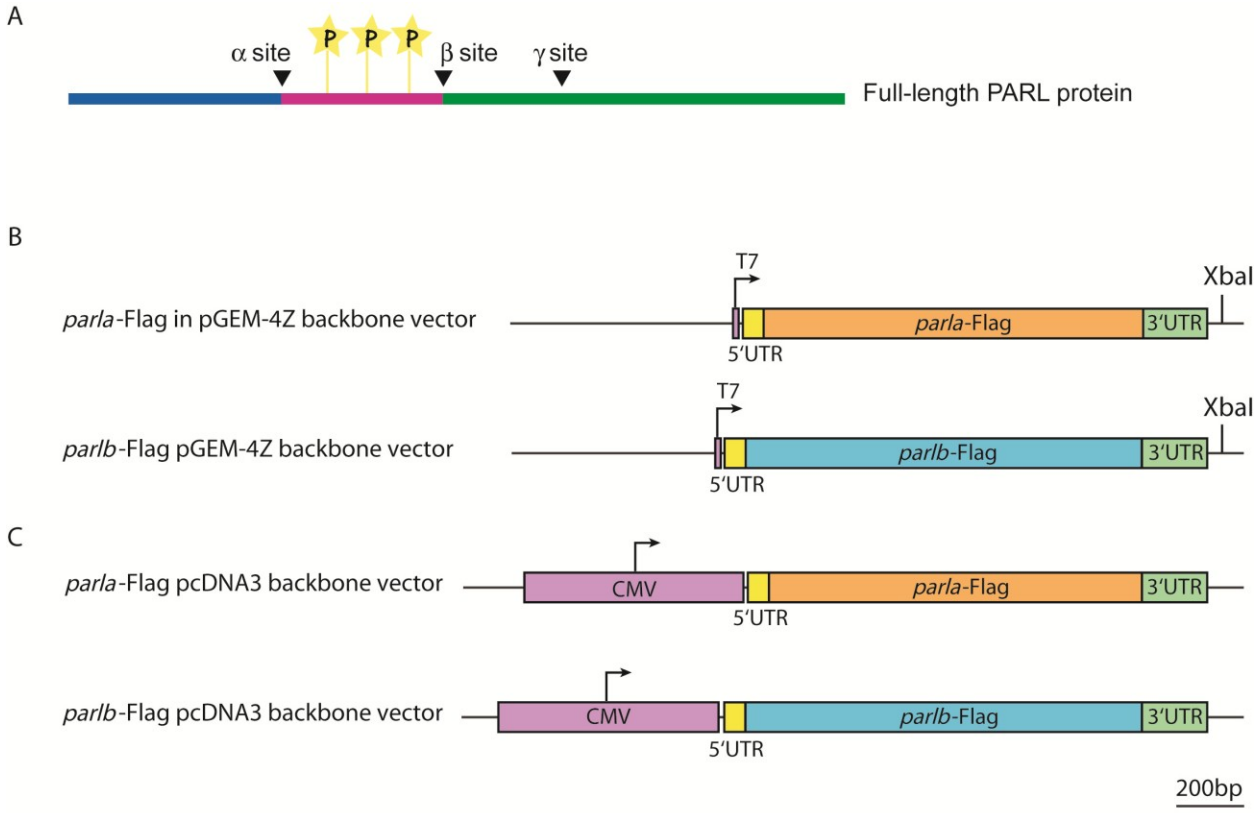
A
α site
P
P
P
β site
γ site
Full-length PARL protein
B
parla-Flag in pGEM-4Z backbone vector
T7
XbaI
parla-Flag
3'UTR
5'UTR
parlb-Flag pGEM-4Z backbone vector
T7
XbaI
parlb-Flag
3'UTR
5'UTR
C
parla-Flag pcDNA3 backbone vector
CMV
parla-Flag
3'UTR
5'UTR
parlb-Flag pcDNA3 backbone vector
CMV
parlb-Flag
3'UTR
5'UTR
200bp
D
parla-Flag
parlb-Flag
~ 1.2 kbases

The β-cleavage of PARL releases a Pβ peptide that may mediate mitochondria-to-nucleus signaling which appears to be under developmental control and might be linked to neuronal development (Sik et al., 2004). Phosphorylation of residues Ser-65, Thr-69, and Ser-70 within the Pβ domain inhibits PARL β-cleavage, and ultimately inhibits mitochondrial fragmentation (by preventing cytochrome c release) which subsequently promotes cell survival (Jeyaraju et al., 2006).

Recently, (Jeyaraju et al., 2011) mapped a third cleavage site, termed γ-cleavage. This site is likely located in Loop-A (amino acids 121-167 of mammalian PARL). Deleting $_{155}$INKWW$_{159}$, blocks the γ-cleavage product. This suggests that the γ-cleavage site is located within or near this sequence. The Jeyaraju group (2011) has suggested that in mammalian systems, γ-cleavage destabilizes PARL and may serve to negatively regulate PARL activity in mitochondria. The Jeyaraju group (2011) report that γ-cleavage is tissue specific in rats (spleen and kidney). Perhaps this tissue-specific negative regulation of PARL through γ-cleavage may explain how PARL plays a cell-specific role in DA neurons with respect to PD.

Commercially available anti-human PARL antibodies do not recognize the zebrafish Parls in either zebrafish or cell culture lysates. In addition, we tried making anti-Parla and anti-Parlb custom antibodies (Open Biosystems, 2 rabbit 70-day protocol) which did not result in specific bands in zebrafish lysates and no signal in immunoprecipitation (IP) experiments in cultured cells. The epitope for the rabbit anti-zebrafish Parla antibody was DAKADWLDKVRPQKHGD. The epitope for the rabbit anti-zebrafish Parlb antibody was RKREPLIKEWHELR.

We performed a number of experiments to test the Parla and Parlb antisera and affinity purified antibodies. We performed dot-blots to determine if we could detect any immuno-reactivity,

which we did, but this did not tell us if the detection was specific. In order to determine if the signal was specific to the Parl proteins, we ran lysates from WT zebrafish embryos and larvae as well as from embryos injected with *parla*-Flag and *parlb*-Flag mRNA. We compared the bands obtained following western blotting with the pre-bleed serum provided from Open Biosystems and the antisera and affinity purified antibodies. If any of the bands detected with the antisera or affinity purified antibody had been specific, then the band(s) should not have been detected in the blot incubated with the pre-bleed sera. This was not the case. We also blotted with a rabbit anti-Flag antibody; however, a number of non-specific bands were detected.

We pre-absorbed the rabbit anti-zebrafish Parla antibody and the rabbit anti-zebrafish Parlb antibody with their respective purified peptides which were used as antigens to immunize the rabbits. Any specific bands in the blot should not have been detected in the blot incubated with the pre-absorbed antibodies versus the non pre-absorbed antibodies. This was not the case.

We also ran an SDS-PAGE gel with a curtain of zebrafish protein lysates and tested a number of dilutions of the rabbit anti-zebrafish Parla antibody and rabbit anti-zebrafish Parlb antibody. Again, this did not result in better resolution of which bands were specific.

To overexpress the Parla-Flag and Parlb-Flag proteins as a positive control for western blotting, we performed an *in vitro* transcription and translation reaction using the TNT® Coupled Reticulocyte Lysate System (Promega, Madison, WI, USA). Unfortunately, this approach did not give us specific signal(s) above background, as all bands detected were also present in the negative control samples.

To concentrate the sample, we isolated mitochondrial fractions from cytosolic fractions, but again this did not help to clarify which bands were specific.

Finally, we transfected cells with the *parla*-Flag and *parlb*-Flag CMV constructs and isolated proteins by immunoprecipitation. We were able to detect specific bands of the correct sizes from blots with these eluates using a rabbit anti-Flag antibody (see below); however, the affinity purified Parla and Parlb antibodies showed no immuno-reactivity.

In this study, we investigated the cleavage patterns of the two zebrafish Parl proteins in zebrafish embryos and in neuronal as well as non-neuronal cell lines and compared them to the pattern described in mammals. This will help determine whether or not the zebrafish Parl proteins are structurally and functionally similar to their mammalian counterparts.

4.2 MATERIALS AND METHODS

4.2.1 ANIMAL MAINTENANCE

All experiments were performed according to the guidelines of the Canadian Council on Animal Care and were approved by the University of Ottawa animal care committee. Zebrafish and embryos were maintained at 28.5°C according to methods described in Westerfield (2000). Wild-type adult zebrafish were kept and bred in circulating fish water at 28.5°C with a controlled 14-h light cycle. Embryos were collected at the one-cell-stage. A Narishige IM300 microinjector was used for microinjection.

4.2.2 CONSTRUCT DESIGN FOR *PARLA*-FLAG AND *PARLB*-FLAG MRNA EXPRESSION IN ZEBRAFISH

parla and *parlb* cDNA sequences were PCR amplified with primers containing a 5' *Not*I site (*parla* forward primer: 5'GCGGCCGCATGGCGGTGAGGGGT3'; *parlb* forward primer: 5'GCGGCCGCATGGCATGGAGGAGCTGCTT3') and 3' *Xho*I site (*parla* reverse primer: 5' CTCGAGCTATCACTTATCGTCGTCATCCTTGTAATCCATAATGGAGCCGTTGCTGCCA

C3’; *parlb* reverse primer: 5’CTCGAGCTATCACTTATCGTCGTCATCCTTGTAATCCATACCCCCACCTCCACCTGG TC3’) immediately following an in frame Flag tag sequence followed by two stop sequences. Each amplicon was TA cloned into pDrive and subcloned using the *Not*I and *Xho*I enzymes between two *Xenopus* globin UTRs in the pGEM-4Z backbone vector containing a T7 promoter. The identity of the amplicons was verified by sequencing. The *parla*-Flag in pGEM-4Z and the *parlb*-Flag in pGEM-4Z were linearized with *Xba*I. *In vitro* mRNA synthesis was carried out using the T7 polymerase mMESSAGEmMACHINE kit (Ambion, Streetsville, ON, Canada). 50 pg of synthetic mRNA were microinjected into zebrafish embryos at the one-cell stage.

4.2.3 CONSTRUCT DESIGN FOR *PARL*-FLAG AND *PARLB*-FLAG TRANSFECTION IN CELL CULTURE

The *parla*-Flag and *parlb*-Flag sequences along with the *Xenopus* globin UTRs were subcloned from the pGEM-4Z vector using *Hind*III and *Xba*I into the pcDNA3 backbone vector containing a CMV promoter. WT human *PARL*-Flag and the PD-related mutant S77N human *PARL*-Flag constructs were a gift from Dr. Angus McQuibban (University of Toronto, Ontario, Canada). HEK cells were transfected using a calcium phosphate transfection method with 5 µg of plasmid in two 10-cm dishes. HeLa and SH-SY5Y cell lines were transfected in 10-cm dishes or 6-well plates with either 10 µg or 2 µg of plasmid, respectively using SuperFect® Transfection Reagent (Qiagen, Mississauga Ontario, Canada).

4.2.4 CELL CULTURE

A human HeLa cell line, a human HEK cell line and a human SH-SY5Y neuroblastoma dopaminergic neuron cell line were used. HeLa cells were cultured in EMEM supplemented with 10% FBS, 1% penicillin-streptomycin and 0.1% gentamicine. HEK cells were cultured in

EMEM supplemented with 10% FBS, 1% penicillin-streptomycin and 0.1% gentamicine. SH-SY5Y cells were cultured on poly-D-lysine (Sigma, Saint Louis, Missouri, US) coated plates in 1:1 Ham's F-12:EMEM supplemented with 10% FBS, 1% penicillin-streptomycin and 0.1% gentamicine. All cells were cultured at 37°C in 5% CO_2. HEK cells were a gift from Dr. Mario Tiberi and SH-SY5Y cells were a gift from Dr. Michael Schlossmacher.

4.2.5 IMMUNOPRECIPITATION AND WESTERN BLOTTING

At least 150 zebrafish embryos were manually dechorionated and deyolked prior to homogenization with a pestle and mortar. Cell lines were washed in PBS prior to solubilisation. Samples from both zebrafish and cells were solubilised in RIPA buffer containing protease inhibitors and solubilised for two hours. Protein concentration was quantified by protein BCA assay. Solubilised protein lysates were centrifuged and incubated with anti-Flag M2 mouse IgG antibody covalently linked to agarose beads (Sigma, Saint Louis, Missouri, US). Samples were centrifuged and washed with RIPA buffer. Samples were eluted using Laemmli buffer containing 5% β-mercaptoethanol overnight, glycine elution buffer, urea elution buffer, Laemmli buffer containing 2% β-mercaptoethanol overnight or Laemmli buffer containing 5% β-mercaptoethanol for 2 hours. IP samples were loaded into a 12% SDS-PAGE gel. The following antibodies were used for western blotting: rabbit anti-Flag primary antibody (1:1000) (Sigma, Saint Louis, Missouri, US) and donkey anti-rabbit-IgG-HRP secondary antibody (1:5000) (GE Healthcare, Little Chalfont, Buckingshire, UK). 12% gels were stained with Coomassie blue (Sigma, Saint Louis, Missouri, US) or 0.1% silver nitrate (Sigma, Saint Louis, Missouri, US) using a standard protocol.

4.3 RESULTS

4.3.1 PARL CLEAVAGE IN ZEBRAFISH EMBRYOS

We have previously identified two *parl* genes in the zebrafish genome, *parla* and *parlb* (Noble et al., 2012). The overall percent identity of amino acid sequences among the different PARLs is shown in Table 4.1. Based on amino acid sequence alignments between zebrafish Parla, zebrafish Parlb and human PARL it appears that the sequence of the α-cleavage site ($_{52}$GF$_{53}$) is conserved while those of the β-cleavage ($_{77}$SA$_{78}$) and γ-cleavage (near $_{155}$INKWW$_{159}$) sites are not conserved in the zebrafish sequences, unless they are cryptic. Presently, it is unknown if the same cleavage patterns occur in zebrafish to regulate mitochondrial targeting of Parl or its predicted catalytic site. First, we sought to determine if the zebrafish Parl proteins are cleaved at all, we prepared fusion constructs (figure 4.1B) containing either the *parla* or *parlb* cDNA sequence fused to a C-terminal Flag tag sequence. These fusion constructs were sub-cloned downstream of a T7 promoter and between flanking *Xenopus* globin 5' and 3'UTRs (for stability) into an adapted pGEM-4Z backbone vector. The construct was linearized using the *Xba*I enzyme and mRNA was synthesized using a T7 polymerase (figure 4.1D). The mRNA was injected into WT zebrafish embryos at the one cell stage.

Table 4.1. Comparison of the overall amino acid percent identity between the PARL sequences.

Protein Sequences	Human PARL	Zebrafish Parlb
Zebrafish Parla	67%	60%
Zebrafish Parlb	55%	100%

In one experiment, the embryos were collected at 1 dpf and 3 dpf and total proteins were extracted and run on an SDS-PAGE gel followed by western blotting for Flag-tagged proteins. In a second experiment, cytosolic and mitochondrial fractions were isolated and run on a protein gel and blotted using an anti-Flag antibody. Unfortunately, both approaches produced a large number of bands which were not consistently reproducible, likely due to the anti-Flag antibody non-specifically recognizing various endogenous zebrafish proteins.

In a third experiment, we performed an immunoprecipitation (IP) using anti-Flag antibodies covalently linked to agarose beads to try to reduce the abundance of confounding non-specific proteins and to enrich and concentrate the sample with Flag-containing protein to load into the SDS-PAGE gel. Eluates collected from *parla*-Flag or *parlb*-Flag injected embryos at 3 dpf resulted in non-specific bands which were also present in WT uninjected zebrafish samples (see below).

4.3.2 PARL CLEAVAGE IN NON-NEURONAL AND NEURONAL CELL LINES

We also prepared two other constructs. From the *parla*-Flag and *parlb*-Flag constructs in pGEM-4Z (figure 4.1B), we subcloned the Flag-tagged *parl* sequences along with the UTRs downstream of a CMV promoter in the pcDNA3 backbone vector (figure 4.1C) which allowed us to express the Parl proteins in cultured cells.

We transfected the two CMV-driven zebrafish *parl*-Flag constructs, a WT human *PARL*-Flag construct, a mutant human *PARL*-Flag construct containing the PD-related S77N mutation and a mock transfection of the pcDNA3 vector only. Based on a paper by Shi and colleagues (Shi et al., 2011), we used the WT human PARL-Flag construct as a positive control to detect cleaved

PARL and the PD mutant construct in which β-cleavage is abolished as a reference point to help determine the approximate cleavage pattern in the zebrafish *parl* constructs.

These five constructs were transfected into HEK cells and 3 days after transfection, an IP was performed on cell lysates. This resulted in bands in the experimental lanes which were not present in the mock pcDNA3 vector only transfected cells (figure 4.2). Despite having loaded too much protein into the gel, making it difficult to accurately calculate the sizes of the bands obtained, this gave us a good indication that the IP experiments were successful in isolating bands of the correct size range which could be the Parl-Flag proteins.

Figure 4.2. Human HEK cells transfected with PARL-Flag tagged constructs. Following transfection, Flag-tagged proteins were immunoprecipitated with an anti-Flag antibody bound to agarose beads and eluted overnight using an SDS buffer containing 5% β-mercaptoethanol. Proteins were run on a 12% SDS-PAGE gel and detected by western blot using a rabbit anti-Flag antibody and an anti-rabbit-HRP antibody. Cells were transfected in two 10-cm dishes. The entire eluate sample was loaded into the gel. The mock lane represents cells transfected with empty pcDNA3 vector only. The label "Mouse IgG LC" band is a non-specific band. Molecular weight ladder is indicated on the far left. These results are representative of at least three independent experiments.

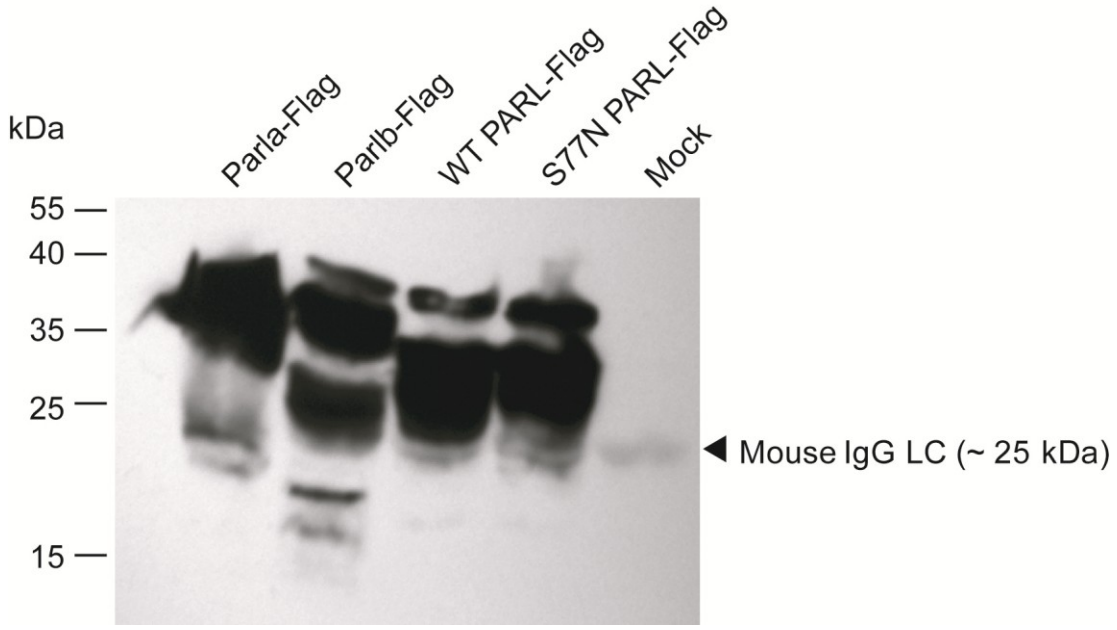
kDa
Parla-Flag
Parlb-Flag
WT PARL-Flag
S77N PARL-Flag
Mock
55
40
35
25
15
Mouse IgG LC (~ 25 kDa)

To determine the cleavage pattern in a human cell line we transfected the PARL constructs in HeLa cells. This resulted in a clear band pattern by western blotting. According to our analysis, Parla was cleaved in at least one location resulting in an ~ 31 kDa band (figure 4.3A, lane 1), while Parlb was cleaved in at least two locations producing bands of ~ 34 kDa and ~ 27 kDa (figure 4.3A, lane 2). As seen in the western blot performed in zebrafish following an IP with anti-Flag antibodies linked to agarose beads, a non-specific band of ~ 25 kDa was present in all samples including the pcDNA3 mock transfected sample (see below for a detailed explanation). Full length Parla and Parlb are predicted to be approximately 42 kDa and 43 kDa, respectively, and are not observed by western blotting. This is consistent with observations in mammals where PARL is constitutively α-cleaved and full length protein is thus undetectable (Sik et al., 2004).

Next we transfected the same constructs into SH-SY5Y dopaminergic neuroblastoma cells in order to compare the cleavage pattern seen in dopaminergic versus non-dopaminergic cells. Western blot analysis of total cell lysates from SH-SY5Y cells following transfection produced a large number of bands which were also present in non-transfected cells. However, IP experiments resulted in the same cleavage pattern of Parla, Parlb, WT PARL and S77N PARL as in HeLa cells (figure 4.3). Parla was cleaved in at least one location resulting in an ~ 32 kDa band (figure 4.4, lane 1), while Parlb was cleaved in at least two locations producing bands of ~ 35 kDa and ~ 28 kDa (figure 4.4, lane 2). Bands at ~ 19 kDa, ~ 25 kDa and ~ 50 kDa were believed to be non-specific as they were also present in eluates from vector only mock transfected SH-SY5Y cells (discussed below). Theses molecular weights were determined experimentally using a standard curve by plotting the molecular weight of the protein ladder against migration distance.

Assuming that α-cleavage occurs between the conserved GF amino acids (which aligns with G52-F53 of human PARL), the predicted theoretical molecular weight of α-cleaved Parla is ~ 37 kDa and it migrated experimentally to ~ 31 – 32 kDa in both HeLa cells and SH-SY5Y cells. The predicted theoretical molecular weight of α-cleaved Parlb is ~ 39 kDa and it migrated experimentally to ~ 34 – 35 kDa in both HeLa cells and SH-SY5Y cells. The Parlb β-cleaved band migrated to ~ 27 – 28 kDa experimentally. To map the β-cleavage site *in silico*, we removed amino acids from the N-terminal of Parlb until a fragment between 28 kDa and 27 kDa remained. This indicated that the β-cleavage site could be somewhere near or within this sequence: $_{132}$TTYWHNWWNQLSN$_{144}$. A closer look at the amino acids neighbouring this sequence revealed another candidate β-cleavage site: $_{152}$LISA$_{155}$. This sequence was remarkably reminiscent of the $_{76}$RSALI$_{80}$ site where β-cleavage is found in mammals.

Figure 4.3. Human HeLa cells transfected with PARL-Flag tagged constructs. Following transfection, Flag-tagged proteins were immunoprecipitated with an anti-Flag antibody bound to agarose beads and eluted overnight using an SDS buffer containing 5% β-mercaptoethanol. Proteins were run on a 12% SDS-PAGE gel and detected by western blotting using a rabbit anti-Flag antibody and an anti-rabbit-HRP antibody. Cells were transfected in 10-cm dishes. **(A)** $1/50^{th}$ of the IP eluate was loaded into the gel. **(B)** $1/500^{th}$ of the IP eluate was loaded into the gel. The mock lanes represent cells transfected with empty pcDNA3 vector only. α-, β- and γ-cleavage fragments of the PARL proteins are denoted on the blot as α, β and γ, respectively. The Mouse IgG bands (arrowheads) are non-specific bands. Molecular weight ladder is indicated on the far left. These results are representative of at least 6 independent experiments.

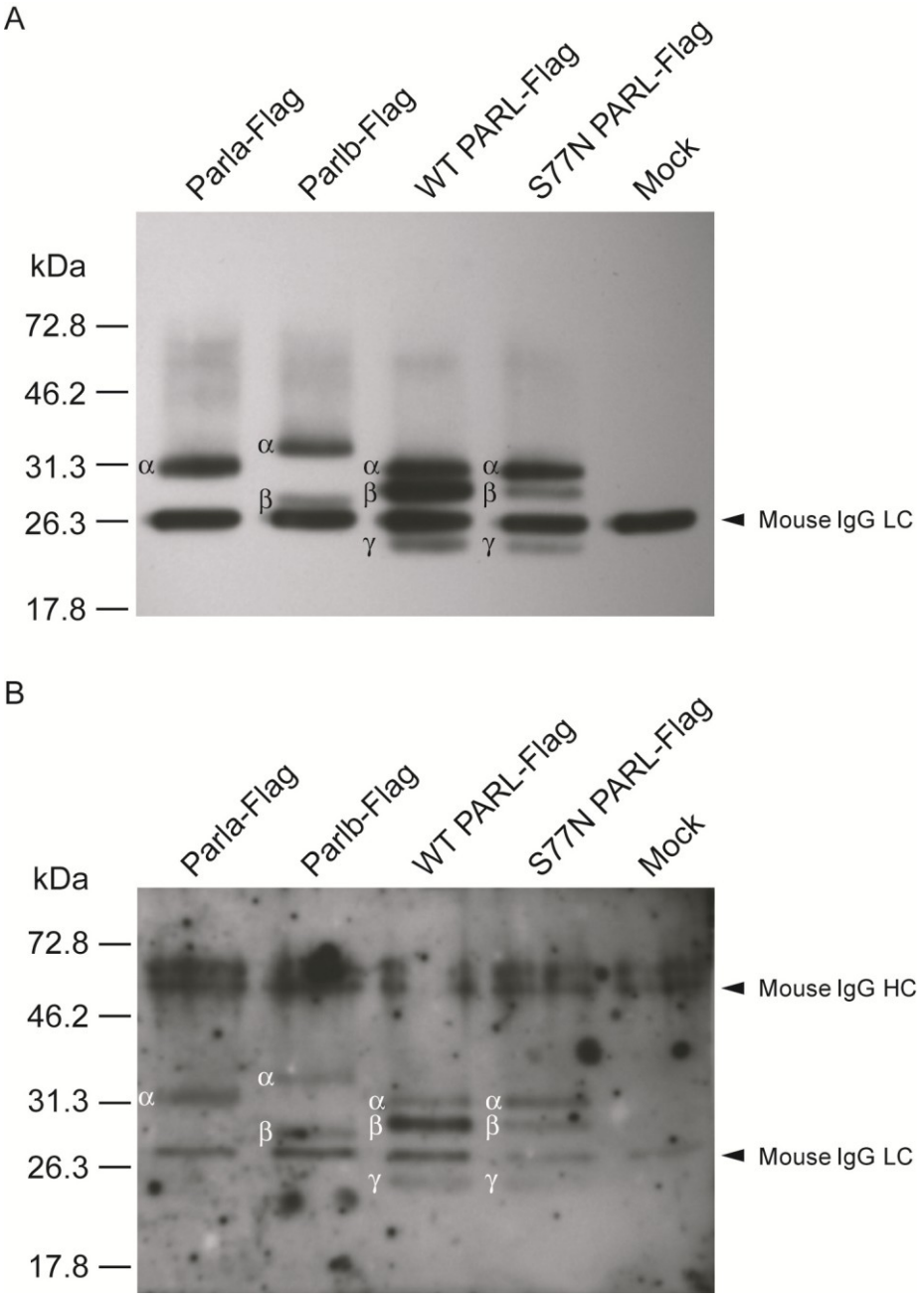
A
Parla-Flag
Parlb-Flag
WT PARL-Flag
S77N PARL-Flag
Mock
kDa
72.8
46.2
31.3
26.3
17.8
α
β
γ
Mouse IgG LC
B
Parla-Flag
Parlb-Flag
WT PARL-Flag
S77N PARL-Flag
Mock
kDa
72.8
46.2
31.3
26.3
17.8
α
β
γ
Mouse IgG HC
Mouse IgG LC

Figure 4.4. Human SH-SY5Y neuroblastoma dopaminergic neuron cells transfected with PARL-Flag tagged constructs. Following transfection, Flag-tagged proteins were immunoprecipitated with an anti-Flag antibody bound to agarose beads and eluted overnight using an SDS buffer containing 5% β-mercaptoethanol. Proteins were run on a 12% SDS-PAGE gel and detected by western blot using a rabbit anti-Flag antibody and an anti-rabbit-HRP antibody. Cells were transfected in 6-well dishes. $1/10^{th}$ of the IP eluate was loaded into the gel. The mock lanes represent cells transfected with empty pcDNA3 vector only. α-, β- and γ-cleavage fragments of the PARL proteins are denoted on the blot as α, β and γ, respectively. The Mouse IgG LC band (arrowhead) is a non-specific band. Molecular weight ladder is indicated on the far left. These results are representative of at least three independent experiments.

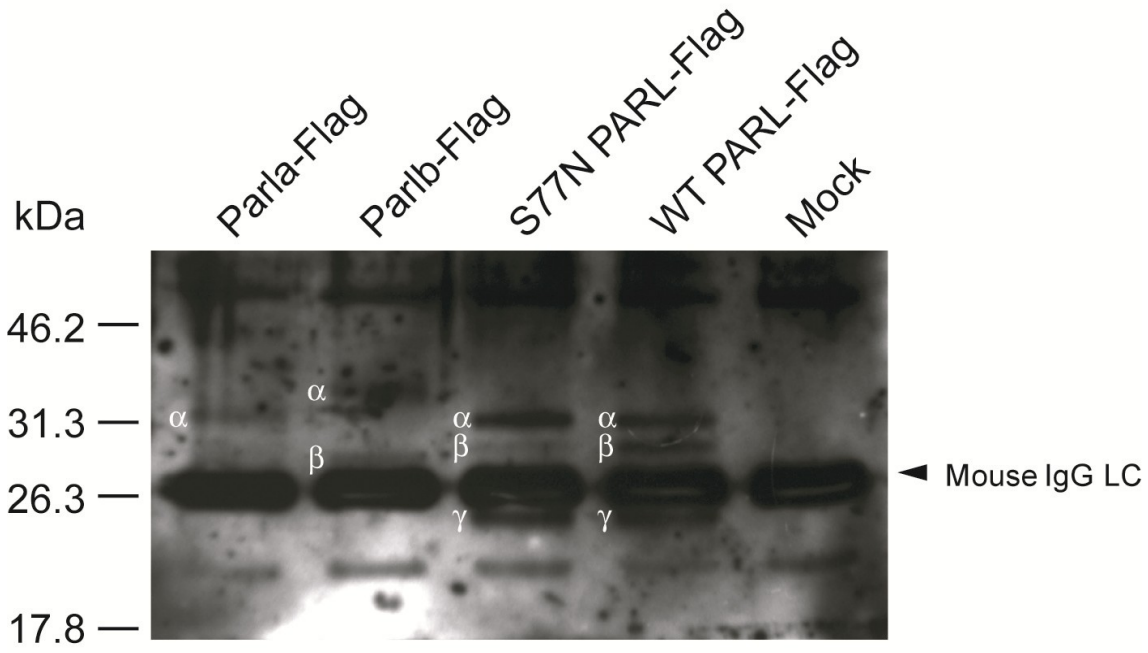
Parla-Flag
Parlb-Flag
S77N PARL-Flag
WT PARL-Flag
Mock
kDa
46.2
31.3
26.3
17.8
α
α
β
α
β
γ
α
β
γ
Mouse IgG LC

To address the identity of two non-specific bands of ~ 25 kDa and ~ 50 kDa observed with both zebrafish samples and samples from cell lines, we performed a number of experiments. Ultimately, we wanted to eliminate the ~ 25 kDa band, due to the possibility that it may be masking a cleaved form of Parla and/or Parlb of the same size. While trouble-shooting (figure 4.5A and 4.5B), we found the identity of these bands to be the IgG light chain (LC, ~ 25 kDa) and the IgG heavy chain (HC, ~ 50 kDa) of the anti-Flag mouse IgG antibody that was bound to the agarose beads used for the IP. Western blotting using only an anti-mouse IgG-HRP secondary antibody revealed two bands at ~ 25 kDa and ~ 50 kDa, indicating that the anti-rabbit IgG-HRP secondary antibody was cross-reacting with mouse IgG from the IP beads. Further evidence to support the idea that the ~ 25 kDa and ~ 50 kDa bands originated from the bead-bound antibody was observed when IP samples from transfected HeLa cells were run on an SDS-PAGE gel which was stained with Coomassie Blue (figure 4.5B). We only observed a high abundance of the two non-specific bands and this indicated that these IgG proteins, corresponding to the LC and HC, originating from the eluates that were run through the gel and did not originate from non-specific binding of either the rabbit anti-Flag or anti-rabbit-HRP antibodies to the membrane. Thus, during the elution step, the antibody's LC and HC were likely being stripped off the beads and eluting along with the Parl-Flag proteins which were attached to the antibody.

Figure 4.5. Determining the identity of the ~ 25 kDa non-specific band in HeLa cells. (A) Following transfection, HeLa cell eluates from immunoprecipitations were run on an SDS-PAGE gel and blotted with secondary anti-mouse-HRP antibody only. Two bands of ~ 25 kDa and ~ 50 kDa were detected. They represent the mouse IgG heavy chain (HC) and mouse IgG light chain (LC) which were originally linked to the agarose beads. **(B)** The same samples as in (A) were run on as SDS-PAGE gel and stained with Coomassie blue. The gel reveals the abundance of bead-bound HC and LC antibody fragments. Parl bands do not show up because they are present in low abundance compared to the mouse antibody fragments in the sample. This indicates that the source of the non-specific bands originated from the sample loaded into the gel and not the blotting procedure. The mock lanes represent cells transfected with empty pcDNA3 vector only. Molecular weight ladder is indicated on the far left.

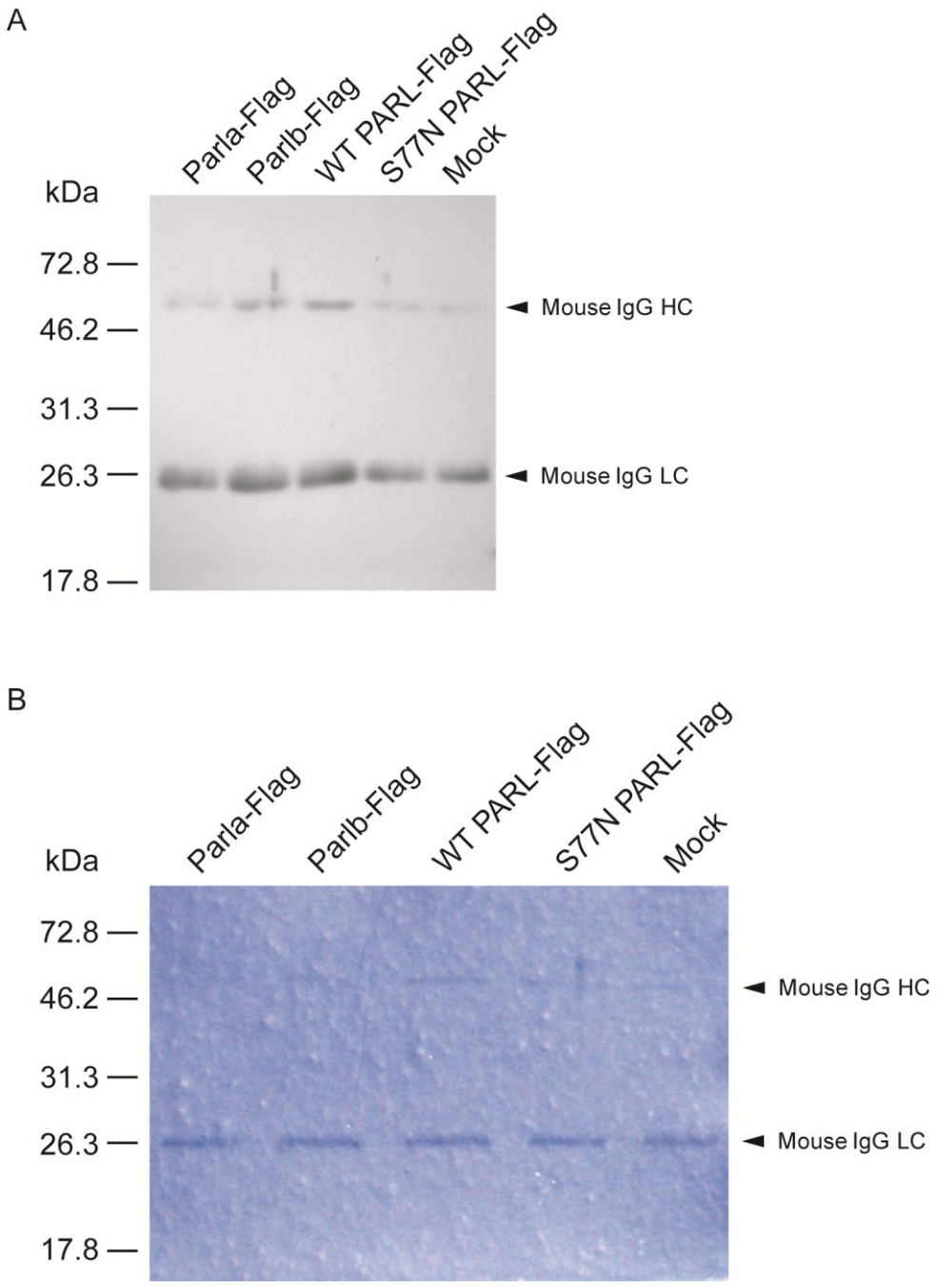
A
Parla-Flag
Parlb-Flag
WT PARL-Flag
S77N PARL-Flag
Mock
kDa
72.8
46.2
31.3
26.3
17.8
Mouse IgG HC
Mouse IgG LC
B
Parla-Flag
Parlb-Flag
WT PARL-Flag
S77N PARL-Flag
Mock
kDa
72.8
46.2
31.3
26.3
17.8
Mouse IgG HC
Mouse IgG LC

We initially eluted the proteins from the beads with Laemmli buffer containing 5% β-mercaptoethanol overnight. To try to prevent the antibody from eluting along with the Parl-Flag tagged proteins, we tried elution buffers and conditions which were less harsh. These included: 1) glycine elution buffer; 2) urea elution buffer; 3) Laemmli buffer containing 2% β-mercaptoethanol overnight; and 4) Laemmli buffer containing 5% β-mercaptoethanol for 2 hours (figure 4.6A). Of these methods, both the glycine and urea elution buffers best eliminated the ~ 25 kDa LC band (figure 4.6A, lanes 3 and 4). To see if these milder alternative elution methods were strong enough to elute the Flag tagged proteins from the antibodies, we transfected HeLa cells with the *parlb*-Flag construct and performed an IP and western blot (figure 4.6B). This resulted in no detectable ~ 25 kDa LC band (figure 4.6B, lane 2). We chose the urea elution method for future experiments as it seemed to perform well in transfection experiments.

Figure 4.6. Determination of the optimal immunoprecipitation elution method. (A) Untransfected HeLa cells were tested in a standard immunoprecipitation experiment and eluted under the following conditions: SDS elution buffer containing 5% β-mercaptoethanol overnight (O/N); SDS elution buffer containing 5% β-mercaptoethanol for 2 hours; urea elution buffer; glycine elution buffer. **(B)** HeLa cells transfected with *parlb*-Flag construct followed by a standard immunoprecipitation experiment and eluted using the following conditions: SDS elution buffer containing 5% β-mercaptoethanol overnight (O/N); SDS elution buffer containing 5% β-mercaptoethanol overnight (O/N); urea elution buffer; glycine elution buffer. Arrowheads pointing to α-cleaved and β-cleaved Parlb-Flag are labeled. The band representing the mouse IgG LC is also labeled.

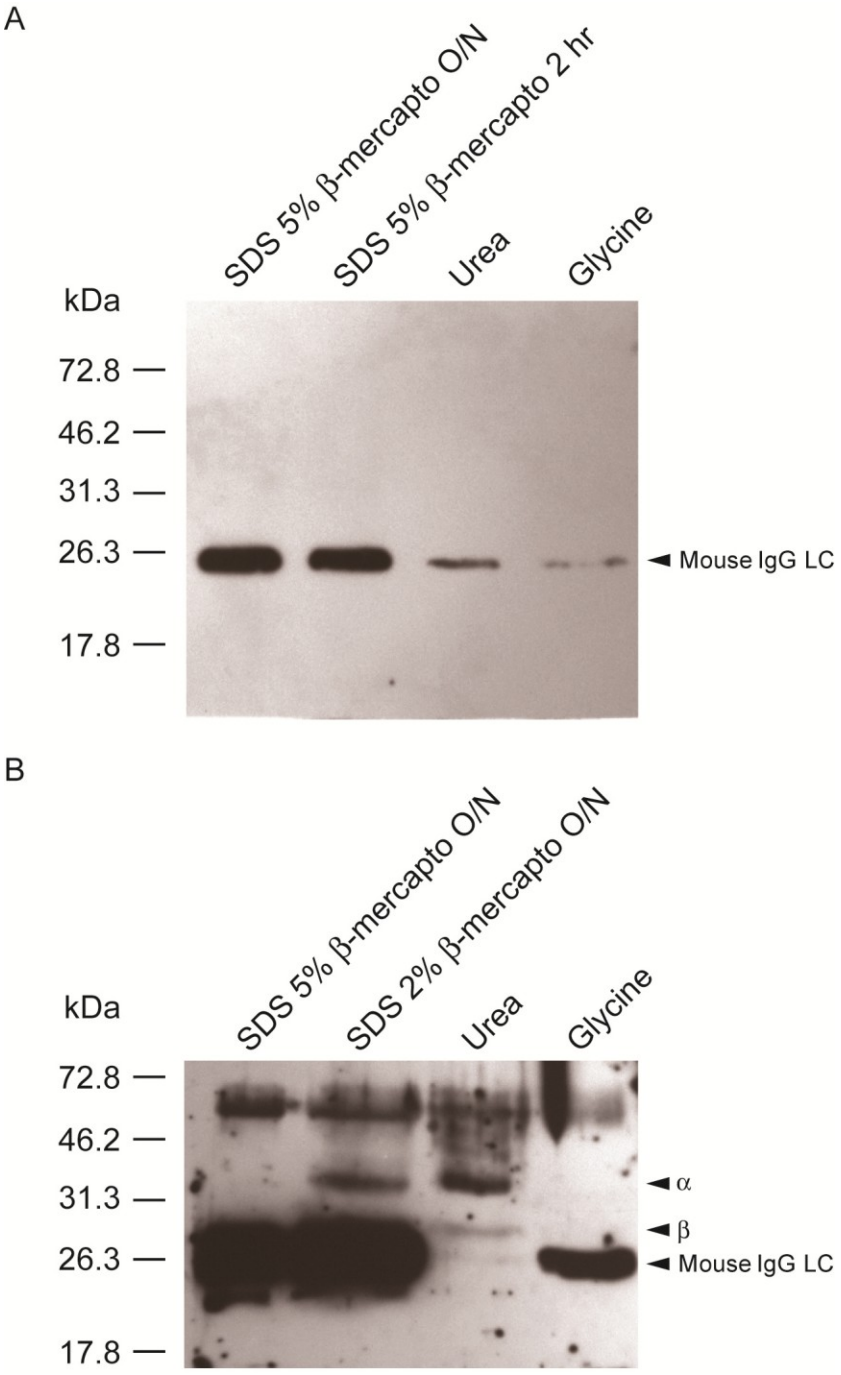
A
SDS 5% β-mercapto O/N
SDS 5% β-mercapto 2 hr
Urea
Glycine
kDa
72.8
46.2
31.3
26.3
17.8
Mouse IgG LC
B
SDS 5% β-mercapto O/N
SDS 2% β-mercapto O/N
Urea
Glycine
kDa
72.8
46.2
31.3
26.3
17.8
α
β
Mouse IgG LC

In order to confirm that the identity of the Flag tagged proteins are indeed Parla and Parlb, we used eluates prepared previously using the harsher method of Laemmli buffer containing 5% β-mercaptoethanol overnight from Parlb-Flag transfected HeLa cells. These eluates were run on an SDS-PAGE gel which was subsequently stained with silver nitrate (figure 4.7) with the intent of excising the Flag-tagged bands to send them for mass spectrometry. Although silver nitrate staining is a much more sensitive method than Coomassie blue staining, this did not result in two clearly defined bands (as previously seen in western blotting with HeLa cells (figure 4.3A)) which were abundant enough to excise and send for mass spectrometry analysis.

Figure 4.7. Silver stain of an SDS-PAGE gel. The immunoprecipitation eluate sample was from HeLa cells transfected with the *parlb*-Flag construct. Nearly the entire eluate sample was loaded into the gel. Arrowheads pointing to putative α-cleaved and β-cleaved Parlb-Flag are labeled. Bands representing the mouse IgG HC and LC are also labeled. This gel is representative of two experiments.

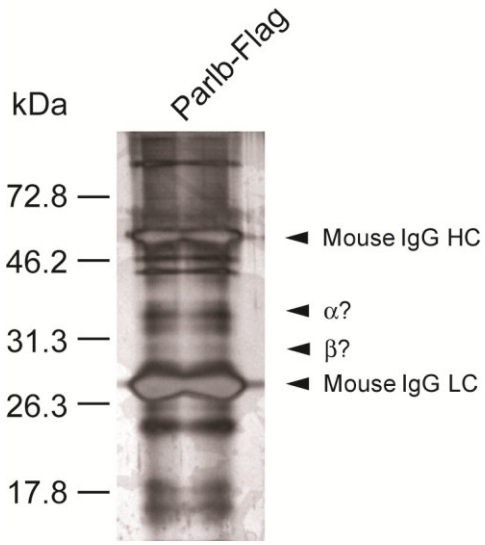
kDa
Parlb-Flag
72.8
46.2
31.3
26.3
17.8
Mouse IgG HC
α?
β?
Mouse IgG LC

4.4 CONCLUDING REMARKS

Once cleavage patterns are established, then additional tags, one at the N-terminal and one in the putative Pβ peptide of each Parl protein will allow us to localize Parl cleavage products to different subcellular fractions (i.e. mitochondrial, cytosolic and/or nuclear) in cells from zebrafish embryos. This work could also be done both quantitatively and qualitatively in cell culture followed by western blotting and immunofluorescence microscopy, respectively. For immunofluorescence microscopy, fluorochrome-conjugated secondary antibodies can be used on these transfected cells to visually co-localize the PARL cleavage products with mitochondrial, cytosolic, and/or nuclear markers.

Furthermore, if a β-cleavage site is mapped in Parla and Parlb, it could undergo site directed mutagenesis to elucidate the effect this may have in zebrafish and their DA neurons.

As 80-95% of PD cases are sporadic and may be due to an environmental insult, the same experiments could be done in transfected cells and in zebrafish pre- and post-exposure to MPTP treatment, to see if a change in PARL cleavage or sub-cellular localization occurs in response to a DA neurotoxin.

Finally, in addition to HEK (human kidney) and HeLa (cervical cancer) cells, several other cell lines could be tested to assay cleavage patterns in different cell types of the body.

CHAPTER 5.

GENERAL CONCLUSIONS AND PERSPECTIVES

5.1 THE *PARL*-DEFICIENCY MODEL

We identified two *parl* sequences within the zebrafish genome which we named *parla* and *parlb* and used antisense morpholino oligonucleotides to knockdown these genes (Chapter 2). The *parla* and *parlb* genes are the zebrafish orthologs of the human PARL that was recently associated with some cases of familial Parkinson's disease. Loss of zebrafish *parl* function resulted in a perturbation of dopaminergic neuron patterning as well as decreased embryonic survival. We were able to rescue the morphant phenotype with a zebrafish *pink1* mRNA demonstrating for the first time that a genetic pathway involving PARL and PINK1 is conserved in a vertebrate model.

Increased mortality was not observed with the loss-of-function of only one *parl* paralog. This observation leads us to believe that there must be an advantage to having two functionally redundant genes in the zebrafish (Postlethwait et al., 2004). Perhaps functional redundancy was advantageous to the fish during the knockdown of either *parla* or *parlb* alone, which resulted in one paralog compensating for the loss of the other. In fact, through semi-quantitative RT-PCR, we observed an increase in the expression of both *parla* and *parlb* mRNA, following *parla* knockdown using translation blocking morpholinos. However, the knockdown of *parlb* did not noticeably effect transcription of either *parla* or *parlb* (data not shown).

Despite having to target two genes at once, studying the Parl proteins in zebrafish was ideal for visualizing the effects gene knockdown had on an organism as a whole. Due to the amenability of zebrafish to morpholino knockdown and their optical clarity, which is advantageous for

whole-mount staining, we were able to visualize DA neurons within the intact brains of *parl* morphants. In addition, there is an overall identity between zebrafish and human in terms of the amino acid sequences of the Parl proteins: zebrafish Parla is ~ 67% identical to human PARL; zebrafish Parlb is ~ 55% identical to human PARL (Table 4.1). This suggests that zebrafish can be used as a suitable model to study the function of the PARL protein found in humans. Moreover, the observation that the human PARL mRNA sequence rescues *parla* and *parlb* double morphants, suggests that the processing machinery may be conserved between zebrafish and humans.

The PD-related mutation in PARL is located in a cleavage site of the mammalian protein, which is necessary for the production of the β peptide; however, this site is predicted to be absent in the zebrafish Parls. Our analysis of cleavage patterns of the zebrafish Parla and Parlb proteins in cultured cells has helped us establish the cleavage patterns of the zebrafish Parls and allowed us to compare them to those of human PARL (Chapter 4). Since starting the Parl project, this was the first time we had detected zebrafish Parla and Parlb using western blotting, for which we detected one band for Parla-Flag and two bands representing Parlb-Flag.

Mapping the location of each cleavage site using mass spectrometry and Edman degradation will be valuable in identifying the exact amino acid location of the α- and β-cleavage sites of Parla and Parlb in order to determine which amino acid corresponds to the serine at position 77 which is mutated to an asparagine in some PD patients.

If we determine that there is indeed a β-cleavage site in Parlb, we should perform site-directed mutagenesis of a mis-matched *parlb* cDNA sequence (which will not bind the morpholinos) at the β site and test its ability to rescue *parl* morphants and the effect it has on DA neuron patterning. Although morpholino knockdown is rarely 100% efficient at abolishing protein

function, this suggested experiment could closely mimic the scenario in PD patients with the S77N mutation.

Other alternative approaches which could be considered are zinc finger nuclease (ZFN) technology and clustered regularly interspaced short palindromic repeats (CRISPRs), both of which generate targeted genomic deletions. Moreover, with ZFN technology the endogenous parl sequences could be deleted and replaced with a β-cleavage *parl* mutant sequence.

5.2 ESTABLISHMENT OF THE CLEAVAGE PATTERNS OF THE PARL PROTEINS

If the second band in the *parlb*-Flag transfected cells does indeed represent β-cleaved Parlb, then the site could be a cryptic cleavage site, perhaps composed of amino acids of the same properties, such as size, charge and/or polarity — i.e. likely small and polar as is the case with serine. Alternatively, we cannot rule out that there could be a different Parlase which targets the Parl proteins in zebrafish cells. This could be tested using a zebrafish cell line such as the ZF4 embryonic zebrafish cell line.

Likewise, if the single band in the *parla*-Flag transfected cells represents α-cleaved Parla and no β-cleaved species of Parla exists, then perhaps the function of the β-cleavage site and the Pβ peptide is the responsibility of Parlb only, pointing to the subfunctionalization of the *parl* genes in zebrafish following the whole genome duplication event that occurred in the teleost lineage.

Once the Pβ peptide of Parlb is mapped, it can be tagged and its localization within the cell can be tracked to give us clues to its function. For example, is it actually targeted to the nucleus as has been observed with its mammalian ortholog (Sik et al., 2004)? This can be achieved in a number of ways. The tagged protein could be followed by fluorescent labeling or staining and

co-localized with a nuclear, cytosolic, organelle or membrane-bound marker. Another approach could involve the preparation of sub-cellular protein fractions combined with western blotting to detect the tagged protein in specific cellular fractions. Ultimately, the location of the Pβ peptide may provide insight into its possible function.

Another avenue of research would be to find out what cleaves the Parls at each cleavage site. At the time of writing of this thesis, nothing has been published about the protease which cleaves PARL at the α-cleavage site. Although it has been shown that β-cleavage of PARL occurs through a mechanism of proteolysis that requires an active form of PARL supplied *in trans* and is thus thought to be executed either by PARL itself, supplied *in trans* (Sik et al., 2004), an unidentified PARLase may still be at play.

In addition to being its own substrate (Sik et al., 2004), PARL itself has been shown to have a number of substrates, including OPA1 (Cipolat et al., 2006), PINK1 (Whitworth et al., 2008; Meissner et al., 2011), and Omi/HtrA2 (Chao et al., 2008). However, some of the interactions involving PINK1 and Omi/HtrA2 have been debated by other groups (Hill and Pellegrini, 2010; Narendra et al., 2010). Finally, one could search for the kinase that phosphorylates PARL at S65, T69 and S70; three important sites which regulate β-cleavage.

5.3 THE TG(*DAT:TOM20 MLS-MCHERRY*) LINE PROVIDES A TOOL TO ASSESS MITOCHONDRIA IN DA NEURONS

Our laboratory previously located the *cis*-regulatory elements of the *dopamine transporter* (*dat*) (Xi et al., 2011b) which we used to drive the expression of a fusion protein between the mitochondrial localising signal (MLS) of a subunit of the translocase of the outer mitochondrial membrane (Tom20) and the fluorescent reporter mCherry to specifically visualise the

mitochondria in dopaminergic neurons of zebrafish *in vivo* (Chapter 3). We generated a transgenic zebrafish line Tg(*dat:tom20 MLS-mCherry*) using this construct and characterised the expression of Tom20-mCherry to the mitochondria of the majority of DA neuron groups. Following MPTP exposure of live fish, we observed a significant decrease in mCherry fluorescence in the olfactory bulb, pretectum, subpallium, and diencephalic clusters 2 and 3 and caudal hypothalamus.

This is the first zebrafish model that labels mitochondria exclusively in DA neurons in the brain. This transgenic line will allow us to observe mitochondrial dynamics using time-lapse confocal microscopy in live zebrafish embryos and look for defects in mitochondrial fusion and fission following neurotoxin exposure or the knockdown of PD-related genes, such as *parla* and *parlb*. That being said, imaging mitochondria in the zebrafish embryonic and larval brain has been challenging, due to the requirement of a high numerical aperture in combination with a high magnification objective to be able to clearly resolve individual mitochondria *in vivo* in DA neuron clusters which are not located in a superficial layer. Previous studies have only been successful in imaging mitochondrial transport in sensory nerve cells at the thin rim of the fin fold (Plucińska et al., 2012) and in superficial mitochondria in the pharyngeal arch and somites at 32 hpf (Kim et al., 2008). One way to approach this obstacle may be to prepare vibrotome tissue sections containing mCherry labeled cells at the immediate surface of the section which could be kept alive in culture for live imaging. This would reduce the distortion caused by the depth of the sample and could help increase resolution.

In addition, examination of *parla* and *parlb* morphants with mCherry labeled mitochondria in DA neurons by anti-mCherry and immunogold staining combined with electron microscopy would allow us to observe the mitochondrial cristae and to determine if the mechanism leading

to cell death in zebrafish is indeed by means of widening the cristae junctions, resulting in the release of cytochrome c and the apoptotic cascade. This would be especially useful, since it is not known whether the mechanism by which the loss-of-function of the *parl* genes specifically leading to mortality in larval zebrafish is conserved and whether it is the same for both of the zebrafish Parls in terms of mitochondria dynamics and cristae remodelling in zebrafish.

The current mechanism proposed is one in which PARL's normal protease function is involved in cleaving the transmembrane domain of OPA1 in the IMM to release a soluble form of OPA1 which is available to oligomerize with IMM-tethered OPA1 to plug the mitochondrial cristae junction and prevent cytochrome c release, which, in turn, guards against apoptosis.

5.4 CONCLUSION

Overall, the *parla* and *parlb* deficiency model along with the characterization of the cleavage patterns of Parl have helped characterize the function of the Parl proteins in zebrafish. The Tg(*dat*:*tom20 MLS-mCherry*) transgenic zebrafish line is a valuable tool which will help elucidate the role mitochondrial proteins and environmental toxins play in Parkinson's disease etiology. In combination, these zebrafish models are remarkable systems in which to study human disease.

APPENDIX A.

TILLING (TARGETING INDUCED LOCAL LESIONS IN GENOMES) RESULTS

TILLING (Targeting Induced Local Lesions in Genomes) is a method for identifying mutations in specific genes in a library of mutagenized organisms (Moens et al., 2008). In zebrafish, these single point mutations were chemically induced by ENU (*N*-ethyl-*N*-nitrosourea). The Zebrafish TILLING Consortium is a joint effort between Dr. Cecilia Moens' lab at the Fred Hutchinson Cancer Research Center (FHCRC) (Seattle, Washington), Dr. Lilianna Solnica-Krezel's lab at Vanderbilt University (Nashville, Tennessee) and Dr. John Postlethwait's lab at the University of Oregon (Eugene, Oregon). The Consortium has established vast libraries of cryopreserved ENU-mutagenized zebrafish. The goal of their project is to generate, identify and distribute loss-of-function mutations in genes of interest to the zebrafish community.

To be eligible for TILLING each fragment must be less than 1.4 Kb in length and contain at least 350 bp of coding sequence and lie within the first two thirds of the 5' end of the gene of interest. TILLING was performed for the regions of both *parla* and *parlb* described in Table A.1.

Table A.1. Regions of *parla* and *parlb* submitted for TILLING.

Gene	Genomic position of TILLING fragment from start codon	Length of TILLING fragment	Length of coding sequence	Fragment within the 5' 2/3rd of the gene
parla	1181 bp – 2581 bp (exon 2 – exon 4)	1.4 kb	340 bp	Yes
parlb	5053 bp – 6453 bp (intron 2 – intron 5)	1.4 kb	363 bp	Yes

Despite finding the ENU-induced mutations listed in Table A.2, no mutants were thawed since none of these were predicted to produce obvious deleterious mutations (either nonsense or splice site mutations). I have presented this list here to keep a record of the zebrafish *parl* mutants

which could be available to us if in the future we do find evidence, through gene modeling or mapping of the cleavage sites in Parl, that these mutants are likely to be deleterious.

Table A.2. TILLING results for *parla* and *parlb*.

Gene	Genomic position of nucleotide change	Effect	Zygosity	Storage location
parla	G1435A	E49=[a] Exon 2	Homozygous	Dr. Cecilia Moens' lab
	T1585A	Intron 2	Homozygous	Dr. Cecilia Moens' lab
	T1754G	Intron 2	Homozygous	Dr. Cecilia Moens' lab
	T2316A	Intron 2	Homozygous	Dr. Cecilia Moens' lab
	T2327A	Intron 2	Homozygous	Dr. Cecilia Moens' lab
parlb	C5425T	Intron 2	Homozygous	Dr. Cecilia Moens' lab
	C5426A	Intron 2	Homozygous	Dr. Cecilia Moens' lab
	C5445T	Intron 2	Homozygous	Dr. Cecilia Moens' lab
	C5474T	T92I Exon 3	Homozygous	Dr. Cecilia Moens' lab
	T5503C	L102= Exon 3	Homozygous	Dr. Cecilia Moens' lab
	G5539A	A114T Exon 3	Homozygous	Dr. Cecilia Moens' lab
	T5595G	Intron 3	Homozygous	Dr. Cecilia Moens' lab
	T6121A	Intron 4	Homozygous	Dr. Cecilia Moens' lab
	G5568A	R123= Exon 3	Homozygous	Dr. Lilianna Solnica-Krezel's lab
	C5685T	Y134= Exon 4	Homozygous	Dr. Lilianna Solnica-Krezel's lab
	C6166T	V180= Exon 5	Homozygous	Dr. Lilianna Solnica-Krezel's lab
	T6173A	C183S Exon 5 TMD 2	Homozygous	Dr. Lilianna Solnica-Krezel's lab

[a]=silent mutation

APPENDIX B.

LIST OF MY CONTRIBUTIONS TO MANUSCRIPTS AND EXPERIMENTS NOT PRESENTED IN THIS THESIS

B.1 PUBLISHED

B.1.1. Xi, Y., Ryan, J., **Noble, S.**, Yu, M., Yilbas, A. E. and Ekker, M. (2010) Impaired dopaminergic neuron development and locomotor function in zebrafish with loss of *pink1* function. *Eur J Neurosci,* 31, 623-633.

- To check *pink1* mRNA expression in adult zebrafish brain, heart, muscle and liver tissues, I dissected these tissues and performed a total RNA isolation followed by a non-quantitative RT-PCR and DNA gel.
- To confirm the knock down of Pink1 by morpholinos, I performed western blotting with a number of different anti-PINK1 and anti-HA antibodies.
- I critically proof-read the manuscript for publication.

B.1.2. Xi, Y., **Noble, S.** and Ekker, M. (2011) Modeling neurodegeneration in zebrafish. *Curr Neurol Neurosci Rep,* 11, 274-282.

- I am co-first-author on this review paper.
- I wrote the sections on Huntington disease and Alzheimer's disease.

B.1.3. Eisa-Beygi, S., Hatch, G., **Noble, S.**, Ekker, M. and Moon, T. W. (2013) The 3-hydroxy-3-methylglutaryl-CoA reductase (HMGCR) pathway regulates developmental

cerebral-vascular stability via prenylation-dependent signalling pathway. *Dev Biol,* 373, 258-266.

- I mounted drug treated and untreated live embryos in agarose and using an LSM 510 upright confocal microscope acquired composite confocal Z-stack projections and time-lapse videos of the blood vessels and blood cells in the brain in Tg(*fli1:EGFP*);(*gata-1:DsRed*) embryos.

B.2 UNPUBLISHED

B.2.1. Shahram Eisa-Beygi; Raymond W.M. Kwong; **Sandra Noble**; Rafael Godoy; Thomas W. Moon; Marc Ekker, Molecular and Pathophysiological Processes Underlying Spontaneous Intracerebral Hemorrhage (ICH) in Developing Zebrafish (Danio rerio). *PLOS ONE*. Submitted September 13, 2013.

- I mounted drug treated and untreated embryos in agarose and acquired images of blood vessels in the brain using an LSM 510 upright confocal microscope.
- I assisted with zebrafish behavior video acquisition of untreated and treated embryos.

APPENDIX C.

PERMISSION FOR USE OF FIGURES

10/16/13

Hello,

I would like request permission to add all the figures from a paper I published in the Journal of Neurochemistry to my Ph.D. thesis.

Here is the title and info for the paper. I tried to go through the Wiley Online Library but could not submit the application as I do not have a login. I have provided a print screen of the form below.

I am also wondering if I may use my original figures (as they are higher quality than those used to make the pdf for publication)?

> Noble, S., Ismail, A., Godoy, R., Xi, Y. and Ekker, M. (2012) Zebrafish Parla- and Parlb-deficiency affects dopaminergic neuron patterning and embryonic survival. *J Neurochem,* **122,** 196-207.

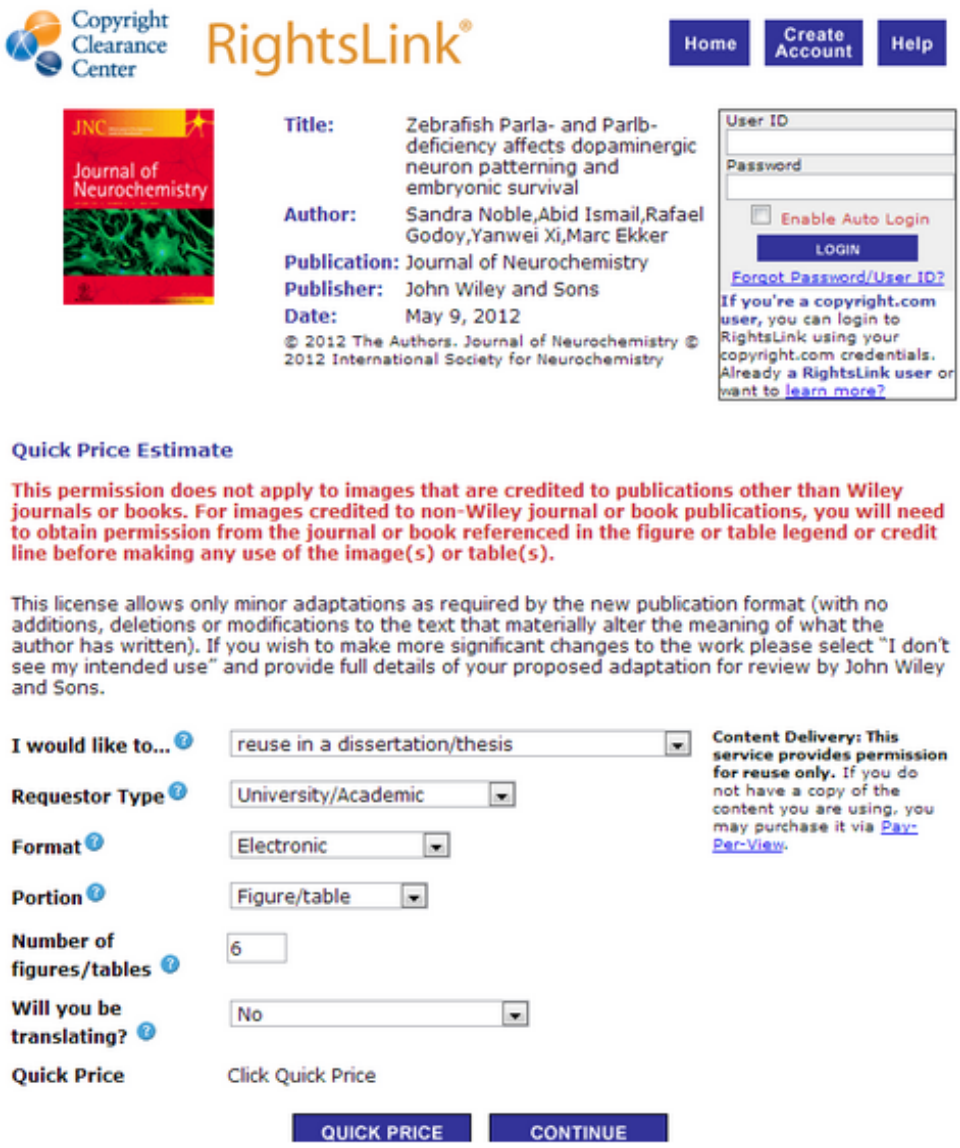

Regards,

Sandra Noble

RightsLink 10/18/13

Dear Sandra Noble

Thank you for your request.

Permission is granted for you to use the material requested for your thesis/dissertation subject to the usual acknowledgements and on the understanding that you will reapply for permission if you wish to distribute or publish your thesis/dissertation commercially.

Permission is granted solely for use in conjunction with the thesis, and the material may not be posted online separately.

Any third party material is expressly excluded from this permission. If any material appears within the article with credit to another source, authorisation from that source must be obtained.

Yours sincerely

Duncan J.
Associate Permissions Manager
John Wiley & Sons Ltd

REFERENCES

Amsterdam A, Burgess S, Golling G, Chen W, Sun Z, Townsend K, Farrington S, Haldi M, Hopkins N (1999) A large-scale insertional mutagenesis screen in zebrafish. Genes Dev 13:2713-2724.

Anichtchik OV, Kaslin J, Peitsaro N, Scheinin M, Panula P (2004) Neurochemical and behavioural changes in zebrafish Danio rerio after systemic administration of 6-hydroxydopamine and 1-methyl-4-phenyl-1,2,3,6-tetrahydropyridine. J Neurochem 88:443-453.

Anichtchik OV, Diekmann H, Fleming A, Roach A, Goldsmith P, Rubinsztein DC (2008) Loss of PINK1 Function Affects Development and Results in

Neurodegeneration in Zebrafish. J Neurosci 28:8199-8207.

Baulac S, Lu H, Strahle J, Yang T, Goldberg MS, Shen J, Schlossmacher MG, Lemere CA, Lu Q, Xia W (2009) Increased DJ-1 expression under oxidative stress and in Alzheimer's disease brains. Mol Neurodegener 4:12.

Bretaud S, Lee S, Guo S (2004) Sensitivity of zebrafish to environmental toxins implicated in Parkinson's disease. Neurotoxicol Teratol 26:857-864.

Bretaud S, Allen C, Ingham P, Bandmann O (2007) p53-dependent neuronal cell death in a DJ-1-deficient zebrafish model of Parkinson's disease. J Neurochem 100:1626-1635.

Brossier F, Jewett TJ, Sibley LD, Urban S (2005) A spatially localized rhomboid protease cleaves cell surface adhesins essential for invasion by Toxoplasma. Proc Natl Acad Sci U S A 102:4146-4151.

Brown MS, Ye J, Rawson RB, Goldstein JL (2000) Regulated intramembrane proteolysis: a control mechanism conserved from bacteria to humans. Cell 100:391-398.

Chao JR, Parganas E, Boyd K, Hong CY, Opferman JT, Ihle JN (2008) Hax1-mediated processing of HtrA2 by Parl allows survival of lymphocytes and neurons. Nature 452:98-102.

Chen H, Detmer SA, Ewald AJ, Griffin EE, Fraser SE, Chan DC (2003) Mitofusins Mfn1 and Mfn2 coordinately regulate mitochondrial fusion and are essential for embryonic development. J Cell Biol 160:189-200.

Cipolat S, Rudka T, Hartmann D, Costa V, Serneels L, Craessaerts K, Metzger K, Frezza C, Annaert W, D'Adamio L, Derks C, Dejaegere T, Pellegrini L, D'Hooge R, Scorrano L, De Strooper B (2006) Mitochondrial rhomboid PARL regulates cytochrome c release during apoptosis via OPA1-dependent cristae remodeling. Cell 126:163-175.

Cookson MR (2005) The biochemistry of Parkinson's disease. Annual Review of Biochemistry 74:29-52.

Curran JE, Jowett JB, Abraham LJ, Diepeveen LA, Elliott KS, Dyer TD, Kerr-Bayles LJ, Johnson MP, Comuzzie AG, Moses EK, Walder KR, Collier GR, Blangero J, Kissebah AH (2010) Genetic variation in PARL influences mitochondrial content. Hum Genet 127:183-190.

Dal-Pra S, Thisse C, Thisse B (2011) FoxA transcription factors are essential for the development of dorsal axial structures. Dev Biol 350:484-495.

Dauer W, Przedborski S (2003) Parkinson's disease: mechanisms and models. Neuron 39:889-909.

Deas E, Plun-Favreau H, Gandhi S, Desmond H, Kjaer S, Loh SH, Renton AE, Harvey RJ, Whitworth AJ, Martins LM, Abramov AY, Wood NW (2011) PINK1 cleavage at position A103 by the mitochondrial protease PARL. Hum Mol Genet 20:867-879.

Dexter DT, Jenner P (2013) Parkinson disease: from pathology to molecular disease mechanisms. Free Radic Biol Med 62:132-144.

Dooley K, Zon LI (2000) Zebrafish: a model system for the study of human disease. Curr Opin Genet Dev 10:252-256.

Driever W, Stemple D, Schier A, Solnica-Krezel L (1994) Zebrafish: genetic tools for studying vertebrate development. Trends Genet 10:152-159.

Driever W, Solnica-Krezel L, Schier AF, Neuhauss SCF, Malicki J, Stemple DL, Stainier DYR, Zwartkruis F, Abdelilah S, Rangini Z, Belak J, Boggs C (1996) A genetic screen for mutations affecting embryogenesis in zebrafish. Development 123:37-46.

Dutt A, Canevascini S, Froehli-Hoier E, Hajnal A (2004) EGF signal propagation during C. elegans vulval development mediated by ROM-1 rhomboid. PLoS Biol 2:e334.

Eisa-Beygi S, Hatch G, Noble S, Ekker M, Moon TW (2013) The 3-hydroxy-3-methylglutaryl-CoA reductase (HMGCR) pathway regulates developmental cerebral-vascular stability via prenylation-dependent signalling pathway. Dev Biol 373:258-266.

Esser K, Tursun B, Ingenhoven M, Michaelis G, Pratje E (2002) A novel two-step mechanism for removal of a mitochondrial signal sequence involves the mAAA complex and the putative rhomboid protease Pcp1. J Mol Biol 323:835-843.

Farrer MJ (2006) Genetics of Parkinson disease: paradigm shifts and future prospects. Nature Reviews Genetics 7:306-318.

Fawcett KA, Wareham NJ, Luan J, Syddall H, Cooper C, O'Rahilly S, Day IN, Sandhu MS, Barroso I (2006) PARL Leu262Val is not associated with fasting insulin levels in UK populations. Diabetologia 49:2649-2652.

Fett ME, Pilsl A, Paquet D, van Bebber F, Haass C, Tatzelt J, Schmid B, Winklhofer KF (2010) Parkin is protective against proteotoxic stress in a transgenic zebrafish model. PLoS One 5:e11783.

Flinn L, Mortiboys H, Volkmann K, Koster RW, Ingham PW, Bandmann O (2009) Complex I deficiency and dopaminergic neuronal cell loss in parkin-deficient zebrafish (Danio rerio). Brain 132:1613-1623.

Freeman M (2004) Proteolysis within the membrane: rhomboids revealed. Nat Rev Mol Cell Biol 5:188-197.

Freeman M (2008) Rhomboid proteases and their biological functions. Annu Rev Genet 42:191-210.

Frezza C, Cipolat S, de Brito OM, Micaroni M, Beznoussenko GV, Rudka T, Bartoli D, Polishuck RS, Danial NN, De Strooper B, Scorrano L (2006) OPA1 controls apoptotic cristae remodeling independently from mitochondrial fusion. Cell 126:177-189.

Gallio M, Sturgill G, Rather P, Kylsten P (2002) A conserved mechanism for extracellular signaling in eukaryotes and prokaryotes. Proc Natl Acad Sci U S A 99:12208-12213.

Gilbert SF (2000) *Developmental Biology*., Sixth Edition ed. Edition.

Gottlieb E (2006) OPA1 and PARL keep a lid on apoptosis. Cell 126:27-29.

Greene AW, Grenier K, Aguileta MA, Muise S, Farazifard R, Haque ME, McBride HM, Park DS, Fon EA (2012) Mitochondrial processing peptidase regulates PINK1 processing, import and Parkin recruitment. EMBO Rep.

Guyon JR, Steffen LS, Howell MH, Pusack TJ, Lawrence C, Kunkel LM (2007) Modeling human muscle disease in zebrafish. Biochim Biophys Acta 1772:205-215.

Haffter P, Granato M, Brand M, Mullins MC, Hammerschmidt M, Kane DA, Odenthal J, van Eeden FJM, Jianmg Y-J, Heisenberg C-P, Kelsh RN, Furutani-Seiki M, Vogelsang E, Beuchle D, Schach U, Fabian C, Nusslein-Volhard C (1996) The identification of genes with unique and essential functions in the development of the zebrafish, *Danio rerio.* Development 123:1-36.

Haque ME, Thomas KJ, D'Souza C, Callaghan S, Kitada T, Slack RS, Fraser P, Cookson MR, Tandon A, ., Park DS (2008) Cytoplasmic Pink1 activity protects neurons from dopaminergic neurotoxin MPTP. Proc Natl Acad Sci USA 105:1716-1721.

Hatunic M, Stapleton M, Hand E, DeLong C, Crowley VE, Nolan JJ (2009) The Leu262Val polymorphism of presenilin associated rhomboid like protein (PARL) is associated with earlier onset of type 2 diabetes and increased urinary microalbumin creatinine ratio in an Irish case-control population. Diabetes Res Clin Pract 83:316-319.

Heinitz S, Klein C, Djarmati A (2011) The p.S77N presenilin-associated rhomboid-like protein mutation is not a frequent cause of early-onset Parkinson's disease. Mov Disord 26:2441-2442.

Herlan M, Vogel F, Bornhovd C, Neupert W, Reichert AS (2003) Processing of Mgm1 by the rhomboid-type protease Pcp1 is required for maintenance of mitochondrial morphology and of mitochondrial DNA. J Biol Chem 278:27781-27788.

Herlan M, Bornhövd C, Hell K, Neupert W, Reichert AS (2004) Alternative topogenesis of Mgm1 and mitochondrial morphology depend on ATP and a functional import motor. J Cell Biol 165:167-173.

Hill RB, Pellegrini L (2010) The PARL family of mitochondrial rhomboid proteases. Semin Cell Dev Biol 21:582-592.

Holzschuh J, Ryu S, Aberger F, Driever W (2001) Dopamine transporter expression distinguishes dopaminergic neurons form other catecholaminergic neurons in the developing zebrafish embryo. Mech Dev 101.

Hukriede NA, Joly L, Tsang M, Miles J, Tellis P, Epstein JA, Barbazuk WB, Li FN, Paw B, Postlethwiat JH, Hudson TJ, Zon LI, McPherson JD, Chevrette M, Dawid IB, Johnson SL, Ekker M (1999) Radiation hybrid mapping of the zebrafish genome. Proc Natl Acad Sci USA 96:9745-9750.

Jenner P (1998) Oxidative mechanisms in nigral cell death in Parkinson's disease. Mov Disord 13 Suppl 1:24-34.

Jeyaraju DV, McBride HM, Hill RB, Pellegrini L (2011) Structural and mechanistic basis of Parl activity and regulation. Cell Death Differ 18:1531-1539.

Jeyaraju DV, Xu L, Letellier MC, Bandaru S, Zunino R, Berg EA, McBride HM, Pellegrini L (2006) Phosphorylation and cleavage of presenilin-associated rhomboid-like protein (PARL) promotes changes in mitochondrial morphology. Proc Natl Acad Sci U S A 103:18562-18567.

Jin SM, Lazarou M, Wang C, Kane LA, Narendra DP, Youle RJ (2010) Mitochondrial membrane potential regulates PINK1 import and proteolytic destabilization by PARL. J Cell Biol 191:933-942.

Kanaji S, Iwahashi J, Kida Y, Sakaguchi M, Mihara K (2000) Characterization of the signal that directs Tom20 to the mitochondrial outer membrane. J Cell Biol 151:277-288.

Keller ET, Murtha JM (2004) The use of mature zebrafish (Danio rerio) as a model for human aging and disease. Comp Biochem Physiol C Toxicol Pharmacol 138:335-341.

Kim MJ, Kang KH, Kim CH, Choi SY (2008) Real-time imaging of mitochondria in transgenic zebrafish expressing mitochondrially targeted GFP. Biotechniques 45:331-334.

Kimmel CB, Ballard WW, Kimmel SR, Ullmann B, Schilling TF (1995) Stages of embryonic development of the zebrafish. Dev Dyn 203:253-310.

Kissebah AH, Sonnenberg GE, Myklebust J, Goldstein M, Broman K, James RG, Marks JA, Krakower GR, Jacob HJ, Weber J, Martin L, Blangero J, Comuzzie AG (2000) Quantitative trait loci on chromosomes 3 and 17 influence phenotypes of the metabolic syndrome. Proc Natl Acad Sci U S A 97:14478-14483.

Klein C, Schlossmacher MG (2006) The genetics of Parkinson disease: Implications for neurological care. Nat Clin Pract Neurol 2:136-146.

Koonin EV, Makarova KS, Rogozin IB, Davidovic L, Letellier MC, Pellegrini L (2003) The rhomboids: a nearly ubiquitous family of intramembrane serine proteases that probably evolved by multiple ancient horizontal gene transfers. Genome Biol 4:R19.

Lam CS, Korzh V, Strahle U (2005) Zebrafish embryos are susceptible to the dopaminergic neurotoxin MPTP. Eur J Neurosci 21:1758-1762.

Lang AE, Lozano AM (1998a) Parkinson's disease. First of two parts. N Engl J Med 339:1044-1053.

Lang AE, Lozano AM (1998b) Parkinson's disease. Second of two parts. N Engl J Med 339:1130-1143.

Lemberg MK, Freeman M (2007) Functional and evolutionary implications of enhanced genomic analysis of rhomboid intramembrane proteases. Genome Res 17:1634-1646.

Lemberg MK, Menendez J, Misik A, Garcia M, Koth CM, Freeman M (2005) Mechanism of intramembrane proteolysis investigated with purified rhomboid proteases. EMBO J 24:464-472.

Lieschke GJ, Currie PD (2007) Animal models of human disease: zebrafish swim into view. Nat Rev Genet 8:353-367.

Link V, Shevchenko A, Heisenberg CP (2006) Proteomics of early zebrafish embryos. BMC Dev Biol 6:1.

Liu P, Jenkins NA, Copeland NG (2003) A highly efficient recombineering-based method for generating conditional knockout mutations. Genome Res 13:476-484.

Ma PM (2003) Catecholaminergic systems in the zebrafish. IV. Organization and projection pattern of dopaminergic neurons in the diencephalon. Journal of Comparative Neurology 460:13-37.

Mann VM, Cooper JM, Krige D, Daniel SE, Schapira AH, Marsden CD (1992) Brain, skeletal muscle and platelet homogenate mitochondrial function in Parkinson's disease. Brain 115 (Pt 2):333-342.

Mayer U, Nüsslein-Volhard C (1988) A group of genes required for pattern formation in the ventral ectoderm of the Drosophila embryo. Genes Dev 2:1496-1511.

McKinley ET, Baranowski TC, Blavo DO, Cato C, Doan TN, Rubinstein AL (2005) Neuroprotection of MPTP-induced toxicity in zebrafish dopaminergic neurons. Brain Res Mol Brain Res 141:128-137.

McQuibban GA, Saurya S, Freeman M (2003) Mitochondrial membrane remodelling regulated by a conserved rhomboid protease. Nature 423:537-541.

McQuibban GA, Lee JR, Zheng L, Juusola M, Freeman M (2006) Normal mitochondrial dynamics requires rhomboid-7 and affects Drosophila lifespan and neuronal function. Curr Biol 16:982-989.

Meissner C, Lorenz H, Weihofen A, Selkoe DJ, Lemberg MK (2011) The mitochondrial intramembrane protease PARL cleaves human Pink1 to regulate Pink1 trafficking. Journal of Neurochemistry 117:856-867.

Moens CB, Donn TM, Wolf-Saxon ER, Ma TP (2008) Reverse genetics in zebrafish by TILLING. Brief Funct Genomic Proteomic 7:454-459.

Narendra DP, Jin SM, Tanaka A, Suen DF, Gautier CA, Shen J, Cookson MR, Youle RJ (2010) PINK1 is selectively stabilized on impaired mitochondria to activate Parkin. PLoS Biol 8:e1000298.

Nasevicius A, Ekker SC (2000) Effective targeted gene "knockdown" in zebrafish. Nature Genet 26:216-220.

Noble S, Ismail A, Godoy R, Xi Y, Ekker M (2012) Zebrafish Parla- and Parlb-deficiency affects dopaminergic neuron patterning and embryonic survival. J Neurochem 122:196-207.

Olanow CW (1992) A rationale for dopamine agonists as primary therapy for Parkinson's disease. Can J Neurol Sci 19:108-112.

Paffett-Lugassy NN, Zon LI (2005) Analysis of hematopoietic development in the zebrafish. Methods Mol Med 105:171-198.

Parkkinen L, O'Sullivan SS, Kuoppamäki M, Collins C, Kallis C, Holton JL, Williams DR, Revesz T, Lees AJ (2011) Does levodopa accelerate the pathologic process in Parkinson disease brain? Neurology 77:1420-1426.

Pellegrini L, Scorrano L (2007) A cut short to death: Parl and Opa1 in the regulation of mitochondrial morphology and apoptosis. Cell Death Differ 14:1275-1284.

Pellegrini L, Passer BJ, Canelles M, Lefterov I, Ganjei JK, Fowlkes BJ, Koonin EV, D'Adamio L (2001) PAMP and PARL, two novel putative metalloproteases interacting with the COOH-terminus of Presenilin-1 and -2. J Alzheimers Dis 3:181-190.

Penberthy WT, Shafizadeh E, Lin S (2002) The zebrafish as a model for human disease. Front Biosci 7:d1439-1453.

Phasukkijwatana N, Kunhapan B, Stankovich J, Chuenkongkaew WL, Thomson R, Thornton T, Bahlo M, Mushiroda T, Nakamura Y, Mahasirimongkol S, Tun AW, Srisawat C, Limwongse C, Peerapittayamongkol C, Sura T, Suthammarak W, Lertrit P (2010) Genome-wide linkage scan and association study of PARL to the expression of LHON families in Thailand. Hum Genet 128:39-49.

Plucińska G, Paquet D, Hruscha A, Godinho L, Haass C, Schmid B, Misgeld T (2012) In vivo imaging of disease-related mitochondrial dynamics in a vertebrate model system. J Neurosci 32:16203-16212.

Postlethwait J, Amores A, Cresko W, Singer A, Yan YL (2004) Subfunction partitioning, the teleost radiation and the annotation of the human genome. Trends Genet 20:481-490.

Powell BL, Wiltshire S, Arscott G, McCaskie PA, Hung J, McQuillan BM, Thompson PL, Carter KW, Palmer LJ, Beilby JP (2008) Association of PARL rs3732581 genetic variant with insulin levels, metabolic syndrome and coronary artery disease. Hum Genet 124:263-270.

Rahn JJ, Stackley KD, Chan SS (2013) Opa1 is required for proper mitochondrial metabolism in early development. PLoS One 8:e59218.

Rajput AH, Fenton M, Birdi S, Macaulay R (1997) Is levodopa toxic to human substantia nigra? Mov Disord 12:634-638.

Ren G, Li S, Zhong H, Lin S (2013) Zebrafish tyrosine hydroxylase 2 gene encodes tryptophan hydroxylase. J Biol Chem 288:22451-22459.

Ren G, Xin S, Li S, Zhong H, Lin S (2011) Disruption of LRRK2 does not cause specific loss of dopaminergic neurons in zebrafish. PLoS One 6:e20630.

Rink E, Wullimann MF (2002) Development of the catecholaminergic system in the early zebrafish brain: an immunohistochemical study. Developmental Brain Research 137:89-100.

Robu ME, Larson JD, Nasevicius A, Beiraghi S, Brenner C, Farber SA, Ekker SC (2007) p53 activation by knockdown technologies. PLoS Genet 3:e78.

Sallinen V, Kolehmainen J, Priyadarshini M, Toleikyte G, Chen YC, Panula P (2010) Dopaminergic cell damage and vulnerability to MPTP in Pink1 knockdown zebrafish. Neurobiol Dis 40:93-101.

Sallinen V, Torkko V, Sundvik M, Reenilä I, Khrustalyov D, Kaslin J, Panula P (2009) MPTP and MPP+ target specific aminergic cell populations in larval zebrafish. J Neurochem 108:719-731.

Santoriello C, Zon LI (2012) Hooked! Modeling human disease in zebrafish. J Clin Invest 122:2337-2343.

Schapira AH (2007) Mitochondrial dysfunction in Parkinson's disease. Cell Death Differ 14:1261-1266.

Schapira AH (2011) Mitochondrial pathology in Parkinson's disease. Mt Sinai J Med 78:872-881.

Sheng D, Qu D, Kwok KH, Ng SS, Lim AY, Aw SS, Lee CW, Sung WK, Tan EK, Lufkin T, Jesuthasan S, Sinnakaruppan M, Liu J (2010) Deletion of the WD40 domain of LRRK2 in Zebrafish causes Parkinsonism-like loss of neurons and locomotive defect. PLoS Genet 6:e1000914.

Shi G, Lee JR, Grimes DA, Racacho L, Ye D, Yang H, Ross OA, Farrer M, McQuibban GA, Bulman DE (2011) Functional alteration of PARL contributes to mitochondrial dysregulation in Parkinson's disease. Human Molecular Genetics 20:1966-1974.

Shibata A, Hattori M, Suda H, Sakaki Y (1996) Identification of cis-acting elements involved in an alternative splicing of the amyloid precursor protein (APP) gene. Gene 175:203-208.

Sik A, Passer BJ, Koonin EV, Pellegrini L (2004) Self-regulated cleavage of the mitochondrial intramembrane-cleaving protease PARL yields Pbeta, a nuclear-targeted peptide. J Biol Chem 279:15323-15329.

Tang H, Liu J, Niu L, He W, Xu Y (2009) Variation in gene expression of presenilins-associated rhomboid-like protein and mitochondrial function in skeletal muscle of insulin-resistant rats. Endocrine 36:524-529.

Tay TL, Ronneberger O, Ryu S, Nitschke R, Driever W (2011) Comprehensive catecholaminergic projectome analysis reveals single-neuron integration of zebrafish ascending and descending dopaminergic systems. Nat Commun 2:171.

Thisse C, Thisse B (2008) High-resolution in situ hybridization to whole-mount zebrafish embryos. Nature Protocols 3:59-69.

Tropepe V, Sive HL (2003) Can zebrafish be used as a model to study the neurodevelopmental causes of autism? Genes Brain Behav 2:268-281.

Walder K, Kerr-Bayles L, Civitarese A, Jowett J, Curran J, Elliott K, Trevaskis J, Bishara N, Zimmet P, Mandarino L, Ravussin E, Blangero J, Kissebah A, Collier GR (2005) The mitochondrial rhomboid protease PSARL is a new candidate gene for type 2 diabetes. Diabetologia 48:459-468.

Wang Y, Maegawa S, Akiyama Y, Ha Y (2007) The role of L1 loop in the mechanism of rhomboid intramembrane protease GlpG. J Mol Biol 374:1104-1113.

Wen L, Wei W, Gu W, Huang P, Ren X, Zhang Z, Zhu Z, Lin S, Zhang B (2008) Visualization of monoaminergic neurons and neurotoxicity of MPTP in live transgenic zebrafish. Dev Biol 314:84-92.

Westerfield M (2000) The zebrafish book. Eugene: University of Oregon Press.

Whitworth AJ, Lee JR, Ho VMW, Flick R, Chowdhury R, McQuibban GA (2008) Rhomboid-7 and HtrA2/Omi act in a common pathway with the Parkinson's disease factors Pink1 and Parkin. Disease Models & Mechanisms 1:168-174.

Xi Y, Noble S, Ekker M (2011a) Modeling neurodegeneration in zebrafish. Curr Neurol Neurosci Rep 11:274-282.

Xi Y, Ryan J, Noble S, Yu M, Yilbas AE, Ekker M (2010) Impaired dopaminergic neuron development and locomotor function in zebrafish with loss of pink1 function. Eur J Neurosci 31:623-633.

Xi Y, Yu M, Godoy R, Hatch G, Poitras L, Ekker M (2011b) Transgenic zebrafish expressing green fluorescent protein in dopaminergic neurons of the ventral diencephalon. Dev Dyn 240:2539-2547.

Yamamoto K, Ruuskanen JO, Wullimann MF, Vernier P (2011) Differential expression of dopaminergic cell markers in the adult zebrafish forebrain. J Comp Neurol 519:576-598.

Zebrafish (2002), First ed. Practical Approach, ed. Edition. New York: Oxford University Press.